الجمهورية الجزائرية الديمقراطية الشعبية

République Algérienne Démocratique et Populaire

Ministère de L'Enseignement Supérieur et de la Recherche Scientifique

Université Ferhat ABBAS Sétif 1

UNIVERSITÉ FERHAT ABBAS - SETIF1

FACULTÉ DE TECHNOLOGIE

THÈSE

Présentée au Département de Génie des Procédés

Pour l'obtention du diplôme de

DOCTORAT

Domaine : Sciences et Technologie

Filière: Génie des Procédés **Option: Matériaux Polymères**

Par

Mr.BELHAOUES Abderrahmane

THÈME

Compatibilisation du Mélange Caoutchouc Naturel/Polypropylène (NR/PP)

Soutenue le 09/Juin/2021 devant le Jury:

BENACHOUR Djafer	**Professeur**	**Univ. Ferhat Abbas Sétif 1**	**Président**
RIAHI Farid	**Professeur**	**Univ. Ferhat Abbas Sétif 1**	**Directeur de Thèse**
ÁNGEL ANTONIO Marcos-Fernández	**Professeur**	**ICTP–CSIC, Madrid-Spain**	**Co-Directeur**
DOUFNOUNE Rachida	**Professeur**	**Univ. Ferhat Abbas Sétif 1**	**Examinatrice**
HELLATI Abdelhak	**Maitre de Conférence Classe A**	**Univ. M.B.I Bordj Bou Arréridj**	**Examinateur**
BAOUZ Toufik	**Maitre de Conférence Classe A**	**Univ. Abderrahmane Mira Bejaia**	**Examinateur**

Dedication

DEDICATION

I would like to dedicate my thesis:

- To my family and my dearest parents especially my mother whose unbelievable endurance, unconditional love, and untouchable devotion have been monumental;

-To all my brothers: Seifeddine; Mouhamed Amin and Adel;

-To my wife who has been of great motivation and inspiration and for the countless ways she ensured that I finished this study this year;

-To those who will be happy for this new goal in my study career;

-To my best friends: Seifeddine, Islam, Abdeelhalim, Ali, Walid, Farouk, Fayçal, Moncef, Wassim, Fares, kamar-zaman, Soltan.

- To anyone who has ever taught me anything;

There are many friends and other family members who need to be listed for their part in this thesis;

Finally, this thesis is dedicated to all those who believe in the richness of learning and to all those who have devoted their lives to bring the faded light of ambiguity to the complete shininess of clarity.

Mr. BELHAOUES Abderrahmane

Acknowledgements

Acknowledgements

In the name of Allah,

The Most Beneficent and the Most Merciful. All praises to Allah the Almighty for giving me the strengths, guidance and patience in completing this thesis. With his blessing, this thesis is finally accomplished.

First of all, there are a lot of people who significantly helped me significantly throughout these years to reach the end of this beautiful journey. All those people were very influential and supportive, and I would like to thank them and show my appreciation for what they did.

I would like to take this opportunity, first and foremost, to express my heartiest thanks and deep gratitude to my supervisor, **Prof. Riahi Farid** for his helpful guidance, valuable discussions and support throughout this research. I also would like to express my gratitude and my deep appreciation accorded to my co-supervisor, **Prof. Ángel Antonio Marcos-Fernández** for spending his time and his thoughtful discussions, encouragement, patience, and kindness in the preparation of this thesis and for allowing me to use the facilities of the laboratories of the Department of Polymer Physics, Elastomers and Energy Applications, Institute of Polymer Science and Technology, CSIC, Madrid, Spain.

I would like to thank the jury members; namely: **Prof. Benachour Djafer**, **Prof. Doufnoune Rachida**, **Dr. Hellati Abdelhek** and **Dr. Baouz Toufik**, for reviewing this thesis. Their effort to examine this work is much appreciated.

I also would like to thank **Dr. Benmesli Samia** who provided the materials used in this study.
This work was performed in a collaboration between the Department of Process Engineering, Faculty of Technology, Ferhat Abbas University, Setif 1, Algeria and the Department of Polymer Physics, Elastomers and Energy Applications, Institute of Polymer Science and Technology, CSIC, Madrid, Spain with a financial grant for Ph.D students by The Algerian Ministry of Higher Education and Scientific Research (Grant Ph.D. Program **PNE 2019-2020**).

I also would like to thank **Dr. Alberto Fernández Torres**, **Dr. Juan Lopez Valentin,** and **Dr. Rodrigo Navarro Crespo** with whom I had useful discussions. Sincere thanks are also extended to all laboratory technicians for their valuable help and advice.

I would like also to place on record my great appreciation to all my teachers in Ferhat Abbas Setif -1- University, where I have studied Polymer Engineering and Science.

I would like to express my gratitude and my deep appreciation to **Prof. Benachour Djafer** for his constructive and scientific guidance, and kindness. He is my inspiration for what academic life should be about.

These acknowledgments would not be complete without a thought for my family. I want to express my deep gratitude to my dearest parents for their endless support. They have always been there for me during all these years of study and encouraged me to finish Ph.D study.

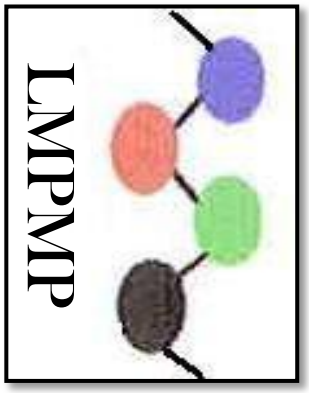

Mr. BELHAOUES Abderrahmane

Abstract

Abstract

Polymer blends emerge as one of the most important research areas in macromolecular science. The study of polymer blends structures, properties, and processing from academics and industries has been observed for decades. Due to their wide potential applications such as electronics, packaging, automotive, household appliances, etc., polymer blends have shown a growing development.

As we know that polymer blending is a mixing of at least two polymers to produce new materials with quite different properties. But unfortunately, most of the polymer pairs are thermodynamically immiscible, and the resulting blends exhibit poor mechanical performance due to the weak interfacial adhesion between the phases. Compatibilization of such polymer blends has been carried out to modify the interface and to improve their properties. The incorporation of compatibilizers as a third component in immiscible blends is effectively used to improve the phase compatibility.

Thermoplastic Elastomers (TPEs) are an important class of polymer blends that exhibit the typical advantages of conventional rubbers but can be processed with the thermoplastic processing methods. Among different kinds of thermoplastic elastomers, those based on polypropylene (PP) and natural rubber (NR). Considering the commercial significance of the mentioned blends, different approaches have been used during the last few decades to improve their compatibility/or their engineering properties to expand their fields of applications.

The objective of this work was to investigate the effects of a 50/50 blend of epoxidized natural rubber (ENR)/maleic anhydride grafted polypropylene (PP-g-MA) as a compatibilizing agent (CA).The incorporation of these modified forms of NR and PP, through their functional groups would promote the interactions with their parent elastomer and thermoplastic phases. The effects were investigated through the measurements of the rheological, mechanical, dynamic mechanical, morphological, and thermal properties of a 70/30 NR/PP thermoplastic elastomeric blend. The chemical structure of raw materials, as well as the compatibilizer was identified by fourier transform infrared spectroscopy (FTIR) and proton nuclear magnetic resonance (^{1}H-NMR).

FTIR analysis has confirmed the occurrence of reactions between the maleic anhydride groups of PP-g-MA and the epoxy groups in ENR and produced ENR-grafted PP with an ester and acid-based linkages. Moreover, ^{1}H-NMR results revealed that the CAs were

insoluble and did not dissolve in the different solvents but swelled only confirming hence the chemical reaction that took place between ENR and PP-g-MA.

Rheological properties of the blends have been investigated using a Brabender Plastograph, and Rubber Process Analyzer (RPA). The Brabender plastograms of the 70/30 NR/PP blends containing the compatibilizers showed a moderate increase of the torque when the CAs were added. It was also found that, compared to ENR_{25}; the ENR_{50}-based CA caused a plastization effect by reducing the viscosity which was reflected by the value of the final torque. For the dynamically vulcanized blends, it was found that the torque also increased as a result of the incorporation of the CA as well as the dynamic vulcanization which was carried out using a mixture of the tetramethylthiuram disulfide (TMTD), 4,4'-Dithiodimorpholine (DTDM), and N-Cyclohexyl-2-benzothiazole sulfenamide (CBS).

The RPA measurements indicated that the viscosity of both types of the CAs was higher than that of their respective individual values, confirming hence the grafting and crosslinking reaction which results from reaction between functional groups of ENR with PP-g-MA. Moreover, the RPA results revealed that, the viscosity of both thermoplastic elastomers and that of thermoplastic vulcanizates (TPVs) increased with increasing the concentration of both types of the CAs. The same trends were observed for the effects on the storage modulus.

The degree of crosslinking of the elastomer phase in the blends dynamically vulcanized by sulfur donors at different amounts of CAs was estimated by measuring the swelling index. It was found that the swelling index decreases continuously with increasing the CA concentration. It can therefore be inferred that changes down to the molecular level have taken place due to the interactions of Compatibilizing $Agent_{25}$ and Compatibilizing $Agent_{50}$ with PP and NR, and that the vulcanizates changed to stiffer and less penetrable materials by the solvent.

The mechanical properties results confirmed the enhancement of the interphase interactions for both the unvulcanized blends and the dynamically vulcanized ones. This was reflected by the increase of tensile strength, Young's modulus, and a decrease of the elongation at break.

Characterization by dynamic mechanical thermal analysis (DMTA) showed also an enhancement in the compatibility of the TPE and TPV blends. DMTA results indicated that the compatibilization and dynamic vulcanization lead to a significant enhancement in the storage modulus of the blends. Moreover, an increase in the glass transition temperatures of the blends was produced, due to the chain motion restriction imposed by their stronger interfacial interactions. The DMTA results revealed also that the T_β transition peak, relative to

the PP phase in the blend, disappeared for the unvulcanized CA_{25} or CA_{50}-containing blends but was more pronounced and shifted by almost 9°C for the dynamically vulcanized system with respect to the control blend.

The morphology of the blends was examined by using scanning electron microscopy (SEM), and atomic force microscopy (AFM). SEM and AFM micrographs revealed a more homogeneous distribution of the dispersed PP phase for the CA-containing TPE systems and good interfacial adhesion between all the phases compared to the control NR/PP TPE blend. Dynamic vulcanization produced a significant morphological transformation. The CA-containing TPVs exhibited a morphology characterized by finely dispersed NR particles in the PP matrix indicating the occurrence of phase inversion.

The thermal properties of the blends were measured by means of Differential Scanning Calorimetry (DSC).The melting behaviour of the blends revealed that, the CA has no significant influence on the melting temperature, it was also found that the CA was responsible for the reduction of the % crystallinity for the unvulcanized TPEs but an increase for the TPVs; which was attributed to phase inversion. The analysis of thermal stability of polymer blends is necessary for the development of durable products. The thermal degradation of the 70/30 NR/PP blends was investigated using the thermogravimetric analysis (TGA) method. The thermogravimetric studies revealed that the addition of CA did not have any significant effect on the thermal stability of the TPE blends. However, it was found that the decomposition temperatures of the two phases (elastomeric phase and thermoplastic phase) decreased for the dynamically vulcanized blends compared to the TPE blends, an unexpected result that reflects the complexity of the system studied which involves many conflicting factors.

Table of contents

Table of contents

Table of contents

Chapter II Materials and Experimental Procedures

Table of contents

Table of contents

Table of contents

List of Tables

List of Tables

List of Figures

List of Figures

List of Abbreviations

List of Abbreviations

Abbreviations	Description
ABS	Acrylonitrile Butadiene Styrene
AFM	Atomic Force Microscopy
BR	Butadiene Rubber
CBS	N-Cyclohexyl-2-benzothiazole sulfenamide
CPE	Chlorinated Polyethylene
CNR	Cyclic Natural Rubber
DTDM	Dithiodimorpholine
DMTA	Dynamic Mechanical Thermal Analysis
DSC	Differential Scanning Calorimetry
DCP	Dicumyl Peroxide
ENR/PP-g-MA	Epoxidized Natural Rubber/ Polypropylene-grafted-Maleic Anhydride
ENR	Epoxidized Natural Rubber
ELNR	Epoxidized Liquid Natural Rubber
EPDM	Ethylene Propylene Diene Rubber
EPDM-g-MA	Ethylene Propylene Diene Rubber –grafted- Maleic anhydride
EVA	Ethylene Vinyl Acetate
EPR	Ethylene Propylene Rubber
HDPE	High Density Polyethylene
HBTP	Hexamethylene N, N′ Bis (Tert-Butyl Peroxy Carbamate)
ISO	International Standards Organization
LNR	Liquid Natural Rubber
LLDPE	Linear Low Density Polyethylene
MA	Maleic Anhydride
MNR	Maleated Natural Rubber
PP-g-MA	Polypropylene-grafted- Maleic Anhydride
Mn	Number Average Molecular Weight
Mw	Molecular Weight
MFI	Melt Flow Index
NR/PP	Natural Rubber/ Polypropylene
NBR	Acrylonitrile Butadiene Rubber
NMR	Nuclear Magnetic Resonance
NR	Natural Rubber

List of Abbreviations

NRL	Natural Rubber Latex
NR-g-MMA	Natural Rubber -graft-Methyl Methacrylate
NR-g-PMMA	Natural Rubber -graft-Poly(Methyl Methacrylate)
NR-g-PS	Natural Rubber -graft-Polystyrene
PA	Polyamide
PA-6	Polyamide-6
PA-12	Polyamide-12
PE	Polyethylene
PLA	Polylactide
PLLA	Poly(L-Lactide)
PMMA	Poly(Methyl Methacrylate)
PVDF	Polyvinyl Diene Fluoride
PP	Polypropylene
PVC	Polyvinyl Chloride
PS	Polystyrene
Ph-PP	Phenolic Modified Polypropylene
SBR	Styrene Butadiene Rubber
SAN	Styrene-Acrylonitrile
SEBS	Styrene Ethylene/Butylene Styrene block copolymer
SEBS-g-MA	Styrene-Ethylene-Butylene-Styrene-graft-Maleic Anhydride
SEM	Scanning Electron Microscope
TEM	Transmission Electron Microscope
TGA	Thermogravimetric Analysis
TPEs	Thermoplastic Elastomers
TPVs	Thermoplastic Vulcanizates
TMTD	Tetramethylthiuram Disulfide
TBBS	N-Tert-Butyl-2-Benzothiazole sulphenamides
TPNR	Thermoplastic Natural Rubber
TPO	Thermoplastic Polyolefin
Tg	Glass Transition Temperature

Symbols	Description
E	Young's Modulus
E'	Storage Modulus
E"	Loss Modulus
ΔHm	Melting Enthalpy of Sample
ΔH_0	Theoretical Enthalpy for 100 % Crystalline
Tan δ	Loss Tangent
Tc	Crystallization Temperature
Tm	Melting Temperature
ω	Frequency
Ɛb	Elongation at Break
TS	Tensile Strength
Xc	Degree of % Crystallinity
ε	Strain
η	Viscosity
η*	Complex Viscosity

Introduction

Introduction

Blending of two or more types of polymers such as blending natural rubber with polyolefins is a useful technique for the preparation and development of materials with properties superior to those of the individual constituents **[1]**. However, most polymer blends are immiscible and usually exhibit phase-separated morphologies and poor interfacial adhesion between their phases **[2]**. The interfacial adhesion can be improved by introducing a third component into the binary system that will either chemically interact with both the phases or will have specific interactions with one phase and physical interactions with the other **[3]**. This phenomenon can be explained as an improvement in the compatibilization of the blend. Commonly, compatibilization can lead to a finer phase structure and enhanced interfacial adhesion **[4]**.

A particular type of polymer blends is thermoplastic elastomers (TPEs). TPEs play an important role in the polymer industry due to their good processability and their elastomeric properties. There has been a growth of subcategories of TPEs to distinguish between different types of materials. Several examples are block copolymers, thermoplastic/rubber blends, and ionomers. Extensive studies have been carried out in the area of TPEs based on blends of elastomers with thermoplastics **[5]**. TPEs based on rubber- thermoplastic blends are classified into two distinct types. One type consists of a simple blend where the rubber known as a thermoplastic elastomer polyolefin (TPE-O) or a thermoplastic polyolefin (TPO). The rubber phase of the thermoplastic polyolefin is an unvulcanized material. In the other type, the rubber singular phase is dynamically vulcanized during melt mixing with a thermoplastic polymer, giving rise to thermoplastic vulcanizates (TPVs), dynamic vulcanizates (DVs), or elastomeric alloys (EAs) **[6]**.

TPEs prepared from blends of natural rubber and various types of thermoplastic are known as thermoplastic natural rubbers (TPNRs) **[7]**. These include polyolefins, such as polypropylene **[8-13]**, polystyrene (PS) **[14]**, polyamide-6 (PA-6) **[15]**, poly (methyl methacrylate) (PMMA) **[16-18]**, ethylene vinyl acetate copolymer (EVA) **[19]**, low-density polyethylene (LDPE) **[20-21]**, and linear low-density polyethylene (LLDPE) **[22-24]**. Polypropylene is considered to be the best choice for blending with NR due to its high softening temperature of about 150°C and low glass transition temperature of about - 60°C for the blend, giving rise to a very versatile thermoplastic applicable over a wide range of temperatures **[25]**.

Research on TPNR is very extensive and can be divided in three main fields which are the development of view types of TPNR by varying blend components, the investigation of

different crosslinking agents for the dynamic vulcanization, and study of the effects of the chemical modification of the NR and/or the polyolefin part in the blend **[26]**.

Several researchers have investigated the compatibilization of TPNRs based on modified forms of NR and reported enhanced properties of the resulting blends **[27-41]**.

The objective of the present study is to investigate the effects of the incorporation of a 50/50 blend of ENR/PP-g-MA as a compatibilizing agent (CA) on the rheological, mechanical, dynamic mechanical, morphological, and thermal properties of a 70/30 NR/PP TPE and TPV blends.

The incorporation of a blend of ENR with PP-g-MA through the functional groups enhanced by the epoxy groups and the anhydride groups would promote the interactions with their parent elastomer (NR) and thermoplastic (PP) phase, respectively in the resulting TPEs.

This thesis is composed of four chapters. The first of which presents a theoretical background on the main polymers used in the study and a state of the art of the research carried out in the field of compatibilization of polymer blends as well as the chemical modification of NR and PP. The second chapter describes the materials and the experimental procedures. In the third chapter, characterizations of the produced compatibilizing agents by FTIR and ^{1}H-NMR analyses as well as the rheological properties of the CA-containing blends are discussed. The results of the effect of addition of the 50/50 blend of ENR with PP-g-MA to the 70/30 NR/PP TPE and TPV on the mechanical, dynamic mechanical, morphological, and thermal properties are discussed in the last chapter.

The main results obtained are summarized in the conclusion, and recommendations for future work are also proposed.

References

[1] Findik, F.; Yilmaz, R.; Köksal, T. Investigation of Mechanical and Physical Properties of Several Industrial Rubbers. *Materials & Design*.**2004**, *25* (4), 269–276. https://doi.org/10.1016/j.matdes.2003.11.003.

[2] Soares, B. G.; Almeida, M. S. M.; Guimarães, P. I. C. The Reactive Compatibilization of NBR/EVA Blends with Oxazoline-Modified Nitrile Rubber. *Eur Polym J*.**2004**, *40* (9), 2185–2194. https://doi.org/10.1016/j.eurpolymj.2004.04.006.

[3] Tedesco, A.; Barbosa, R. V.; Nachtigall, S. M. B.; Mauler, R. S. Comparative Study of PP-MA and PP-GMA as Compatibilizing Agents on Polypropylene/Nylon 6 Blends. *Polym Test*.**2002**, *21* (1), 11–15. https://doi.org/10.1016/S0142-9418(01)00038-1.

[4] Mangaraj, D. Elastomer blends. *Rubber Chem Technol*.**2002**, 75(3), 365-427. https://doi.org/10.5254/1.3547677.

[5] Abdou-Sabet,S; Raman P. Patel, Morphology of Elastomeric Alloys. *Rubber Chem Technol*.**1991**, 64 (5), 769–779.https://doi.org/10.5254/1.3538589.

[6] Abdou-Sabet, S.; Puydak, R. C.; Rader. Dynamically vulcanized thermoplastic elastomers. C. P. *Rubber Chem Technol*.**1996**, 69(3), 476-494.https://doi.org/10.5254/1.3538382.

[7] Nakason, C.; Jarnthong, M.; Kaesaman, A.; Kiatkamjornwong, S. Thermoplastic Elastomers Based on Epoxidized Natural Rubber and High-Density Polyethylene Blends: Effect of Blend Compatibilizers on the Mechanical and Morphological Properties. *J. Appl. Polym. Sci*.**2008**, *109* (4), 2694–2702. https://doi.org/10.1002/app.28265.

[8] Varghese, S.; Alex, R.; Kuriakose, B. Natural Rubber-Isotactic Polypropylene Thermoplastic Blends. *J. Appl. Polym. Sci*.**2004**, *92* (4), 2063–2068. https://doi.org/10.1002/app.20077.

[9] Kuriakose, B.; De, S. K.; Bhagawan, S. S.; Sivaramkrishnan, R.; Athithan, S. K. Dynamic Mechanical Properties of Thermoplastic Elastomers from Polypropylene–Natural Rubber Blend. *J. Appl. Polym. Sci.***1986**, *32* (6), 5509–5521. https://doi.org/10.1002/app.1986.070320619.

[10] Al-Malaika, S.; Amir, E. J. Thermoplastic Elastomers: Part III Ageing and Mechanical Properties of Natural Rubber-Reclaimed Rubber/Polypropylene Systems and Their Role as Solid Phase Dispersants in Polypropylene/Polyethylene Blends. *Polym Deg Stab*.**1989**,26(1),31–41. https://doi.org/10.1016/0141-3910(89)90026-8.

[11] Ismail, H.; Suryadiansyah. Thermoplastic Elastomers Based on Polypropylene/Natural Rubber and Polypropylene/Recycle Rubber Blends. *Polym Test*.**2002**, *21* (4), 389–395. https://doi.org/10.1016/S0142-9418(01)00101-5.

[12] Kuriakose, B.; Chakraborty, S. K.; De, S. K. Scanning Electron Microscopy Studies on Tensile Failure of Thermoplastic Elastomers from Polypropylene-Natural Rubber Blends. *Mat Chem Phys*.**1985**, *12* (2), 157–170. https://doi.org/10.1016/0254-0584(85)90053-7.

[13] Roy Choudhury, N.; Chaki, T. K.; Bhowmick, A. K. Thermal Characterization of Thermoplastic Elastomeric Natural Rubber-Polypropylene Blends. *Thermo Acta*.**1991**, *176*, 149–161. https://doi.org/10.1016/0040-6031(91)80270-S.

[14] Asaletha, R.; Groeninckx, G.; Kumaran, M. G.; Thomas, S. Melt Rheology and Morphology of Physically Compatibilized Natural Rubber-Polystyrene Blends by the Addition of Natural Rubber-g-Polystyrene.*J. Appl. Polym. Sci.***1998**, 69(13), 2673–2690. https://doi.org/10.1002/(SICI)1097-4628(19980926)69:13<2673::AID-APP18>3.0.CO;2-V

[15] Carone, E.; Kopcak, U.; Gonçalves, M. C.; Nunes, S. P. In Situ Compatibilization of Polyamide 6/Natural Rubber Blends with Maleic Anhydride. *Polymer*.**2000**, *41* (15), 5929–5935. https://doi.org/10.1016/S0032-3861(99)00800-9.

[16] Suriyachi P, Kiatkamjonwong S, Prasassarakich P. Natural Rubber-g-Glycidyl Methacrylate/Styrene as a Compatibilizer in Natural Rubber/PMMA Blends. *Rubber Chem Technol*.**2004**,77(5), 914–930. https://doi.org/10.5254/1.3547859.

[17] Thiraphattaraphun, L.; Kiatkamjornwong, S.; Prasassarakich, P.; Damronglerd, S. Natural Rubber-g-Methyl Methacrylate/Poly(Methyl Methacrylate) Blends. *J. Appl. Polym. Sci.* **2001**, *81* (2), 428–439. https://doi.org/10.1002/app.1455.

[18] Nakason, C.; Panklieng, Y.; Kaesaman, A. Rheological and Thermal Properties of Thermoplastic Natural Rubbers Based on Poly(Methyl Methacrylate)/Epoxidized-Natural-Rubber Blends. *J. Appl. Polym. Sci*.**2004**, *92* (6), 3561–3572. https://doi.org/10.1002/app.20384.

[19] Thongpin, C.; Muanwong, A.; Yanyongsak, J.; Lorphaitoon, P. Effect of ENR Contents on Cure Characteristic and Properties of NR/ENR/EVA Foam. MSF.**2017**, 889, 45–50, doi:10.4028/www.scientific.net/MSF.889.45.

[20] Bhowmick, A. K.; Heslop, J.; White, J. R. Effect of Stabilizers in Photodegradation of Thermoplastic Elastomeric Rubber–Polyethylene Blends—a Preliminary Study. *Polym Deg Stab*.**2001**, *74* (3),513–521. https://doi.org/10.1016/S0141-3910(01)00188-4.

[21] Mahapram, S.; Poompradub, S. Preparation of Natural Rubber (NR) Latex/Low Density Polyethylene (LDPE) Blown Film and Its Properties. *Polymer Test*.**2011**, *30*, 716–725, doi:10.1016/j.polymertesting.2011.06.006.

[22] Dahlan, H. M.; Khairul Zaman, M. D.; Ibrahim, A. The Morphology and Thermal Properties of Liquid Natural Rubber (LNR)-Compatibilized 60/40 NR/LLDPE Blends. *Polym Test*.**2002**, *21* (8), 905–911. https://doi.org/10.1016/S0142-9418(02)00027-2.

[23] Abdullah, I.; Ahmad, S.; Sulaiman, C. S. Blending of Natural Rubber with Linear Low-Density Polyethylene. *J. Appl. Polym. Sci.***1995**, *58* (7), 1125–1133. https://doi.org/10.1002/app.1995.070580706.

[24] Guo, B.; Cao, Y.; Jia, D.; Qiu, Q. Thermoplastic Elastomers Derived from Scrap Rubber Powder/LLDPE Blend with LLDPE-Graft-(Epoxidized Natural Rubber) Dual Compatibilizer. *Macromol. Mater. Eng.***2004**, *289* (4), 360–367. https://doi.org/10.1002/mame.200300311.

[25] Ibrahim, A, Dahlan, H. M. Thermoplastic Natural Rubber Blends. *Prog Polym Sci*.**1998**, *23* (4), 665–706. https://doi.org/10.1016/S0079-6700(97)00052-X.

[26] Belhaoues, A.; Benmesli, S.; Riahi, F. Compatibilization of Natural Rubber–Polypropylene Thermoplastic Elastomer Blend. *J Elastomers Plast*.**2020**, *52* (8), 728–746. https://doi.org/10.1177/0095244319891231.

[27] Choudhury, N. R.; Bhowmick, A. K. Compatibilization of Natural Rubber–Polyolefin Thermoplastic Elastomeric Blends by Phase Modification. *J. Appl. Polym. Sci.***1989**, *38* (6), 1091–1109. https://doi.org/10.1002/app.1989.070380609.

[28] Pichaiyut, S.; Nakason, C.; Kaesaman, A.; Kiatkamjornwong, S. Influences of Blend Compatibilizers on Dynamic, Mechanical, and Morphological Properties of Dynamically Cured Maleated Natural Rubber and High-Density Polyethylene Blends. *Polym Test*.**2008**, *27* (5), 566–580. https://doi.org/10.1016/j.polymertesting.2008.03.004.

[29] Thitithammawong, A.; Noordermeer, J. W. M.; Kaesaman, A.; Nakason, C. Influence of Compatibilizers on the Rheological, Mechanical, and Morphological Properties of Epoxidized Natural Rubber/Polypropylene Thermoplastic Vulcanizates. *J. Appl. Polym. Sc.* **2008**, 107(4), 2436–2443. https://doi.org/10.1002/app.27233.

[30] Mahendra, I. P.; Wirjosentono, B.; Tamrin; Ismail, H.; Mendez, J. A.; Causin, V. The Influence of Maleic Anhydride-Grafted Polymers as Compatibilizer on the Properties of Polypropylene and Cyclic Natural Rubber Blends. *J Polym Res*.**2019**, *26* (9), 215. https://doi.org/10.1007/s10965-019-1878-2.

[31] Chuayjujit, S.; Sakulkijpiboon, S.; Potiyaraj, P. Preparation of Thermoplastic Elastomer from Epoxidised Natural Rubber and Polystyrene. *Polym & Polym Compos*.**2010**, *18* (3), 139–144. https://doi.org/10.1177/096739111001800303.

[32] Benmesli, S.; Riahi, F. Dynamic Mechanical and Thermal Properties of a Chemically Modified Polypropylene/Natural Rubber Thermoplastic Elastomer Blend. *Polym Test*.**2014**, *36*, 54–61. https://doi.org/10.1016/j.polymertesting.2014.03.016.

[33] Setua, D. K.; Gupta, Y. N. On the Use of Micro Thermal Analysis to Characterize Compatibility of Nitrile Rubber Blends. *Thermo Acta*.**2007**, *462* (1–2), 32–37. https://doi.org/10.1016/j.tca.2007.06.004.

[34] Datta, S.; Lohse, D. J. Polymeric Compatibilizers: Uses and Benefit in Polymer Blend; Polymer Chemistry; Hanser: New York,.**1996, 542 p.**

[35] Markham, R. L. Introduction to Compatibilization of Polymer Blends; CRC: Boca Raton, FL. Advances in Polymer Technology.**1993**, 10 (3), 231-236. https://doi.org/10.1002/adv.1990.060100307.

[36] Panigrahi, H.; Sreenath, P. R.; Bhowmick, A. K.; Dinesh Kumar, K. Unique Compatibilized Thermoplastic Elastomer from Polypropylene and Epichlorohydrin Rubber. *Polymer*.**2019**, *183*, 121866. https://doi.org/10.1016/j.polymer.2019.121866.

[37] George, S.; Reethamma, J.; Sabu, T. Blends of Isotactic Polypropylene and Nitrile Rubber: Morphology, Mechanical Properties and Compatibilization. *Polymer*.**1995**, 36(23), 4405-4416. https://doi.org/10.1016/0032-3861(95)96846-Z.

[38] Hashim, A. S.; Ong, S. Study on Polypropylene/Natural Rubber Blend with Polystyrene-Modified Natural Rubber as Compatibilizer. *Polym Int.***2002**, *51* (7), 611–616. https://doi.org/10.1002/pi.920.

[39] Phinyocheep, P.; Axtell, F. H.; Laosee, T. Influence of Compatibilizers on Mechanical Properties, Crystallization, and Morphology of Polypropylene/Scrap Rubber Dust Blends. *J. Appl. Polym. Sci.***2002**, *86* (1), 148–159. https://doi.org/10.1002/app.10917.

[40] Nakason, C.; Saiwari, S.; Kaesaman, A. Rheological Properties of Maleated Natural Rubber/Polypropylene Blends with Phenolic Modified Polypropylene and Polypropylene-g-Maleic Anhydride Compatibilizers. *Polym Test*.**2006**, *25* (3), 413–423. https://doi.org/10.1016/j.polymertesting.2005.11.006.

[41] Nakason, C.; Wannavilai, P.; Kaesaman, A. Thermoplastic Vulcanizates Based on Epoxidized Natural Rubber/Polypropylene Blends: Effect of Compatibilizers and Reactive Blending. *J. Appl. Polym. Sci.***2006**, *100* (6), 4729–4740. https://doi.org/10.1002/app.23260.

Chapter I

Theoretical Background and Literature Review

In this chapter we present an overview of the polymers involved in this study. Emphasis is made on thermoplastic elastomers (TPEs) and those based on natural rubber (NR) and the different strategies used for compatibilization. In the second part, a literature review concerning the research studies published in the field of thermoplastic natural rubber (TPNRs) is presented.

I.1 Introduction

Natural Rubber (NR) products are undoubtedly a part of our everyday life and can be seen in applications across a number of industries, including some we may have never even thought about. Also known as gum rubber, it is a substance which is heavily desired because of its favorable physical properties and the potential to be improved chemically so that it will become even more useful **[1]**. The history of natural rubber has seen its evolution from a product that was originally used primitively and only for simple functions. Nowadays natural rubber is used in modern industries such as aerospace, automotive, transportation, and petroleum industries. With continued research and advances in technology, we can be sure to find the uses of natural rubber to expand alongside these applications **[2]**.

Chemical modification of NR has become an important method for improving its properties and widening its range of uses **[3-7]**. The epoxidation of NR, to produce epoxidized natural rubber (ENR) is an attractive method of its modification as it improves its properties as damping, air permeability, as well as oil and solvent resistance **[8]**. Another route of modification of Natural Rubber, which gained great importance, as far as optimizing the materials performance and processing, is the development of Thermoplastic Natural Rubber (TPNR). TPNR is a material blend made from Natural Rubber (NR) and a polyolefin, such as polypropylene. Thus, it shows intermediate properties between the NR and the plastic, which provides flexibility in shaping, great recyclability of scrap, and low production cost. Its outstanding feature, as for all thermoplastic elastomers (TPEs), is its combined excellent processing characteristics of thermoplastic materials and the wide range of physical properties of the base elastomer at service temperature **[9-10]**.

I.2 Natural Rubber

Among of the range of elastomers available to technologists, NR is among the most important, because it is the building block of most rubber compounds used in products today. NR, which is a truly renewable resource (**Figure I.1**), comes primarily from Indonesia, Malaysia, India, and the Philippines, though many more additional sources of good quality

rubber are becoming available. NR is a material that is capable of rapid deformation and recovery, and it is insoluble in a range of solvents, though it will swell when immersed in organic solvents at elevated temperatures. Its many attributes include abrasion resistance, good hysteretic properties, high tear strength, high tensile strength, and high green strength. However, it may also display poor fatigue resistance. It is difficult to process in factories, and it can show poor tire performance in areas such as traction or wet skid compared to selected synthetic elastomers **[11].**

Natural Rubber, consisting of cis-1,4-polyisoprene (**Figure I.2**) as a major polymeric material, is a useful material with a high amount of production and consumption throughout the world. NR has been used as a raw material in many industries, particularly for the manufacture of rubber tires, consumer products and medical sectors, such as footwear, rubber band, rubber toys, medical gloves, etc.

Figure I.1 Photographic images of Natural Rubber latex from Hevea brasiliensis tree.

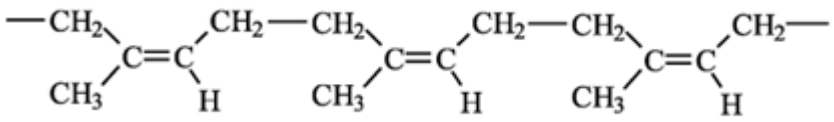

cis-Polyisoprene (repeat units, n = 1500 to 15,000: M_w = 100,000 to 1,000,000)

Figure I.2 Chemical structure of natural rubber.

The chemical structure of Natural Rubber comprises of 99% of cis-1,4-polyisoprene. The remaining 1% is a mixture of non-rubber components such as protein, amino acids, sugar, fatty acids and other substances. The high content of cis-1,4-polyisoprene in NR, contributes to high degree of strain-induced crystallization as well as high mechanical properties **[11].**

I.2.1 Properties of Natural Rubber

Natural Rubber has certain unique properties such as:

- It combines high strength (tensile and tear) with an outstanding resistance to fatigue.
- It has excellent green strength and tack which means that it has the ability to stick to itself and to other materials which makes it easier to fabricate.
- It has moderate resistance to environmental damage by heat, light and ozone which is one of its drawback.
- Natural Rubber has excellent adhesion to brass-plated steel cord, which is ideal in rubber tyres.
- It has low hysteresis which leads to low heat generation, and this in turn maintains new tyre service integrity and extends retreadability.
- Natural Rubber has low rolling resistance with enhanced fuel economy.
- It has high resistance to cutting, chipping and tearing **[12].**

I.2.2 Applications of Natural Rubber

Owing to its excellent properties, NR is an essential component of many products used in various applications. Rubber products can be classified into five sectors as follows:

1. Tyre products: Major products of dry NR for over 70% of NR consumption is used in tyres, especially heavy-duty tyres for trucks, buses and airplanes, and tyre products, such as pneumatic tyres and inner tubes for automotive use. The ability of NR to resist heat build-up makes the heavy-duty tyres much safer than those made from synthetic rubber.
2. Moulded products: Prepared by compression or injection of rubber compound into a closed mould. Typical products are sponges, carpet underlay, sandals, shoes, rubber bands, connectors, curing tubes, and curing flaps, lining mats, O-rings, rollers, bumpers, heavy-duty pads, seals, gaskets and wheels.
3. Extruded products: Rubber is extruded through dies to form various shapes and profiles. Examples of extruded products are hoses, pipes, electric cables, refrigerator seals, window/door seals, insulators, rollers and erasers.
4. Calendered products: Calendered rubber sheets are widely used in various applications such as conveyer belts, bumpers, gaskets, roll coverings, brake linings, seals and tyre patches.

5. Adhesives: Solution adhesives consist of a mixture of solid rubber and other components dissolved in a solvent. Several adhesive systems are used to produce pressure-sensitive adhesives. The applications of solid NR are adhesives, electrical insulation tapes, adhesive tapes, packaging tapes, surgical tapes and plasters **[12].**

I.3 Modified forms of Natural Rubber

NR has been modified in a number of ways in line with several developments that have taken place in the field of synthetic rubbers. Physical blending with other materials or polymers is commonly referred to as physical modification while direct reaction of the polyisoprene molecule with appropriate reagents results in chemically modified forms. NR was found to be suitable for different types of chemical modification resulting in the production of a number of polymeric materials of very interesting properties **[13].**

NR can be modified by physical or chemical means and in some cases by a combination of the two. Physical methods involve incorporation of additives that do not chemically react with rubber. Examples are oil extension, blending with other polymers, masterbatching, etc. Although a limited level of chemical reaction may take place between the rubber and some of the added materials, the modification in properties is brought about mostly by the physical combination of materials. A chemical modification on the other hand, depends on the chemical reactivity of NR molecule. Being unsaturated, it is highly reactive and many chemical reactions could be carried out on NR resulting in materials having entirely different properties. The most widely practiced chemical reaction on NR is vulcanization. It is an integral part of most of the product manufacturing processes. There are a number of other reactions on NR which yield products with novel properties. These reactions could be broadly divided into three categories: intermolecular changes without introduction of a new chemical group, attachment of a pendant functional group, grafting of different polymers at one or more points along the NR molecule **[13-14].**

I.3.1 Chemical modification of Natural Rubber

NR shows a very uniform microstructure that provides unique and important characteristics to the material, namely the ability to crystallize under strain, a phenomenon known as “strain induced crystallization”, and very low hysteresis. From these properties; i.e: good tensile strength, high resilience, excellent flexibility, and resistance to impact and tear NR is very useful in many applications. However, NR shows low resistance to oxidation, UV radiation, weathering, and a wide range of chemicals and solvents, mainly due to its unsaturated chain

structure and low polarity. These inherent drawbacks apparently cause limitations in NR usage, particularly for technical and engineering applications. In order to extend the uses of NR, a chemical modification of its structure have been envisaged for many years and was shown as an interesting method for producing new NR-derived materials and modifying its intrinsic properties such as chemical resistance, weathering resistance, and thermal stability. Chemical modification of NR can be classified in three main categories **[13-14]:**

I.3.1.1 Modification by bond rearrangement without introducing new atoms

Carbon-carbon crosslinking, carbon-carbon isomerization, hydrogenation, cyclization, and depolymerization are among the main examples of this type of modification applied to NR. For instance, hydrogenated NR is thermally more stable than NR, and more resistant to oxidation and radiation effects, because of its saturated structure. Hydrogenated NR has a structure of alternated copolymer of ethylene and propylene as shown in **Figure I.3.** It can be performed with elemental hydrogen in the presence of a transition metal catalyst **[15-16]** or by a non-catalytic method **[17].** Hydrogenated NR shows a higher degree of crystallinity and a slightly higher glass transition temperature (Tg) than NR, as well as a better thermal stability **[18].** Such hydrogenated NRs have the potential to be used in fields where good thermal properties are required, for instance to prepare vibration isolators at high temperature **[18].**

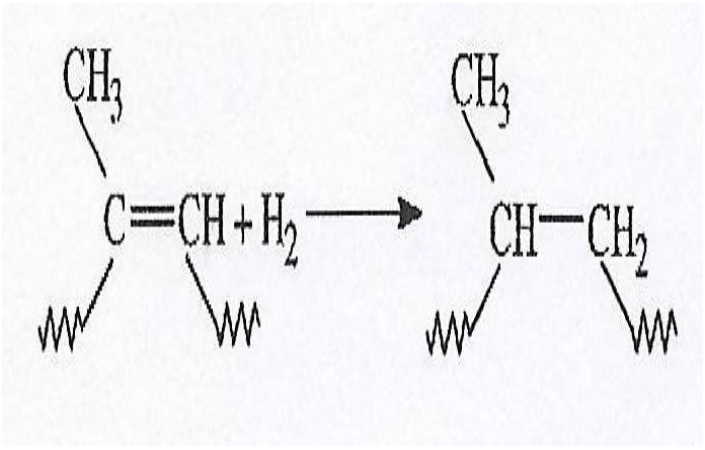

Figure I.3 Hydrogenation of natural rubber **[18]**.

I.3.1.2 Modification by bonding of new chemical groups or atoms through addition or substitution reactions performed on carbon-carbon double bonds.

Chlorinated NR, hydrochlorinated NR and, epoxidized NR are some examples of commercially available modified NR by attachment of new chemical groups. Epoxidation of NR has been done since 1922, but commercial grades and potential applications of epoxidized natural rubber were only developed in the 1980. Epoxidation can be carried out in solution or

in the latex form but only the latter is of commercial grade. A peracid is commonly used to carry out the epoxidation of NR in the latex form. The epoxidation occurs via a transition state mechanism as shown in **Figure I.4.** It was found that, depending on the reaction conditions, it is possible to modulate the level of epoxidation **[19-21].** Two ENR grades defined by their content in epoxidized 1,4-polyisoprene units, i.e., 25 % and 50 %, are commercially available. The Tg of ENR increases linearly with the content in epoxidized units. Due to its higher Tg, ENR shows improved tensile strength and fatigue compared to NR, and the bonding to metal and wet grip is also better than with NR **[22].**

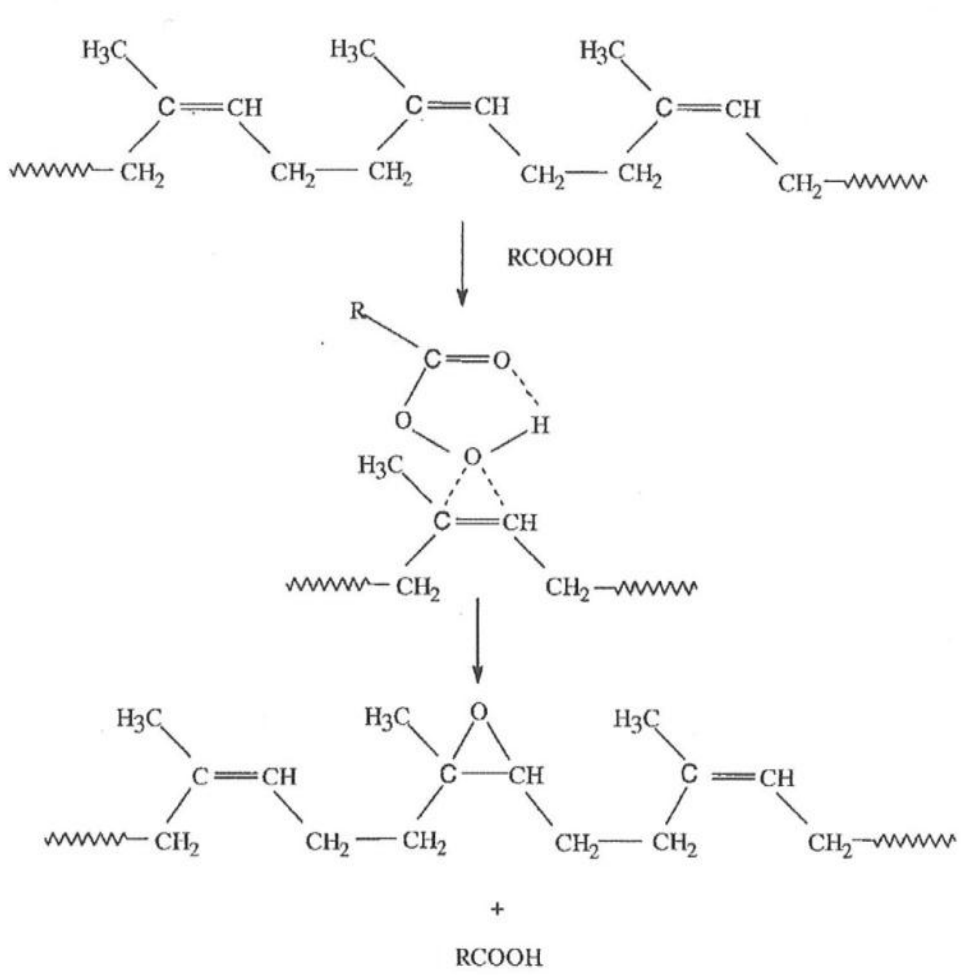

Figure I.4 Mechanism of the epoxidation of NR by the peracid **[21]**.

I.3.1.3 Grafting of a polymer onto the NR backbone

Grafting has been frequently performed using vinyl monomers like methyl methacrylate and styrene. Graft copolymers of NR and poly(methyl methacrylate) (NR-g-PMMA) known as Heveaplus MG, are commercially available in two grades: 30 % (MG 30) and 49 % (MG49) of PMMA **[23].** Heveaplus MG shows superior properties like hardness, modulus, abrasion,

electrical resistance, and light color. It has been used to improve the impact properties of polystyrene, and to blend with NR as reinforcing agent. The solution or latex form of Heveaplus MG was used as adhesive or bonding agent to bond rubber to poly(vinyl chloride) (PVC), leather, textiles, and metals. Recently, Derouet et al **[24],** synthesized well-defined NR-g-PMMAs by MMA photopolymerization initiated from N, N-diethyldithiocarbamate functions previously created along the NR chains (**Figure I.5**). They found that the thermal stability of NR was improved after the introduction of PMMA grafts onto NR chains.

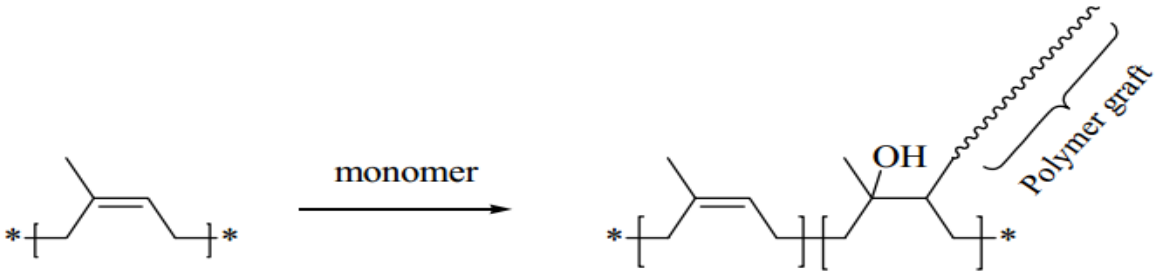

Figure I.5 Grafting of a second polymer onto the NR backbone **[24].**

I.4 Polypropylene

Polypropylene is a tough, rigid and semi crystalline thermoplastic produced from propene (or propylene) monomer. It is a linear hydrocarbon resin. The chemical formula of polypropylene is $(C_3H_6)_n$. Polypropylene is a vinyl polymer in which every carbon atom is attached to a methyl group and can be expressed as shown in **Figure I.6.**

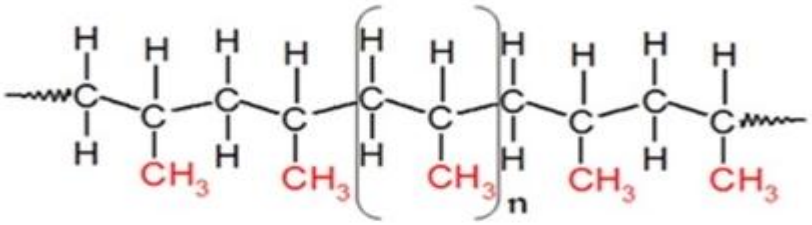

Figure I.6 Chemical structure of polypropylene.

Polypropylene shows many good properties such as excellent chemical and thermal resistance, high melting point, stiffness, chemical inertness and low density, a high tensile modulus, and easy recyclability **[25].** Polypropylene offers a very attractive combination of physical and mechanical properties at a relatively low cost with continuously increasing applications. Some of the characteristics of this material are suitable for common service conditions. Due to its high transition temperature and high crystallinity, PP exhibits poor low temperature impact resistance. Polypropylene forms very poor blends with other polymers. It has no chemical functionalities. Polypropylene is one of the most important commercial

polymers; it is a highly versatile material with an outstanding combination of cost performance and excellent physical properties. The property range of PP can be broadened by physically blending it with other polymers. It has a hydrophobic, low-free-energy, chemically inert surface. Polypropylene shows brittleness, low mechanical performance and low impact resistance at below or around glass transition temperature.

Polypropylene is made from polymerization of propene monomer by: Ziegler-Natta polymerization or Metallocene catalysis polymerization.

Upon polymerization, PP can form three basic chain structures depending on the position of the methyl groups (**Figure I.7)**: 1-Atactic (aPP) - Irregular methyl group (CH_3) arrangement, 2-Isotactic (iPP) – Methyl groups (CH_3) arranged on one side of the carbon chain. 3-Syndiotactic (sPP) - Alternating methyl group (CH_3) arrangement **[26].**

1- Atactic polypropylene (aPP)

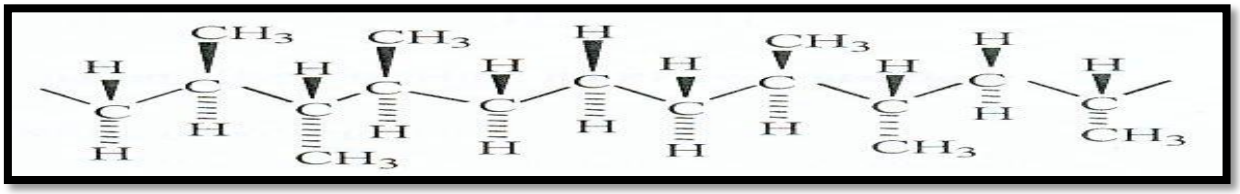

2- Isotactic polypropylene (iPP)

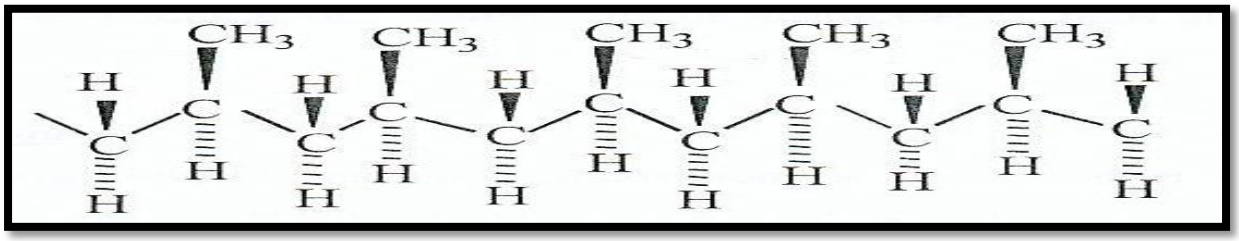

3- Syndiotactic polypropylene (sPP)

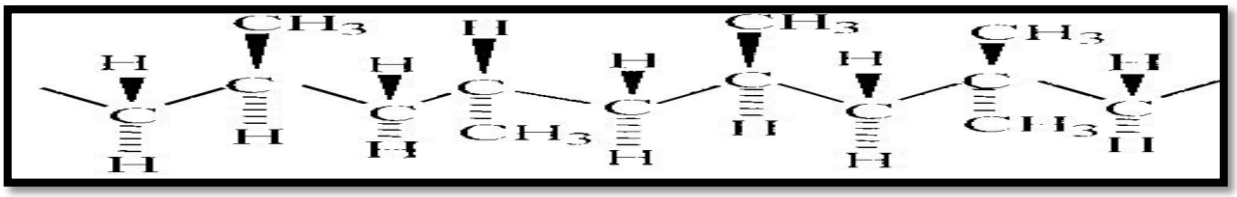

Figure I.7 The Ziegler-Natta catalytic polymerization of propene with three different stereoregular structures **[26].**

I.4.1 Advantages of polypropylene

1. Polypropylene is readily available and relatively inexpensive.
2. It has high flexural strength due to its semi-crystalline nature.
3. It has also a relatively slippery surface.
4. It is very resistant to absorbing moisture.
5. Polypropylene has good chemical resistance over a wide range of bases and acids.

6. It possesses good fatigue resistance.
7. Polypropylene has good impact strength.
8. Polypropylene is also a good electrical insulator **[27]**.

I.4.2 Drawbacks of polypropylene

1. Polypropylene has a high thermal expansion coefficient which limits its high temperature applications.
2. It is susceptible to UV degradation.
3. Polypropylene has poor resistance to chlorinated solvents and aromatics.
4. It is known to be difficult to paint as it has poor bonding properties.
5. Polypropylene is highly flammable.
6. It is susceptible to oxidation **[27].**

I.4.3 Applications of polypropylene

Polypropylene is widely used in various applications due to its good chemical resistance and weldability. Some common uses of polypropylene include:

1. Packaging Applications

Good barrier properties, high strength, good surface finish, and low cost make polypropylene ideal for several packaging applications.

a. **Flexible packaging.** PP films' excellent optical clarity and low moisture-vapor transmission make it suitable for use in food packaging. Other markets include shrink-film overwrap, electronic industry films, graphic arts applications, and disposable diaper tabs and closures. PP film is available either as cast film or bi-axially orientated PP (BOPP).
b. **Rigid packaging.** PP is blow molded to produce crates, bottles, and pots. PP thin-walled containers are commonly used for food packaging.

2. Consumer goods. Polypropylene is used in several household products and consumer goods applications, including translucent parts, house wares, furniture, appliances, luggage, and toys.

3. Automotive applications. Due to its low cost, outstanding mechanical properties, and moldability, polypropylene is widely used in automotive parts. Main applications include battery cases and trays, bumpers, fender liners, interior trim, instrumental panels, and door trims. Other key features of automotive applications of PP include low coefficient of linear

thermal expansion and specific gravity, high chemical resistance and good weatherability, processability, and impact/stiffness balance.

4. Fibers and Fabrics. A large volume of PP utilized in the market segment known as fibers and fabrics. PP fiber is utilized in a host of applications including raffia/slit-film, tape, strapping, bulk continuous filament, staple fibers, spun bond and continuous filament. PP rope and twine are very strong and moisture resistant very suitable for marine applications.

5. Medical Applications. Polypropylene is used in various medical applications due to its high chemical and bacterial resistance. Also, the medical grade PP exhibits good resistance to steam sterilization. Disposable syringes are the most common medical application of polypropylene. Other applications include medical vials, diagnostic devices, petri dishes, intravenous bottles, specimen bottles, food trays, pans, pill containers **[28].**

I.5 Thermoplastic elastomers from Rubber/Plastics blends

Thermoplastic elastomers combine the service properties of elastomers with the processing advantages of thermoplastics. This combination of properties can be obtained through the simultaneous presence of soft, elastic segments that have a high extensibility and a low glass transition temperature and hard, crystallizable segments which have a lower extensibility and a high Tg value. This means that TPE properties are characterized more by their morphological behavior than by their chemical composition. The ratio of soft and hard segments determines the hardness and the modulus of elasticity and also comparable properties of TPE. The chemical nature of the soft segments has an influence on the elastic behavior and the low temperature flexibility, whilst the hard segments, which act as crosslink points, determine the heat resistance, the strength and the swelling behavior **[29].**

I.5.1 The major advantages of TPEs

1. TPEs do not require any compounding steps which are necessary for thermoset rubbers, i.e. TPE pellets itself can be used for the fabrication of products.
2. The processing of TPE is much simpler than thermoset rubbers which require multisteps for fabrication of products. This reduces the final cost of the product.
3. TPEs can be processed using thermoplastic fabrication methods such as blow moulding, heat welding and thermoforming, but are not practical for thermoset rubbers.
4. TPEs require shorter cycle times for the fabrication of a product compared to thermoset rubbers and this increases the production rate. The lower density of TPEs

compared to thermoset rubbers leads to the production of a large number of articles from a given weight. Both these factors lead to cost reduction.

5. TPE scrap can be reused with negligible loss of properties. However thermoset rubber scrap cannot be reprocessed.
6. TPEs are flexible and break at large elongation.
7. TPEs have good compression set and superior vibration damping characteristics.
8. TPEs can be reinforced with fillers such as carbon black and silica.
9. TPEs have good resistance to impact, compressive and flexural loads.
10. TPEs have high fatigue to failure resistance **[30].**

I.5.2 Drawbacks of TPEs

Countering these advantages of TPEs are certain disadvantages which must be considered:

1. Thermoplastic processing methods and equipment, foreign to the rubber industry, are required for their fabrication. TPE fabrication by a thermoset rubber processor thus requires a capital investment in thermoplastics equipment, and operators must learn how to use this equipment.
2. The good processing economics of TPEs generally need a relatively high production volume to justify the costs of molds, extrusion dies, and development effort.
3. Drying is usually required before TPE processing. This step, familiar to thermoplastics processors, is unknown in conventional rubber processing **[31].**

I.5.3 Classification of TPEs

TPEs may be rationally divided into the following classes according to their chemistry and morphology:

1) Poly (Styrene-Butadiene-Styrene) (TPE-S)

2) Thermoplastic Polyolefin (TPE-O or TPO)

3) Thermoplastic Vulcanizates (TPE-V or TPV)

4) Thermoplastic Polyurethanes (TPE-U or TPU)

5) Thermoplastic Polyesters (TPE-E)

6) Melt Processable Rubber (MPR) **[32].**

I.5.4 Factors determining the properties of TPEs

The properties of TPEs are determined by a number of factors, which depend on the material properties of the rubber and plastic components. These include:

1. Dynamic shear modulus or Young's modulus: This property is a measure of the stiffness of the polymer.
2. Tensile strength of the hard phase material: This property represents a limit for the strength of TPE.
3. Critical surface tension for wetting: The difference between the critical surface tension for wetting (for the rubber and plastic) is a rough estimate of the interfacial tension between the rubber and the plastic during melt mixing. The interfacial tension is an important factor that determines the extent of phase heterogeneity. It has been found that blends in which the surface energies of the rubber and plastic are closely matched are strong and extensible.
4. Crystallinity: The ultimate strength of rubber-plastic blends shows a definite dependence on the crystallinity of the plastic material component, which improves both mechanical integrity and elastic recovery.
5. Melt viscosity: it has been accepted that melt blending is most efficient (i.e. capable of giving the smallest particles of dispersed phase) when the viscosities of the phases are the same **[33].**

I.6 Thermoplastic vulcanizates

Thermoplastic vulcanizates (TPVs) are prepared by a dynamic vulcanization technique by adding curatives during the mixing operation. The TPVs consist of the dispersion of vulcanized rubber domains in the thermoplastic matrix, which differs from the simple blends. The dynamic vulcanization occurs through two stages: first, blending without crosslinking or simple blending, and second, a superimposed crosslinking and mixing. The viscosity plays a significant role on the formation of TPV morphology. When the degree of vulcanization is high, the rubber particles may be broken into micron size of elastomeric particles. The dynamic vulcanization of the rubber phase in the plastic matrix leads to the formation of materials with improved properties of high elasticity, while the thermoplastic phase provides the melt processing characteristics. Varieties of TPVs have already found commercial applications, especially in the automotive sector **[34-36].**

In the first blending step, the morphology of both phases changes to a co-continuous structure (**Figure I.8** (**a**)). The continuous mixing leads to formation of smaller grains of the co-continuous structure under the action of shear and elongational stresses on a highly viscous co-continuous structure (**Figure I.8** (**b**)). After addition of the curatives, the viscosity of the rubber phase quickly increases and the co-continuous structure is deformed by a shearing process (**Figure I.8** (**c**)). The break-up mechanism of the highly deformed co-continuous structure happens after the blend reaches a critical stress from increased viscosity, which results in the dispersion of the crosslinked rubber phase in the thermoplastic matrix. At high amount of crosslinks in the rubber, the rubber phase will break up into a finely dispersed particles morphology (**Figure I.8** (**d**) and (**e**)) **[34, 36-37].** This is the moment where the co-continuous morphology is transformed into a dispersed matrix phase, which depends on blend composition, viscosity and elasticity ratio, processing conditions and crosslinking conditions. Therefore, TPV morphology typically consists of the crosslinked rubber particles finely dispersed in the thermoplastic matrix. However, at high content of the rubber phase or rubber-rich TPV, the crosslinking is insufficient to enforce phase inversion and it is commonly difficult to separate the rubber particles in the rubber-rich TPV **[34]**.

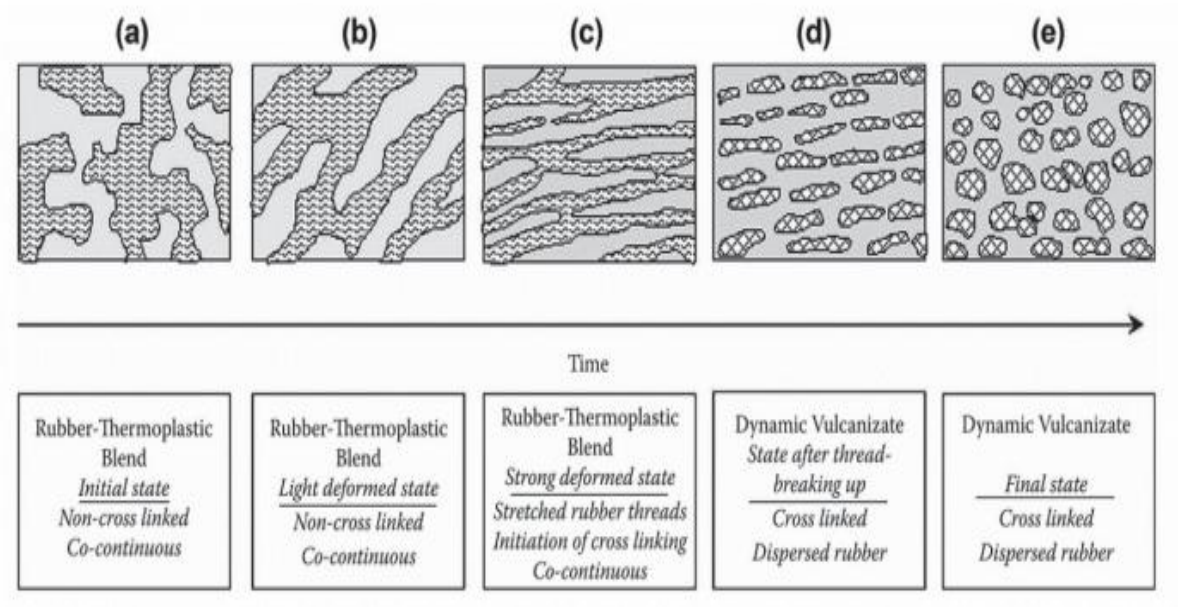

Figure I.8 Schematic diagram of morphology transformation during the dynamic vulcanization of polymer blends **[34]**.

The vulcanization system is one of the most important factor in determining the physical properties of the dynamic vulcanizates. TPVs have been extensively investigated by using various types of the vulcanization system such as a phenolic resin **[34, 38-41],** sulfur **[42, 43],** a peroxide **[44, 45],** and mixed curatives (sulfur and peroxide) **[40, 46].** Recently, the phenolic

cured system has received more attention in TPVs. This is because the fine dispersion of rubber particles in the matrix is obtained. As a consequence, improvement in mechanical properties of the TPV was achieved **[40].** The sulfur cured TPV provided superior mechanical properties in terms of tensile strength and elongation at break as compared with peroxide cure but it always gives an unpleasant smell during processing **[46].** TPV based on the peroxide cured system showed good elastic behavior in particular the compression set, heat resistance and no discoloration of the final products. However, the peroxide cured material shows a blooming effect and a decomposition of the peroxide into smelly by-products along with a β-chain scission reaction of the PP **[40, 44].** The use of multifunctional peroxide may overcome the drawbacks and provide PP-based TPV with appropriate mechanical properties **[47, 48].**

I.7 Thermoplastic Natural Rubber blends

Thermoplastic Natural Rubber blends are a group of thermoplastic elastomers prepared by blending NR with thermoplastics in various proportions. There are several types of thermoplastics that could be used to prepare TPNRs. They include polystyrene **[49],** polypropylene **[50],** high density polyethylene **[51],** linear low density polyethylene **[52-53],** poly(methyl methacrylate) **[54],** and polyamide **[55].**

I.7.1 Natural Rubber-Polypropylene blends

Natural Rubber-Polypropylene blend is the most widely studied system and it is synonymous with TPNR. PP is considered to be the best choice for blending with NR due to its high softening temperature which is about 150°C and low glass transition temperature, about - 60°C for the blend, giving rise to a very versatile thermoplastic applicable over a wide range of temperatures **[56,57].** NR/PP thermoplastic blend compositions can be varied to give materials of different mechanical properties ranging from a soft elastomer to a semi rigid plastic. The soft grade TPNR is produced by blends with compositions richer in rubber while the harder grades can contain up to about 30% NR. The flexural modulus of the blend is determined by NR and the grade of PP, with the homopolymer PP producing higher stiffness while the copolymer PP contributes to a greater ductility and impact strength at low temperatures.

The compatibility of NR and PP can be realised from the microstructures of the individual polymers. At the molecular level, NR and PP are incompatible which will give rise to a

two-phase blend but their solubility parameters are fairly similar and thus a stable dispersion of NR particles in a PP matrix or vice versa is possible **[58,59].** The processing temperature is between 175 and 185°C and higher temperatures are undesirable due to the possibility of oxidation of NR which becomes significant at 200°C and increases with temperature. The effect on the physical properties of TPNR is minimal but oxidation will increase the odour and may affect the ageing of the blend. To overcome incompatibility and produce a homogenised blend, the mixing of the two polymers during blending requires an agent that can induce interactions within the phases, between phases or at the interface **[60].**

In Natural Rubber processing, the normal and most effective crosslinking reagent is either elemental sulfur or sulfur donating compounds where highly crosslinked systems are desired **[61].** However, in TPNR blends, partial crosslinking in the NR phase and the formation of graft copolymers for interfacial adhesion between the NR and PP phases are required. These reactions occur during blending and are induced by the compatibilizer added. This process is categorised as reactive blending or dynamic vulcanization.

Analogous to Natural Rubber vulcanization but with only partial crosslinking within the NR phase, the curing reaction in TPNR can be affected by low concentrations of elemental sulfur or sulfur donor efficient vulcanization systems such as thiuram disulfides or dithiobismorpholine (DTM), dimaleimides, di-isocyanate derivatives and tetramethylthiuram disulfide (TMTD) **[56,62-64].**

The effects of TMTD in the presence of zinc oxide, stearic acid and 3-mercaptobenzothiazole (MBT) on the degree of crosslinking in TPNR was studied in relation to the physical properties exhibited. An improvement in the physical properties observed was related to an increase in the crosslinking density. However, surface blooming and odour resulting from residual chemicals in the TPNR were observed. Dynamic curing of NR/PP blends by a mixture containing equal amounts of TMTD, DTM and N-cyclohexyl- benzothiazole-2-sulphenamide (CBS) was also investigated and it was found that the mechanical and physical properties were optimised at about 2 phr of each component **[65].**

Addition of free sulfur caused the properties to degrade. The sulfur releasing compounds are also unsuitable to coexist with UV inhibitors (hindered amines) which are widely

used in the stabilization of PP. Morphological studies by SEM showed that crosslinking the elastomeric phase caused a change in the flow behavior of the materials which accounted for the increase in tear resistance of the sulfur-cured TPNR in comparison to the uncured system **[66].**

I.8 Theoretical aspects of compatibilization

A good compatibilizer should migrate to the interface and reduce the interfacial tension coefficient, decreasing the dispersed phase dimensions, thereby stabilizing the blend morphology and enhancing the adhesion between phases in the solid-state. Compatibilizing agents often provide additional morphology stabilization by acting as a surfactant and decreasing the interfacial surface tension. In general, the added compatibilizers, if compatible with both phases, segregate preferentially at the interface and ensure strong interfacial adhesion **[67, 68].**

A successfully compatibilized blend of moderate composition (up to 30 wt% minority component) exhibits spherical dispersed phases with consistent diameters, averaging on the micron and submicron scale. Such consistent morphologies can be achieved when the compatibilizing agent provides a steric hindrance to the dispersed phase coalescence. Compatibilizers which provide steric hindrances act as anchors for minority phase droplets in the matrix, and also serve as repulsive "springs" when two droplets are in proximity **[69].**

I.8.1 Role of compatibilizers in blending processes

Compatibilizers are macromolecular species exhibiting interfacial activities in heterogeneous polymer blends. Usually the chains of a compatibilizer have a blocky structure, with one constitutive block miscible with one blend component and a second block miscible with the other blend component. These blocky structures can be pre-made and added to the immiscible polymer blend, but they can also be generated in-situ during the blending process. The latter procedure is called reactive compatibilization, and mutual reactivity of both blend components is required.

The lower the interfacial tension, the longer the stretching of the thread will proceed, the smaller the diameter of the resulting thread will become, and, consequently, the smaller the size of the generated droplets of polymer will be. Usually, an average particle size in the sub-micron range can be achieved. In addition, the presence of compatibilizer molecules at the surface of the small generated particles prevents coalescence from occurring during

subsequent processing. Compatibilizers are thus able to generate and to stabilize a finer morphology.

Finally, provided that each block of a poly(A-b-B) compatibilizer penetrates the parent phase (A and B, respectively) deeply enough to be entangled with the constitutive chains, the interfacial adhesion is enhanced. Good interfacial adhesion is essential for stress transfer from one phase to the other one to be efficient and for cracks initiated at the interface to be prevented from growth until catastrophic failure occurs. Refinement and stabilization of the phase morphology and the enhancement of the interfacial adhesion usually upgrade an inferior and useless immiscible polymer blend to an interesting material **[70].**

I.8.2 Non-reactive compatibilization (Physical compatibilization)

Non –reactive compatibilization commonly known as physical compatibilization involves the compatibilization of immiscible blends by the addition of a third component as block and graft copolymers, which do not react with the component polymers, or homopolymers. In the compatibilization of an immiscible blend (A/B) by a symmetric copolymer A'-B' the mechanism of the action of compatibilizer can be represented in **Figure I.9**. If the block A' mixes only with A and the block B' with B, the copolymer can located at the interface as shown in the **Figure I.9 [70].**

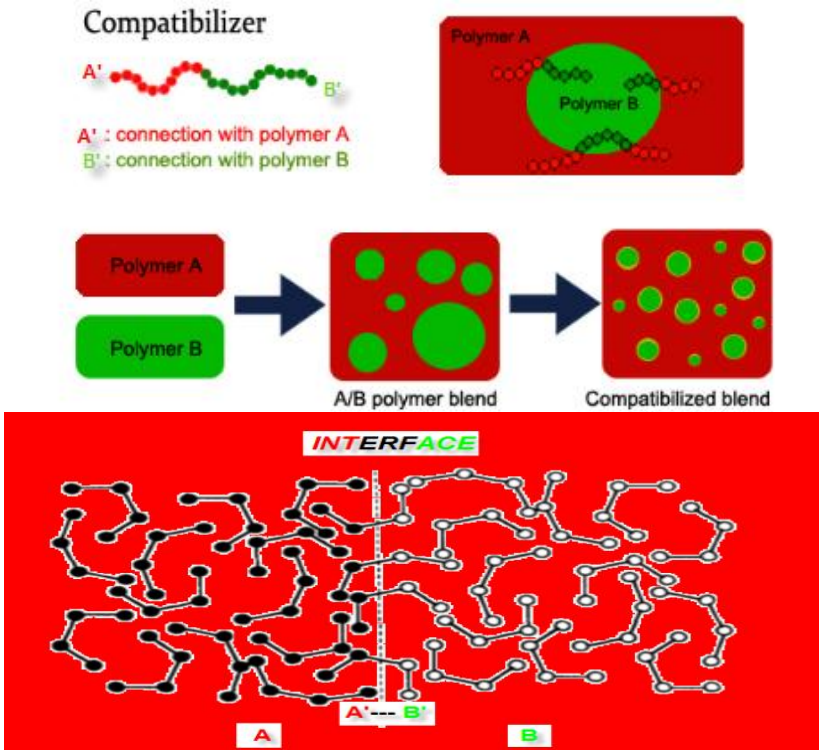

Figure I.9 Effect of compatibilizer A'-B' in the interface between the phases of two homopolymers A and B **[70].**

I.9 Literature Review

Research about TPEs, particularly that on TPNRs is very extensive. It originated in the early 1970's after the successful synthesis of SBS thermoplastic elastomers, NR producers wondering about eventual competition from synthetic rubber producers, had to develop a NR-based thermoplastic elastomer.

Many aspects of this type of material have then been investigated. These include the development of different types of TPNRs, the physical and/or chemical modification of the blend components to meet specific requirements, and the study of different systems for the dynamic vulcanization.

In this section and for the sake of illustration, a brief presentation of some of the works that have been published and which covered different aspects of the subject, will be made.

These studies are presented in a chronological order.

Kuriakose et al. **[71]** investigated the effects of blend ratio, and various vulcanizing agents namely: sulfur, peroxide, and mixed curatives (sulfur and peroxide) on the melt flow behavior of thermoplastic elastomers from Polypropylene- Natural Rubber blends. The proportion of rubber in the blend and the extent of dynamic crosslinking of the rubber phase were found to have a profound influence on the viscosity of the blends. They have found that the viscosity of the blend increased with the increase in the rubber content and the increase in the degree of crosslinking of the rubber phase.

In another publication, Kuriakose et al. **[72]** investigated also the effect of dynamic vulcanization of a 70/30 NR/PP blends on the dynamic mechanical properties. Their results indicated that the increase in storage modulus and decrease in the loss modulus becomes more remarkable as the extent of crosslinking increases.

Namita Roy Choudhury et al. **[73]** studied the thermal behaviour of natural rubber-polypropylene thermoplastic elastomeric blends by a number of different techniques including differential scanning calorimetry, thermogravimetry and dynamic mechanical analysis. EPDM and chlorinated polyethylene (CPE) were added as interfacial agents to NR/PP blends. DSC results showed a drop in the melting temperature (Tm) value with increasing rubber content. The effect of the addition of 20 Phr of an interfacial agent, like EPDM or CPE, showed similar effects. Heat of fusion (ΔHm) values exhibited a similar trend indicating increasing isolation of the crystallizable component at high rubber content. There was a 79%

drop in crystallinity with the incorporation of 70 Phr of natural rubber. They reported that the Tg of the blends was higher than that of neat NR. The elevation of Tg coupled with the depression of Tm indicated the kinetic restriction on the crystallization process. The TGA showed that the onset of degradation for neat PP was delayed with the addition of rubber. Differential thermogravimetry (DTG) curves for the blends displayed two peaks. The highest thermal stability was attained with the addition of ethylene-propylene diene rubber to the NR/PP blend. Dynamic mechanical analysis showed the existence of two *T*g values, one corresponding to the amorphous phase and the other to the polypropylene phase, indicating the incompatibility of the blends. The values of the elastic modulus also displayed a sharp change in magnitude in the vicinity of the glass transition temperature. The intensity of the damping factor (tan δ) peak was found to be governed by the overall blend crystallinity.

In another study, George et al. **[74]** have investigated the effect of blend ratio, compatibilization, and dynamic vulcanization on dynamic mechanical properties of PP/NBR blends using phenolic-modified PP (Ph-PP) and maleic anhydride grafted Polypropylene (MA-g-PP) as compatibilizers. Their results indicated that the storage modulus of the blend decreased with increase in rubber content and shows two relaxation peaks corresponding to the Tg's of PP and NBR indicating the incompatibility of the system. The addition of Ph–PP and MA-g-PP increased the interfacial adhesion between the two phases and improved the storage modulus of the blend at lower temperatures. The effect of dynamic vulcanization using sulfur, peroxide, and mixed sulfur/peroxide system on the viscoelastic behavior was also studied. Among these, the peroxide system shows the highest modulus and the sulfur system the lowest. The mixed system showed an intermediate behavior.

The melt rheological behaviour of a 60/40 Natural Rubber (NR) /poly (methyl methacrylate) (PMMA) compatibilized with Natural Rubber-grafted-poly (methyl methacrylate) (NR-g-PMMA) was investigated by Zachariah Oommen and Sabu Thomas **[75]**. The influence of dynamic vulcanization of the rubber phase on the flow behaviour and morphological properties of the blends were investigated. They have found that the dynamic crosslinking of the natural rubber phase and the addition of the compatibilizer increased the viscosity of the system and reduced the domain size of the dispersed rubber phase in the PMMA thermoplastic phase.

The properties and performance of TPE blends are critically dependent on blend morphology, and the study of this morphology in terms of compatibility between elastomer/thermoplastic

blends has received considerable attention during recent years. By the addition of a compatibilizer to incompatible elastomer/thermoplastic blends, the interfacial tension can be reduced and finer dispersion of the dispersed phase is achieved during mixing. For example, H.M. Dahlan et al, investigated the effects of liquid natural rubber (LNR) as a compatibilizer in binary blends of a 60/40 Natural Rubber/Linear Low Density Polyethylene NR/LLDPE on the thermal, dynamic mechanical and morphological properties. Special emphasis was given to the role of LNR in inducing interactions between NR and LLDPE. It was found that increasing LNR content decreases Tm and ΔHm. The decrease reflects a reduction in the degree of crystallinity of NR/ LLDPE blends. They reported also a shift in Tg of the blends to higher temperatures as observed by DMA thermograms. The compatibilizer creates better interactions between the phases leading to improvements in the compatibility of the blends. Further confirmation was obtained through SEM examination. They have found that the blends containing LNR were more homogeneous with smaller and more spherical honeycomb structures **[76]**.

In recent years, Atomic Force Microscopy (AFM) has also been widely used for the high resolution imaging of TPE surfaces. For TPE and dynamically vulcanized blends, the thermoplastic elastomer behavior is usually obtained for high concentrations of the elastomer phase, e.g., higher than 50 Phr. This single argument on the concentration of the elastomeric component has a huge consequence on the morphology. The simple blends with high elastomer content tend to form a co-continuous morphology, where both elastomer and thermoplastic constituents are interconnected throughout the whole bulk of the material . However, in dynamically vulcanized blends, the elastomer (usually the major and initially part of the co-continuous phase) becomes discontinuous and dispersed during dynamic vulcanization. Eventually, the thermoplastic becomes the continuous phase surrounding the crosslinked elastomer particles. This morphology transformation is known as phase inversion **[77].**

Hua Huang et al. **[78]** used Maleic anhydride-grafted EPDM (EPDM-g-MAH) as a compatibilizing agent for a TPV blend based on Ethylene Propylene Diene Rubber (EPDM)/ Polyamide (PA). The phase morphology of EPDM/PA TPVs was investigated by AFM. AFM images showed that, although there was a compatibilization reaction between EPDM-g-MAH and PA, phase inversion always existed for EPDM/EPDM-g-MAH/PA TPVs and the rubber phase could be finely dispersed in the PA matrix with increasing the compatibilizer content.

In another study, Riahi et al. **[79]**, investigated the effect of Hexamethylene N, N′ bis (tert-butyl peroxy carbamate) (HBTP) on the rheological behaviour of NR/PP blend. It was found that varying the HBTP concentration had a great influence on the rheological behavior as well as the dynamic and tensile properties of the material. The increase of HBTP dosage resulted in an increase of the extent of crosslinking and caused an increase of the elastic modulus and a reduction of the loss modulus.

Nakason and coworkers **[80, 81]** recently reported the effect of a PP-g-MA, and Ph-PP on the properties of TPVs based on NR-g-MA/PP blends and ENR/PP blends using a sulfur vulcanization system. They found that the blend compatibilizers promoted compatibility between the constituent components and resulted in an improvement of the mechanical properties. The increase in chemical interactions between the interfaces caused an improvement of the interfacial adhesion and led to decreasing size of the dispersed domains of the thermoplastic phase in the rubber phase.

In another study, Charoen Nakason et al. **[82]** reported also the influence of various levels of epoxide groups on the mechanical and morphological properties of a TPV based on 75/25 ENR/PP blends using Ph-PP as a compatibilizer and sulfur as a curing system. Their results indicated that the tensile strength and hardness properties increased with increasing levels of epoxide groups in the ENR molecules. They attributed these effects to chemical interactions between the methylol groups of the Ph-PP molecules and the polar functional groups of the ENR molecules. They reported also that from SEM micrographs, a finer dispersion of vulcanized rubber domains in PP matrix was observed with increasing levels of epoxide contents. This corresponds to an increasing trend of strength and hardness properties of the TPVs.

In another publication, Charoen Nakason et al. **[83]** investigated the effect of blend compatibilizers namely: HDPE-g-MA and two types of phenolic modified HDPEs (phenolic resins SP-1045 and HRJ-10518, i.e: PhSP-PE and PhHRJ-PE) on the mechanical properties of thermoplastic elastomers based on ENR/HDPE. They have found that the blend with compatibilizer exhibited superior tensile strength compared to that of the blend without compatibilizer. The ENR and HDPE interaction via the link of compatibilizer molecules was the polar functional groups of the compatibilizer with the oxirane groups in the ENR molecules. Also, another end of the compatibilizer molecules (i.e., HDPE segments) was compatibilizing with the HDPE molecules in the blend components. The blend with

compatibilizer also showed smaller phase morphology than the blend without compatibilizer. Among the three types of the blend compatibilizer, HDPE-g-MA provided the blend with the greatest strength and hardness properties but the lowest set properties.

Thitithammawong et al. **[84]** investigated the influence of various ratios of sulfur to peroxide during vulcanization on the rheological properties of Natural Rubber/Polypropylene thermoplastic vulcanizates (TPVs) blended at a fixed ratio of 60/40. The results showed that the addition of the peroxide into the mixed vulcanization system has an important effect on the properties of the TPVs as a result of two competing reactions which occur simultaneously in the natural rubber and the polypropylene phases. These are crosslinking reactions of NR molecules with different crosslink patterns, crosslink density being caused by the proportions of sulfur and peroxide curing agents and the degradation of the PP through β-chain scission. This caused significant variations in the phase morphology of the TPVs and the crystallization of the PP. Further, different trends of changes in properties were observed according to the peroxide content in the mixed vulcanization system. They have also found that a ratio of 70/30 parts of sulfur to peroxide provided a better overall balance of properties of the NR/PP TPVs than those of TPVs produced using sulfur or peroxide alone or other ratios of mixed sulfur/peroxide vulcanization systems.

The effects of blend ratios and dynamic vulcanization on the rheological, mechanical, thermal and morphological properties of thermoplastic elastomers based on Natural Rubber /Polypropylene were also investigated by Fabio Roberto et al **[85].** The TPVs were obtained by dynamic vulcanization of NR/PP using a sulfur (S)/N-tert-butyl-2-benzothiazolesulphenamide (TBBS) and tetramethylthiuram disulphide (TMTD) curative system during processing in the melt state in an internal mixer. It was reported that the dynamic vulcanization process increases the stiffness of the NR phase and modifies the rheological and thermal behavior of the system compared to the behavior of the basic material PP. The crosslinked NR particles restrict the spherulitic growth and the regular arrangement of the spherulites of PP phase, decreasing the crystallinity degree. On the other hand, a reduction of mobility of the chain segments was also observed and, consequently, an increase of the Tg values. NR/PP TPVs with high content of NR showed superior mechanical performance compared to the uncrosslinked NR/PP blends in terms of tensile strength, and Young's modulus and hardness. An increase of approximately 320% in Young's modulus values was obtained for the NR70/PP30 TPE compared to uncrosslinked NR/PP 70/30.

Morphological studies revealed the formation of large aggregates of NR domains in NR/PP TPEs which increased in size with an increase of the rubber content.

Samia Benmesli and Farid Riahi **[86]** investigated the effects of a chemically modified NR/PP thermoplastic elastomer blend on the dynamic mechanical and thermal properties. They reported that, the dynamic mechanical analysis showed an increase of the glass transition temperature by 5 °C and a disappearance of the β transition peak for NR-g-MAH/PP-g-MAH with respect to the unmodified NR/PP blend. The DSC analysis showed a slight increase of the fractional crystallinity of polypropylene for the dynamically vulcanized and grafted blends, and for whom these effects are due to the enhancement of the interactions that developed between the two polymers as a result of the grafting.

In another publication, Harekrishna Panigrahi et al **[87]** have studied the compatibilization of a thermoplastic elastomer based on PP and epichlorohydrin rubber (ECH) using PP-g-MA as a compatibilizer. They have found that, in the absence of the compatibilizer, PP/ECH blends showed very poor mechanical properties, especially low elongation at break values and higher tension set values. This was attributed to the poor compatibility between PP and ECH. On the other hand, in the case of compatibilized PP/ECH blends, PP-g-MA acted as a strong interfacial agent between PP and ECH phases and led to an outstanding improvement in the mechanical and rheological properties. Compatibilized PP/ ECH blends showed higher mixing torque values in comparison to the incompatible PP/ECH blends due to the existence of a better interaction between PP and ECH in the presence of PP-g-MA.

References

[1] Morton, M., Ed.; *Rubber Technology*; Springer Netherlands.**1999,** Dordrecht. https://doi.org/10.1007/978-94-017-2925-3.

[2] Vaysse, L.; Bonfils, F.; Sainte-Beuve, J.; Cartault, M. Natural Rubber. In *Polymer Science: A Comprehensive Reference*; Elsevier. **2012**, 281–293. https://doi.org/10.1016/B978-0-444-53349-4.00267-3.

[3] Phinyocheep, P. Chemical Modification of Natural Rubber (NR) for Improved Performance. In *Chemistry, Manufacture and Applications of Natural Rubber*; Elsevier, **2014**; 68–118. https://doi.org/10.1533/9780857096913.1.68.

[4] Mohapatra, S.; Nando, G. B. Chemical Modification of Natural Rubber in the Latex Stage by Grafting Cardanol, a Waste from the Cashew Industry and a Renewable Resource. *Ind. Eng. Chem. Res.* **2013**, *52* (17), 5951–5957. https://doi.org/10.1021/ie400195v.

[5] Indah Sari, T.; Handaya Sa, A.; R. Maspang, D.; Bismo, S. Modification of Natural Rubber as a Resistant Material to Dimethyl Ether. *J. Appl. Polym. Sci.* **2017**, *17* (2), 53–60. https://doi.org/10.3923/jas.2017.53.60.

[6] Lal, J., Mark, J. E., Eds., *Advances in Elastomers and Rubber Elasticity*;.; Springer US: Boston, MA. **1986**. https://doi.org/10.1007/978-1-4757-1436-4.

[7] Baker, C. S. L.; Barnard, D. An Overview of the Chemical Modification of Natural Rubber. In *Advances in Elastomers and Rubber Elasticity*; Lal, J., Mark, J. E., Eds.; Springer US: Boston, MA.**1986**;175–188. https://doi.org/10.1007/978-1-4757-1436-4_10.

[8] Azhar, N. H. A.; Md Rasid, H.; M. Yusoff, S. F. Epoxidation and Hydroxylation of Liquid Natural Rubber. *JSM* **2017**, *46* (3), 485–491. https://doi.org/10.17576/jsm-2017-4603-17.

[9] Hj., S.; A. Tarawneh, Mouad.; Y. Yahya, S.; Rasi, R. Reinforced Thermoplastic Natural Rubber (TPNR) Composites with Different Types of Carbon Nanotubes (MWNTS). In *Carbon Nanotubes - Synthesis, Characterization, Applications*; Yellampalli, S., Ed.; In Tech. **2011**. https://doi.org/10.5772/16494.

[10] K. Ravindranadh and MC. Rao, Physical Properties and Applications of Conducting Polymers: An Overview, International Journal Of Advances In Pharmacy, Biology And Chemistry, IJAPBC .**2013**, Vol. 2(1).

[11] Rodgers, B., Ed.; Marcel Dekker: *Rubber Compounding: Chemistry and Applications*; New York, N.Y. **2004**,645.

[12] Janet L. Hamilton (Editor), Natural Rubber: Properties, Behavior and Applications, Series: Polymer Science and Technology. **2016**, 212.

[13] Kadir, A. Modifications of Natural Rubber. In *Progress in Pacific Polymer Science*; Anderson, B. C., Imanishi, Y., Eds.; Springer Berlin Heidelberg: Berlin, Heidelberg, **1991**; 281–282. https://doi.org/10.1007/978-3-642-84115-6_32.

[14] Borowski, T. Modifications of Natural Rubber (Hevea Brasiliensis): Production, Application and Comparison. **2015**, 33. Available online at www.worldscientificnews.com.World Scientific News .7- **2015** 20-52 EISSN 2392-2192.

[15] Hinchiranan, N.; Charmondusit, K.; Prasassarakich, P.; Rempel, G. L. Hydrogenation of Synthetic cis-1,4-Polyisoprene and Natural Rubber Catalyzed by [Ir(COD)Py(PCy_3)]PF6. *J. Appl. Polym. Sci.* **2006**, *100* (5), 4219–4233. https://doi.org/10.1002/app.23710.

[16] Tangthongkul, R.; Prasassarakich, P.; Rempel, G. L. Hydrogenation of Natural Rubber with Ru[CH CH(Ph)]Cl(CO)(PCy3)2 as a Catalyst. *J. Appl. Polym. Sci.* **2005**, *97* (6), 2399–2406. https://doi.org/10.1002/app.21922.

[17] Samran, J.; Phinyocheep, P.; Daniel, P.; Kittipoom, S. Hydrogenation of Unsaturated Rubbers Using Diimide as a Reducing Agent. *J. Appl. Polym. Sci.* **2005**, *95* (1), 16–27. https://doi.org/10.1002/app.20811.

[18] Singha, N.K., De, P.P. and Sivaram, S.. Homogeneous catalytic hydrogenation of natural rubber using RhCl(PPh3)3. *J. Appl. Polym. Sci.* **1997**,66(9): 1647-1625. https://doi.org/10.1002/(SICI)1097-4628(19971128)66:9<1647::AID-APP3>3.0.CO;2-D

[19] Udipi, K. Epoxidation of Styrene–Butadiene Block Polymers. I. *J. Appl. Polym. Sci.* **1979**, *23* (11), 3301–3309. https://doi.org/10.1002/app.1979.070231116.

[20] Ng, S.C. and Gan, L.H.. Reaction of natural rubber latex with performic acid Eur. *Polymer*. **1981**, *17*(10): 1073-1077. https://doi.org/10.1016/0014-3057(81)90030-6.

[21] Burfield, D. R.; Lim, K.-L.; Law, K.-S. Epoxidation of Natural Rubber Latices: Methods of Preparation and Properties of Modified Rubbers. *J. Appl. Polym. Sci.* **1984**, *29* (5), 1661–1673. https://doi.org/10.1002/app.1984.070290520.

[22] Ahmad, H. S.; Ismail, H.; Rashid, A. A. Tensile Properties and Morphology of Epoxidized Natural Rubber/Recycled Acrylonitrile-Butadiene Rubber (ENR 50/NBRr) Blends. *Procedia Chemistry*. **2016**, *19*, 359–365. https://doi.org/10.1016/j.proche.2016.03.024.

[23] Thiraphattaraphun, L.; Kiatkamjornwong, S.; Prasassarakich, P.; Damronglerd, S. Natural Rubber-g-Methyl Methacrylate/Poly(Methyl Methacrylate) Blends. *J. Appl. Polym. Sci.* **2001**, *81* (2), 428–439. https://doi.org/10.1002/app.1455.

[24] Derouet, D.; Tran, Q. N.; Ha Thuc, H. Synthesis of N,N-Diethyldithiocarbamate Functionalized 1,4-Polyisoprene, from Natural Rubber and Synthetic 1,4-Polyisoprene. *Eur Poly J*. **2007**, *43* (5), 1806–1824. https://doi.org/10.1016/j.eurpolymj.2007.02.036.

[25] Stern, C. On the Performance of Polypropylene: Between Synthesis and End-Use Properties, s.n.], S.l., **2005**. PhD thesis, University of Twente, Enschede .

[26] Virkkunen, V. Polymerisation of Propene with Heterogeneous Ziegler-Natta Catalyst: Active Sites and Corresponding Polypropylene Structures, [Ville Virkkunen], Helsinki, **2005**.

[27] John Ducard, Advantages and Disadvantages of Polypropylene, Blog, Plastics.**2019**. Available online at https://kempner.co.uk/2019/04/16/advantages-and-disadvantages-of-polypropylene-blog/.

[28] Tripathi D., "Practical Guide to Polypropylene", 1st edition, Rapra Technology Ltd., UK., **2002**.

[29] S. K. De, Anil K. Bhowmick .Thermoplastic Elastomers from Rubber-Plastic Blends (Ellis Horwood Series in Polymer Science and Technology). **1991**,268.

[30] Sadhan K. De and Jim R. White, Rubber Technologist's Handbook, Rapra Technology Limited Shawbury, Shrewsbury, Shropshire, SY4 4NR, United Kingdom.**2001**

[31] Drobny, J. G. *Handbook of Thermoplastic Elastomers*; PDL handbook series; PDL(Plastics Design Library)/William Andrew Pub: Norwich, NY.**2007**.

[32] Holden, G. Thermoplastic Elastomers. In *Applied Plastics Engineering Handbook*; Elsevier. **2011**; 77–91. https://doi.org/10.1016/B978-1-4377-3514-7.10006-6.

[33] Tommaso Crisenza, Thermoplastic Elastomers from Chlorinated Polyethylene/Nylon Terpolyamide Blends, Ph.D Thesis University of Milano - Bicocca Department of Materials Science. **2012.**

[34] G. O. Shonaike, G. P. Simon , Thermoplastic Rubbers via Dynamic Vulcanization, Edition: 1sr, In book: Polymer Alloys and Blends, Marcel Dekker, N.Y., USA **1999**, DOI: 10.1201/9780203742921-5.

[35] Bhadane, P. A.; Virgilio, N.; Favis, B. D.; Champagne, M. F.; Huneault, M. A.; Tofan, F. Effect of Dynamic Vulcanization on Co-Continuous Morphology. *AIChE J.* **2006**, *52* (10), 3411–3420. https://doi.org/10.1002/aic.10946.

[36] Martin, G.; Barres, C.; Sonntag, P.; Garois, N.; Cassagnau, P. Morphology Development in Thermoplastic Vulcanizates (TPV): Dispersion Mechanisms of a Pre-Crosslinked EPDM Phase. *Eur Polym J* **2009**, *45* (11), 3257–3268. https://doi.org/10.1016/j.eurpolymj.2009.07.012.

[37] Antunes, C. F.; Machado, A. V.; van Duin, M. Morphology Development and Phase Inversion during Dynamic Vulcanisation of EPDM/PP Blends. *Eur Polym J.* **2011**, *47* (7), 1447–1459. https://doi.org/10.1016/j.eurpolymj.2011.04.005.

[38] Abdou-Sabet, S., Puydak, R.C. and Rader, C.P.. Dynamically vulcanized thermoplastic elastomers. *Rubber Chem Technol* .**1996**, 69 (3): 476–494. https://doi.org/10.5254/1.3538382.

[39] Nakason, C.; Kaewsakul, W. Influence of Oil Contents in Dynamically Cured Natural Rubber and Polypropylene Blends. *J. Appl. Polym. Sci.* **2010**, *115* (1), 540–548. https://doi.org/10.1002/app.30909.

[40] Nakason, C.; Worlee, A.; Salaeh, S. Effect of Vulcanization Systems on Properties and Recyclability of Dynamically Cured Epoxidized Natural Rubber/Polypropylene Blends. *Polym Test.* **2008**, *27* (7), 858–869. https://doi.org/10.1016/j.polymertesting.2008.06.011.

[41] Machado, A. V.; van Duin, M. Dynamic Vulcanisation of EPDM/PE-Based Thermoplastic Vulcanisates Studied along the Extruder Axis. *Polymer*.**2005**, *46* (17), 6575–6586. https://doi.org/10.1016/j.polymer.2005.05.011.

[42] Nakason, C.; Tobprakhon, A.; Kaesaman, A. Thermoplastic Vulcanizates Based on Poly(Methyl Methacrylate)/Epoxidized Natural Rubber Blends: Mechanical, Thermal, and Morphological Properties. *J. Appl. Polym. Sci.* **2005**, *98* (3), 1251–1261. https://doi.org/10.1002/app.21908.

[43] Mousa, A.; Ishiaku, U. S.; Mohd Ishak, Z. A. Rheological Properties of Dynamically Vulcanized Poly(Vinyl Chloride)/Epoxidized Natural Rubber Thermoplastic Elastomers: Effect of Processing Variables. *Polym Test.* **2000**, *19* (2), 193–204. https://doi.org/10.1016/S0142-9418(98)00093-2.

[44] Thitithammawong, A.; Nakason, C.; Sahakaro, K.; Noordermeer, J. W. M. Thermoplastic Vulcanizates Based on Epoxidized Natural Rubber/Polypropylene Blends: Selection of Optimal Peroxide Type and Concentration in Relation to Mixing Conditions. *Eur Polym J.* **2007**, *43* (9), 4008–4018. https://doi.org/10.1016/j.eurpolymj.2007.06.035.

[45] Mani, S.; Cassagnau, P.; Bousmina, M.; Chaumont, P. Morphology Development in Novel Composition of Thermoplastic Vulcanizates Based on PA12/PDMS Reactive Blends. *Macromol. Mater. Eng.* **2011**, *296* (10), 909–920. https://doi.org/10.1002/mame.201000406.

[46] Nakason, C.; Wannavilai, P.; Kaesaman, A. Effect of Vulcanization System on Properties of Thermoplastic Vulcanizates Based on Epoxidized Natural Rubber/Polypropylene Blends. *Polym Test.* **2006**, *25* (1), 34–41. https://doi.org/10.1016/j.polymertesting.2005.09.007.

[47] Thitithammawong, A.; Nakason, C.; Sahakaro, K.; Noordermeer, J. W. M. Multifunctional Peroxide as Alternative Crosslink Agents for Dynamically Vulcanized Epoxidized Natural Rubber/Polypropylene Blends. *J. Appl. Polym. Sci.* **2009**, 111, 819-825. https://doi.org/10.1002/app.29129.

[48] Babu, R. R.; Singha, N. K.; Naskar, K. Dynamically Vulcanized Blends of Polypropylene and Ethylene Octene Copolymer: Influence of Various Coagents on Mechanical and Morphological Characteristics. *J. Appl. Polym. Sci.* **2009**, *113* (5), 3207–3221. https://doi.org/10.1002/app.30000.

[49] Asaletha, R.; Kumaran, M. G.; Thomas, S. Thermoplastic Elastomers from Blends of Polystyrene and Natural Rubber: Morphology and Mechanical Properties. *Eur Polym J.* **1999**, *35* (2), 253–271. https://doi.org/10.1016/S0014-3057(98)00115-3.

[50] Ibrahim, A. Thermoplastic Natural Rubber Blends. *Prog Polym Sci.* **1998**, *23* (4), 665–706. https://doi.org/10.1016/S0079-6700(97)00052-X.

[51] Pechurai, W.; Nakason, C.; Sahakaro, K. Thermoplastic Natural Rubber Based on Oil Extended NR and HDPE Blends: Blend Compatibilizer, Phase Inversion Composition and Mechanical Properties. *Polym Test.* **2008**, *27* (5), 621–631. https://doi.org/10.1016/j.polymertesting.2008.04.001.

[52] Obasi, H. C.; Ogbobe, O.; Igwe, I. O. Diffusion Characteristics of Toluene into Natural Rubber/Linear Low Density Polyethylene Blends. *Inter J Polym Sci.* **2009**, 1–6. https://doi.org/10.1155/2009/140682.

[53] Abdullah, I.; Ahmad, S.; Sulaiman, C. S. Blending of Natural Rubber with Linear Low-Density Polyethylene. *J. Appl. Polym. Sci.* **1995**, *58* (7), 1125–1133. https://doi.org/10.1002/app.1995.070580706.

[54] Oommen, Z.; Gopinathan Nair, M. R.; Thomas, S. Compatibilizing Effect of Natural Rubber-g-Poly(Methyl Methacrylate) in Heterogeneous Natural Rubber/Poly(Methyl Methacrylate) Blends. *Polym. Eng. Sci.* **1996**, *36* (1), 151–160. https://doi.org/10.1002/pen.10396.

[55] Coran, A.Y. and Patel, R.P. Thermoplastic elastomers based on dynamically vulcanized elastomer-thermoplastic blends, in thermoplastic elastomers, Holden, G., Legge, N.R., Quirk, R. and Schroeder, H.E., Eds., Hanser Publisher, New York. **1996**

[56] Elliott, D. J. and Tinker, A. J., in Proc. International Rubber Conference 198.5 Kuala Lumpur, Vol. II, ed. J. C. Rajarao and L. L. Amin. RRIM, Kuala Lumpur, Malaysia, **1986**.

[57] Tinker, A. J., Icenogle, R. D. and Whittle, I., Rubber World, **1989**, 199 (6), 25.

[58] Paul, D. R., in Polymer Blends and Mixtures, ed. D. P. Walsh, J. S. Higgins and A. Maconnachie. Martinus Nijhoff, Dordrecht, **1985**, p. 1.

[59] Rostami, S. in 3rd. Internutional Conference on Frontiers of Polymers and Advanced Materials, Kuala Lumpur, Malaysia, **1995**.

[60] Choudhury, N. R.; Bhowmick, A. K. Compatibilization of Natural Rubber–Polyolefin Thermoplastic Elastomeric Blends by Phase Modification. *J. Appl. Polym. Sci.* **1989**, *38* (6), 1091–1109. https://doi.org/10.1002/app.1989.070380609.

[61] Ikeda, Y. Understanding Network Control by Vulcanization for Sulfur Cross-Linked Natural Rubber (NR). In *Chemistry, Manufacture and Applications of Natural Rubber*; Elsevier.**2014**; pp 119–134. https://doi.org/10.1533/9780857096913.1.119.

[62] Posadas, P.; Fernández-Torres, A.; Valentín, J. L.; Rodríguez, A.; González, L. Effect of the Temperature on the Kinetic of Natural Rubber Vulcanization with the Sulfur Donor Agent Dipentamethylene Thiuram Tetrasulphide. *J. Appl. Polym. Sci.* **2010**, *115* (2), 692–701. https://doi.org/10.1002/app.30828.

[63] Mathew, C.; Mini, E.; Kuriakose, A. P.; Francis, D. J.; Amma, G. Effect of Fillers in the Binary Systems Containing TMTD-Amidinothiourea and MBTS-Amidinothiourea in NR Vulcanization. *J. Appl. Polym. Sci.* **1996**, 59(2), 365-381. https://doi.org/10.1002/(SICI)1097-4628(19960110)59:2<365::AID-APP21>3.0.CO;2-

[64] Formela, K.; Wąsowicz, D.; Formela, M.; Hejna, A.; Haponiuk, J. Curing Characteristics, Mechanical and Thermal Properties of Reclaimed Ground Tire Rubber Cured with Various Vulcanizing Systems. *Iran Polym J*. **2015**, *24* (4), 289–297. https://doi.org/10.1007/s13726-015-0320-9.

[65] Coran, A. Y. and Patel, R., U.S. Pat. Elastoplastic compositions of cured diene rubber and polypropylene, **1981**.

[66] Marturano, V.; Cerruti, P.; Ambrogi, V. Polymer Additives. *Physical Sciences Reviews* **2017**, *2* (6). https://doi.org/10.1515/psr-2016-0130.

[67] Ajitha A.R.,Sabu Thomas,Compatibilization of Polymer Blends: Micro and Nano Scale Phase Morphologies, Interphase Characterization and Properties, Book **2020**, 640 P

[68] Utracki, L. A. Compatibilization of Polymer Blends. *Can. J. Chem. Eng.* **2002**, *80* (6), 1008–1016. https://doi.org/10.1002/cjce.5450800601.

[69] Macosko, C. W.; Guégan, P.; Khandpur, A. K.; Nakayama, A.; Marechal, P.; Inoue, T. Compatibilizers for Melt Blending: Premade Block Copolymers. *Macromolecules* **1996**, *29* (17), 5590–5598. https://doi.org/10.1021/ma9602482.

[70] Cor, K.; Martin, V. D.; Christophe, P.; Robert, J. Strategies for Compatibilization of Polymer Blends. *Prog polym sci.* **1998**, *23* (4),707-757.

[71] Kuriakose, B.; De, S. K. Studies on the Melt Flow Behavior of Thermoplastic Elastomers from Polypropylene/Natural Rubber Blends. *Polym. Eng. Sci.* **1985**, *25* (10), 630–634. https://doi.org/10.1002/pen.760251009.

[72] Kuriakose, B.; De, S. K.; Bhagawan, S. S.; Sivaramkrishnan, R.; Athithan, S. K. Dynamic Mechanical Properties of Thermoplastic Elastomers from Polypropylene–Natural Rubber Blend. *J. Appl. Polym. Sci.* **1986**, *32* (6), 5509–5521. https://doi.org/10.1002/app.1986.070320619.

[73] Roy Choudhury, N.; Chaki, T. K.; Bhowmick, A. K. Thermal Characterization of Thermoplastic Elastomeric Natural Rubber-Polypropylene Blends. *Thermo Acta*.**1991**, *176*, 149–161. https://doi.org/10.1016/0040-6031(91)80270-S.

[74] Snooppy George, N. R. Neelakantan, K. T. Varughese, Sabu Thomas, Dynamic Mechanical Properties of Isotactic Polypropylene/ Nitrile Rubber Blends: Effects of Blend Ratio, Reactive Compatibilization, and Dynamic Vulcanization, Journal of Polymer Science: Part B: *Polym Phys*.**1997**,35 (14), 2309–2327. https://doi.org/10.1002/(SICI)1099-0488(199710)35:14<2309::AID

[75] Oommen, Z.; Thomas, S.; Premalatha, C. K.; Kuriakose, B. Melt Rheological Behaviour of Natural Rubber/Poly(Methyl Methacrylate)/Natural Rubber-g-Poly(Methyl Methacrylate) Blends. *Polymer*.**1997**, *38* (22), 5611–5621. https://doi.org/10.1016/S0032-3861(97)00120-1.

[76] Dahlan, H. M.; Khairul Zaman, M. D.; Ibrahim, A. The Morphology and Thermal Properties of Liquid Natural Rubber (LNR)-Compatibilized 60/40 NR/LLDPE Blends. *Polym Test*.**2002**, *21* (8), 905–911. https://doi.org/10.1016/S0142-9418(02)00027-2.

[77] Shant Shahbikian and Pierre J. Carreau, Plasticization and Morphology Development in Dynamically Vulcanized Thermoplastic Elastomers, **2015**, jeneza trdine,51000,rejeka,Croatia. https://doi.org/10.5772/59647

[78] Huang, H.; Ikehara, T.; Nishi, T. Observation of Morphology in EPDM/Nylon Copolymer Thermoplastic Vulcanizates by Atomic Force Microscopy. *J. Appl. Polym. Sci.* **2003**, *90* (5), 1242–1248. https://doi.org/10.1002/app.12629.

[79] Riahi, F.; Benachour, D.; Douibi, A. Dynamically Vulcanized Thermoplastic Elastomer Blends of Natural Rubber and Polypropylene. *Inter J Polym Mater*. **2004**, *53* (2), 143–156. https://doi.org/10.1080/00914030490267564.

[80] Nakason, C.; Saiwari, S.; Kaesaman, A. Rheological Properties of Maleated Natural Rubber/Polypropylene Blends with Phenolic Modified Polypropylene and Polypropylene-g-Maleic Anhydride Compatibilizers. *Polym Test.* **2006**, *25* (3), 413–423. https://doi.org/10.1016/j.polymertesting.2005.11.006.

[81] Nakason, C.; Wannavilai, P.; Kaesaman, A. Thermoplastic Vulcanizates Based on Epoxidized Natural Rubber/Polypropylene Blends: Effect of Compatibilizers and Reactive Blending. *J. Appl. Polym. Sci.* **2006**, *100* (6), 4729–4740. https://doi.org/10.1002/app.23260.

[82] Nakason, C.; Wannavilai, P.; Kaesaman, A. Thermoplastic Vulcanizates Based on Epoxidized Natural Rubber/Polypropylene Blends: Effect of Epoxide Levels in ENR Molecules. *J. Appl. Polym. Sci.* **2006**, *101* (5), 3046–3052. https://doi.org/10.1002/app.23926.

[83] Nakason, C.; Jarnthong, M.; Kaesaman, A.; Kiatkamjornwong, S. Thermoplastic Elastomers Based on Epoxidized Natural Rubber and High-Density Polyethylene Blends: Effect of Blend Compatibilizers on the Mechanical and Morphological Properties. *J. Appl. Polym. Sci.* **2008**, *109* (4), 2694–2702. https://doi.org/10.1002/app.28265.

[84] Thitithammawong, A.; Uthaipan, N.; Rungvichaniwat, A. The Effect of the Ratios of Sulfur to Peroxide in Mixed Vulcanization Systems on the Properties of Dynamic Vulcanized Natural Rubber and Polypropylene Blends. *J. Sci. Technol.* **2012**, 34 (6), 653-662.

[85] Passador, F. R.; Alzate Rojas, G. J.; Pessan, L. A. Thermoplastic Elastomers Based on Natural Rubber/Polypropylene Blends: Effect of Blend Ratios and Dynamic Vulcanization on Rheological, Thermal, Mechanical, and Morphological Properties. *J Macromolecular Sci, Part B* .**2013**, *52* (8), 1142–1157. https://doi.org/10.1080/00222348.2012.756323.

[86] Benmesli, S.; Riahi, F. Dynamic Mechanical and Thermal Properties of a Chemically Modified Polypropylene/Natural Rubber Thermoplastic Elastomer Blend. *Polym Test* **2014**, *36*, 54–61. https://doi.org/10.1016/j.polymertesting.2014.03.016.

[87] Panigrahi, H.; Sreenath, P. R.; Bhowmick, A. K.; Dinesh Kumar, K. Unique Compatibilized Thermoplastic Elastomer from Polypropylene and Epichlorohydrin Rubber. *Polymer*. **2019**, *183*, 121866. https://doi.org/10.1016/j.polymer.2019.121866.

Chapter II

Materials and Experimental Procedures

II.1 Introduction

The materials and experimental methods used for the present investigation are discussed in this chapter. A brief account of the material characteristics, the compatibilizers preparation and characterization of the blends is given. Different instrumentation techniques used for the characterization of the samples are explained. The different methods include spectroscopic structural analysis; melt rheological behavior, mechanical property measurements, dynamic mechanical analysis, scanning electron microscopic analysis, atomic force microscopy, differential scanning calorimetry, and thermogravimetric analysis are also given.
The section covering blend preparation is divided into two parts:

I-First part: Preparation of the thermoplastic elastomer from 70/30 NR/PP blends;

II-Second part: Preparation of the thermoplastic vulcanizate based on70/30 NR/PP systems.

It should be remembered that the main objective of this work is to:

1- Study the effect of the incorporation of two types of compatibilizing agents (i.e: ENR_{25}/PP-g-MA, and ENR_{50}/PP-g-MA) at different concentrations: 5, 10, and 15 Phr on the rheological, mechanical, dynamic mechanical, morphological, and thermal properties of the 70/30 NR/PP blend.
2- Study the effect of the epoxidation level: two levels of epoxidation in ENR (i.e: ENR_{25} and ENR_{50} with 25 and 50 mole % epoxide, respectively) were used to prepare the CAs-containing NR/PP blends.
3- Study the effect of dynamic vulcanization by using a sulfur donor system; namely: Tetramethylthiuram disulfide (TMTD), 4,4'-Dithiodimorpholine (DTDM) , and N-Cyclohexyl-2-benzothiazole sulfenamide (CBS).

First, a preliminary study was carried out in order to choose the best-operating conditions (mixing time, the temperature of the mixing chamber, speed of the rotors, etc.). In fact, in a previous study carried out in Institute of Polymer Science and Technology, CSIC, Madrid, it was found that the formulations with sulfur exhibit higher reversion at high temperature. So in our work, an attempt was made to design a proper formulation for the dynamic vulcanization and which would offer a longer scorch time and a lower reversion. Additionally, the cure characteristics including induction time, vulcanization rate and the reversion behavior were studied using the curing curves obtained from RPA2000. The effect of the vulcanization

system on the rheological, mechanical, dynamic mechanical, morphological and thermal properties of the TPVs was then investigated.

Taking into account the high temperature needed for mixing NR and polypropylene and the advantage of a longer time for mixing to allow a fine dispersion of the rubber phase, several curing systems were designed and the time of curing and reversion at 180ºC and the mechanical properties were measured. From the results, an optimum curing system was selected for TPV formulation.

II.2 Materials used

The characteristics of the materials used in this study are listed below:

II.2.1 Polymers

★ **Natural Rubber (NR)**

The NR was of a commercial grade and was supplied by HB Chemical (Enterprise Parkway Twinsburg, USA). The natural rubber is an SVR-CV60 grade with a density of 0.93 g/cm^3 and a Mooney viscosity M_L(1+4)100 of 60.

★ **Epoxidized natural rubber (ENR)**

The ENR grades contained either 25 or 50 mol % epoxidation (denoted furtheron ENR_{25} and ENR_{50}, respectively) were obtained from Kumpulan Guthrie Sdn.Bhd., Seremban, Malaysia. The Mooney viscosities measured at M_L (1+4) 100 °C were 110 (ENR_{25}) and 140 (ENR_{50}). Their glass transition temperatures were -47 °C, -24°C, and a density of 0.97gr/cm^3, and 1.2gr/cm^3, respectively.

★ **Polypropylene (PP)**

The Polypropylene was of commercial grade and was supplied by Entreprise Nationale des Plastiques et Caoutchoucs (ENPC, Setif), was a commercial injection molding grade (CLYRELL RC1314) from Lyon dell Basel having a density of 0.90 g/cm^3 and a melt flow index (MFI) (230°C/ 2.16 Kg) of 9 g/10 min.

★ **Poly(propylene-g-maleic anhydride) (PP-g-MA)**

Poly (propylene-g-maleic anhydride) copolymer with a MFI of 115 g/10 min at 190°C and 0.6 wt% maleic anhydride content was supplied by Aldrich Chemicals (Germany).

A full description of the polymers used is given in **Table II.1**

Table II.1 Description of the polymers used in this study.

Materials	Commercial designation	Supplier	Properties
NR	SVR-CV60	HB Chemical (Enterprise Parkway Twinsburg, USA).	Mooney viscosity M_L (1+4) = 60 at 100 °C d=0.93 gr/cm^3
ENR_{25}	Epoxyprene $_{25}$	Kumpulan Guthrie Sdn.Bhd., Seremban, Malaysia.	Mooney viscosity M_L (1+4) = 110 at 100 °C d=0.97 gr/cm^3
ENR_{50}	Epoxyprene $_{50}$	Kumpulan Guthrie Sdn.Bhd., Seremban, Malaysia.	Mooney viscosity M_L (1+4) = 140 at 100 °C d=1.2 gr/cm^3
PP	CLYRELL RC1314	Lyon dell Basell.	MFI= 9.0 gr/10 min,d= 0.90 g/cm^3
PP-g-MA	Maleic Anhydrid-grafted Polypropylene	Sigma-Aldrich ,Germany	MFI=115 g/10 min,d= 0,95 g/cm^3

II.2.2 Compatibilizers (CAs)

The compatibilizers that will be referred to as CA_{25} and CA_{50} were a 50/50 blend of ENR_{25}/PP-g-MA and ENR_{50}/PP-g-MA respectively. The CAs were prepared using a Brabender Plastograph^{EC} internal mixer preheated at 180°C, using a cam-type mixer with a rotor speed of 60 rpm.

II.2.3Chemicals

★ **Zinc oxide**

Zinc Oxide (ZnO) was used as a co-activator in the sulfur vulcanization system. It is a white powder with a density of 5.606 g/cm³. It was manufactured by Sigma-Aldrich (Germany).

★ **Stearic acid**

Stearic acid (**$C_{18}H_{36}O_2$**) was used as an activator in the sulfur vulcanization system. It is a waxy white solid with a density of 0.847 g/cm^3. It was manufactured by Sigma-Aldrich (Germany).

★ **N-cyclohexyl-2-bezonthiazole sulfenamide**

N-Cyclohexyl-2-benzothiazole sulfenamide (CBS), is an accelerator of the sulphenamides family. Its molecular formula is **$C_{13}H_{16}N_2S_2$**, and its chemical structure is given in **Figure II.1** below, and it was provided by Flexsys (Brussels, Belgium).

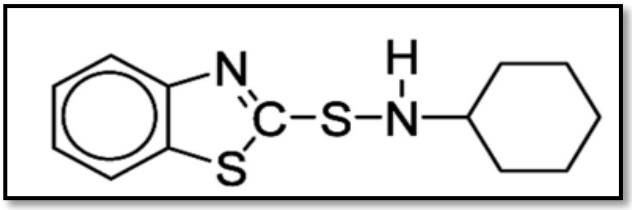

Figure II.1 Chemical structure of N-cyclohexyl-2-bezonthiazole sulfenamide.

★ **Tetramethylthiuram disulfide**

Tetramethylthiuram disulfide (TMTD) is widely used in rubber processing as an ultra accelerator of the thiuram sulphide family (**Figure II.2**). It can be used without sulphur (2 -4% on the weight of the gum) as a sulfur donor. It was manufactured by Sigma-Aldrich, Germany.

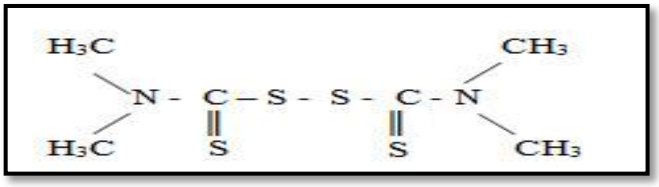

Figure II.2 Chemical structure of tetramethylthiuram disulfide.

★ **4,4'-Dithiodimorpholine**

4,4'-Dithiodimorpholine (DTDM) is mainly used as a vulcanizing agent and accelerator for natural rubber and synthetic rubber (**Figure II.3**). Under vulcanizing temperature, it can decompose as active sulfur, whose content is 27%. In crosslinking reaction, it mainly forms monosulfidic crosslinks. This product, which has the characteristic of processing safely, is usually used together with such accelerators as thiazoles, thiuram, dithiocarbamates, and it was provided by Flexsys (Brussels, Belgium).

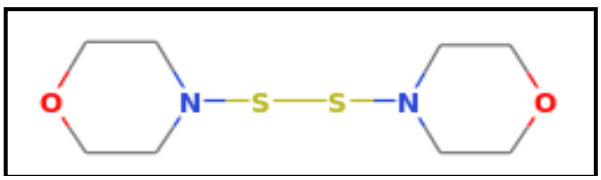

Figure II.3 Chemical structure of 4,4'-Dithiodimorpholine.

The solvents used; namely: toluene, deuterated toluene-d8, xylene, tetrahydrofuran (THF) deuteratedchloroform-d8 ($CDCl_3$), and cyclohexane were of a laboratory reagent grade material and were purchased from Sigma-Aldrich (Germany).

II.3 Experimental procedures

II.3.1 Compatibilizing agents and blends preparation

Melt mixing of CAs as well as TPE blends were carried out in a Brabender Plastograph internal mixer (model EC) with a mixing chamber of 80 cm^3 (**Figure II.4**). The mixer was heated at 180°C, and mixing was carried out using a cam-type mixer with a rotor speed of 60 rpm.

Figure II.4 Brabender Plastograph^{EC} internal mixer.

II.3.1.1 Preparation of the ENR/PP-g-MA compatibilizers (CAs)

PP-g-MA was first incorporated into the mixing chamber of a Brabender Plastograph and preheated for 5 minutes without rotation at 180°C. The polymer was then melt mixed for 3 minutes at a rotor speed of 60 rpm. ENR was then added and mixing was continued for 4 minutes. The final product was cut into small pieces.

II.3.1.2 Preparation of TPE based on NR/PP blends

In this study, all the NR/PP blends contained 70/30 rubber to plastic ratio. In a typical procedure, the control 70/30 NR/PP blend was prepared by first introducing PP in the mixing chamber and preheated for 5 minutes without rotation, and it was let to melt mixed for 2 minutes at a rotor speed of 60 rpm. Then NR was added and the two polymers were allowed to blend for 10 minutes. At the end of the mixing process, the molten mixtures were removed from the plastograph chamber, and cooled down in open air to room temperature.

The blends containing the compatibilizing agents CA_{25} and CA_{50} were prepared in the internal mixer chamber at a three-step process. First, neat PP was introduced and sheared for 2 minutes. Neat NR was then added and mixed with PP for 4 minutes. Finally, the compatibilizing agents were added and mixed for 4 minutes. The compositions and designations of the different studied TPEs are presented in **Table II.2**.

Table II.2 Compositions and designations of the different TPE blends in parts per hundred parts of rubber (phr).

Materials	**Compositions, content (phr)**								
Designations	**CA_{25}**	**CA_{50}**	**B0**	**B1**	**B2**	**B3**	**B4**	**B5**	**B6**
NR	-	-	70	70	70	70	70	70	70
PP	-	-	30	30	30	30	30	30	30
ENR_{25}/PP-g-MA	50/50	-	-	5	10	15	-	-	-
ENR_{50}/PP-g-MA	-	50/50	-	-	-	-	5	10	15

II.3.1.3 Preparation of TPV based on NR/PP blends

The dynamic vulcanized blends were prepared according to the following procedure:

First NR was masticated in a two-roll mill (Comerio Ercole S.P.A model, Busto Arsizio, Italy) at room temperature for 3 minutes before adding the vulcanizing system which consisted of ZnO, stearic acid, CBS, TMTD, DTDM (**Table II.3**). It is to be noted that it was found, after a preliminary study, that the best mechanical properties of the vulcanizates would be obtained if the above ingredients were incorporated in the listed order. The resulting paste (NR/vulcanizing ingredients (VI)) referred to as NR/VI compound was stored in a refrigerator for 12 hours in order to avoid premature vulcanization.

The 70/30 NR/PP TPVs were then prepared via dynamic vulcanization during melt mixing using a Haake Rheocord 90 at 180°C. The PP was first preheated for 5 minutes in the mixing chamber without rotation. It was then melted for 2 minutes at a rotor speed of 60 rpm. The compatibilizer was incorporated and mixed for 2 minutes. The NR/VI compound was then added and mixing was continued until a plateau mixing torque was reached. The blend products were finally pelletized and the final product was cut into small pieces.

The compositions and designations of the different TPVs studied are presented in **Table II.3**

Table II.3 Compositions and designations of the different TPV blends.

Materials	Compositions, content (phr)								
Designations	**CA_{25}**	**CA_{50}**	**B0V**	**B1V**	**B2V**	**B3V**	**B4V**	**B5V**	**B6V**
NR	-	-	70	70	70	70	70	70	70
PP	-	-	30	30	30	30	30	30	30
ENR_{25}/PP-g-MA	50/50	-	-	5	10	15	-	-	-
ENR_{50}/PP-g-MA	-	50/50	-	-	-	-	5	10	15
ZnO	-	-	5	5	5	5	5	5	5
Stearic acid	-	-	2	2	2	2	2	2	2
CBS	-	-	2	2	2	2	2	2	2
TMTD	-	-	2	2	2	2	2	2	2
DTDM	-	-	2	2	2	2	2	2	2

II.4 Moulding of samples

The samples for testing were stamped out from 1 mm thick sheets prepared by compression molding at 180°C and using an electrically heated hydraulic press (Gumix- hydraulic press Model Guix-TP 300/450/1). Teflon sheets were used to allow an easy release of mouldings. The following procedure was used:

First the sheeted blend was put into the cavity of a square mold and pressed under 50 bars for 5 minutes before lowering the pressure back. Second, without taking out the platens the pressure was raised to 150 bars and the material was pressed for 2 minutes. After releasing the pressure again, a final pressure of 200 bars was applied for 8 minutes. Finally, the cooling took place inside the hydraulic press under cold water circulation.

II.5 Characterization techniques

II.5.1 Fourier transform infrared spectroscopy (FTIR)

The FTIR spectra were obtained using a Perkin-Elmer spectrum one series equipment and the attenuated total reflection (ATR) technique was adopted. The selected spectrum resolution and the scanning range were 4 cm^{-1} and 650-2000 cm^{-1}, respectively.

FTIR samples of PP-g-MA, CA_{25}, and CA_{50} were obtained by pressing in an electric press heated at 180°C under a pressure of 150 $kg.cm^{-2}$. But for ENR_{25} and ENR_{50}, it was not possible to obtain thin films by pressing because the material, at such a high temperature,

sticks to the Teflon film used to cover the plates. As a result, the specimen were prepared using the casting method (**Figure II.5**), which consisted of dissolving small chunks (approximately 80 mg) as shown in **Figure II.5.1** in toluene at 80°C for ENR_{25} and in tetrahydrofuran (THF) at 40°C for ENR_{50} under continuous stirring for 12 h (**Figure II.5.2**). The resulting solutions were then poured on glass plates (**Figure II.5.3**), and after drying at room temperature, thin films were peeled off (**Figure II.5.4**).

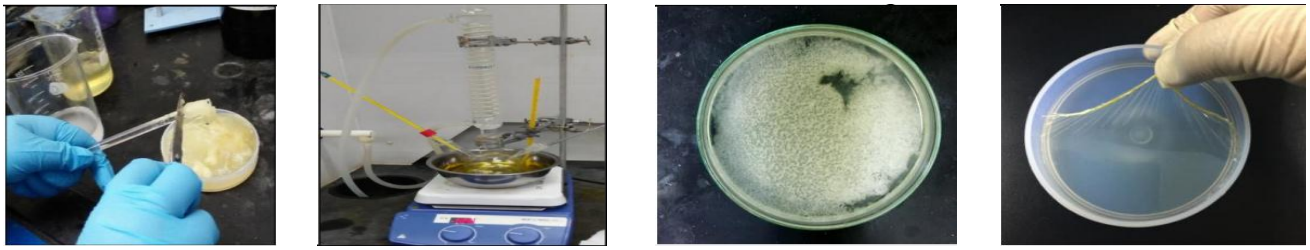

(1) (2) (3) (4)

Figure II.5 Chemical method for the preparation of thin films of ENRs.

II.5.2 Proton Nuclear Magnetic Resonance Spectroscopy (^{1}H-NMR)

The ^{1}H-NMR experiments were performed on a Bruker 400 MHz instrument operating at 400 MHz. The spectra were acquired and processed using the Mestre-Nova software. Deuterated Chloroform and Toluene-d8 were used as solvents as well as internal references $\delta\ [^1H]_{CHCl3}$= 7.26 ppm and $\delta\ [^1H]_{Toluene\text{-}d8}$= 2.08 ppm. Before analysis, a sample of PP-g-MA (about 30 mg) was dissolved in Toluene-d8 (0.7 mL) at 25°C in a 10 mm Wilmad NMR tube (Sigma-Aldrich). However, ENR_{25}, and ENR_{50} were dissolved in Deuterated chloroform $CDCl_3$.In this part also, great efforts have been made to dissolve the compatibilizing agents in many solvents, namely: toluene, deuterated toluene-d8, hot xylene, tetrahydrofuran, and deuterated chloroform-d8.Once the sample was completely dissolved, the tube was inserted in the spectrometer; the homogeneity of the magnetic field (shims) was carefully adjusted before acquisition.

II.5.3 Rheological Measurements

II.5.3.1 Brabender Plastograms

The study of the rheological behavior of CAs as well as the TPE and TPV blends was performed using the rheograms giving the variations of the torque as a function of mixing time, recorded during the blends melt mixing within the internal mixer.

II.5.3.2 Rubber Process Analyzer (RPA)

The processing characteristics of the compounds were monitored using a Rubber Process Analyzer (RPA 2000, Alpha Technologies, USA) which was used to measure the viscoelastic properties of the TPNR. This equipment operates with a temperature accuracy of ±0.1°C and can be operated with strain and frequency sweeps in wide ranges of strain amplitude and temperature. In this work, measurements were carried out following the frequency sweep method.

Approximately 4 g of each sample were charged into the measuring chamber with a bi-conical moving die (**Figure II.6**) and the rheological characteristics for TPE and TPV blends were measured at 150°C, 170°C and 190°C with an applied strain amplitude of 0.5º arc (approximately 5.02% strain). The frequency sweep ranged from 0.018 to 33.33Hz. The shear storage modulus (G'), and complex viscosity (η*) were recorded at each frequency and temperature.

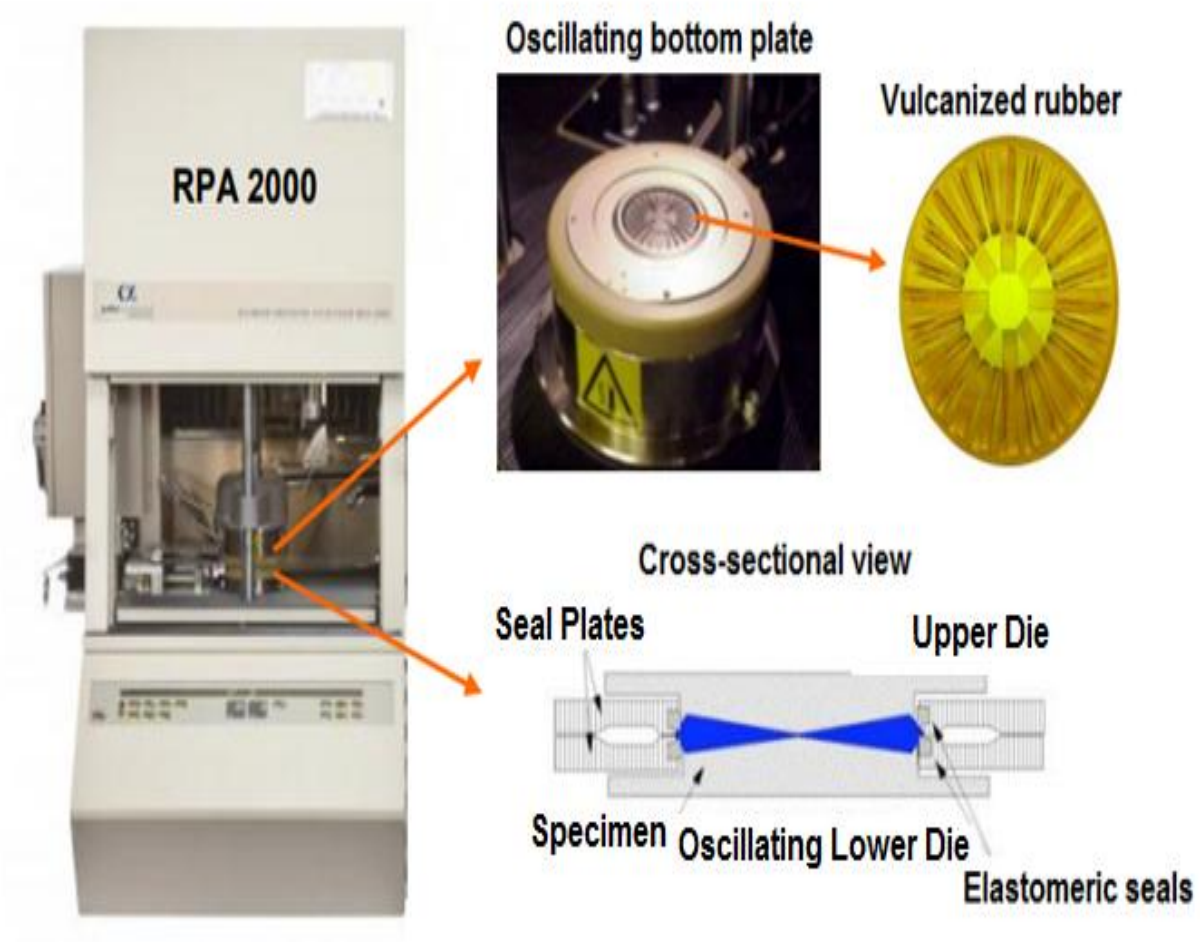

Figure II.6 Rubber Process Analyzer (RPA 2000, Alpha Technologies, USA).

II.5.4 Swelling Index

In order to characterize the extent of crosslinking for the dynamically vulcanized blends, the swelling index was determined by first measuring the weight of a sample before immersion into cyclohexane for 24 hours at room temperature. The rectangular specimen of a length of 1 cm and a width of 1 cm with a thickness of 1mm was then removed from the solvent and wiped thoroughly to remove excessive solvent and reweighed again. The swelling index was calculated as:

Swelling Index= Swollen Weight/ Original Weight.

II.5.5 Stress-Strain behaviour (Tensile Test)

The tensile test was performed on INSTRON-3366 testing machine using dumbbell specimens of Type 4 following the UNE-ISO 37 test method at a cross-head speed of 200mm/min. and the machine recorded the load-extension curve. The tensile strength was calculated as the maximum load divided by the cross-sectional area of the specimen. Average values from seven measurements were calculated for each formulation.

II.5.6 Dynamic Mechanical Thermal Analysis (DMTA)

The dynamic mechanical properties of the blends were determined using a DMA 861^E METTLER- TOLEDO equipment. Measurements of the storage modulus E', the loss modulus E" and the dissipation factor tan δ were carried out in the temperature range of-100 °C to 100 °C at a heating rate of 2°C/min. Rectangular samples (30 x 5 x1) mm^3 were vibrated in tension mode at a frequency of 1Hz and a strain amplitude of 0.2 mm.

II.5.7 Scanning Electron Microscopic Analysis (SEM)

Morphological characterization was performed using a scanning electron microscope (SEM) model SU-8000 for TPE and model XL30 Philips for TPV blends. The molded samples of the thermoplastic elastomers and thermoplastic vulcanizates were cryogenically cracked in liquid nitrogen to avoid any possibility of phase deformation. The PP phase was preferentially extracted by dissolving the fractured surface in hot xylene for 30 min. The specimens were then dried in a vacuum oven at 40°C for 12 h to eliminate the contamination of the solvent. The dried surfaces were later gold-coated and examined by scanning electron microscopy.

II.5.8 Atomic Force Microscopy (AFM)

The sheet sample was cut by a Leica EM UC6 ultra-microtome at -150ºC to obtain a flat surface for AFM analysis.

Atomic force microscopy images were taken using a Multimode AFM (Veeco Instruments Santa Barbara CA, USA) equipped with a Nanoscope Iva control system /software version 6.14r. Topographic height and phase images were recorded in the tapping mode at air, using a tip with 42 N/m of spring constant and the cantilever was oscillated at its resonance frequency of 300 kHz. Scanning was done at least at 3 different positions of each sample, at a resolution of 512x512 pixels. Samples were scanned over square regions of 2 μm size.

Analyses were performed at 25°C and the Nanoscope image processing software was employed to analyze the images.

II.5.9 Differential Scanning Calorimetry (DSC)

Differential Scanning Calorimetry (DSC) analysis was performed to characterize the thermal properties of the blend and to study the effect on the thermal transitions. The test was carried out using a METTLER-TOLEDO DSC 822^E calorimeter under nitrogen atmosphere. The weight of all samples was approximately 12 mg. The samples were programmed to be cooled at a rate of -10° C/min from 25°C to -90°C then heated at 10° C/min to 200° C in nitrogen atmosphere to eliminate previous thermal history and were held at this temperature for 5 min to ensure complete melting before starting the cooling. Cooling was carried out from 200°C to −90°C at -10°C/ min followed by second heating from −90°C to 200°C at 10°C/min.

The fractional crystallinity χ_c was calculated using the following equation, taking into account the PP content in the blends which changes depending on its content in PP-g-MA in the compatibilizing agents:

$$\chi_C(\%) = \left[\Delta H_m / \Delta H_0 \right] x \left[100 / \varphi \right] \quad \text{..... (1)}$$

Where χ_c is the percentage crystallinity of PP in the blend, ΔH_m the fusion enthalpy, ΔH_0 (209.3 J/g) is the fusion enthalpy of a 100% crystalline PP **[1]**, and φ is the weight fraction of PP in the blend.

II.5.10 Thermogravimetric Analysis (TGA)

Thermogravimetric (TGA) analysis of the samples was carried out in a nitrogen atmosphere at a heating rate of 10°C/min in a TGA instrument Q500 V20.13 BUILD 39, with a constant weighed quantity of samples in all cases (10 mg). Thermograms were recorded from room temperature to 600°C. The onset of degradation and the residue left at 600°C were then estimated. The temperature at which the rate of the mass loss is at the maximum (Tmax) was evaluated from the differential thermogravimetry (DTG) curve.

Reference

[1] Passador, F. R.; Alzate Rojas, G. J.; Pessan, L. A. Thermoplastic Elastomers Based on Natural Rubber/Polypropylene Blends: Effect of Blend Ratios and Dynamic Vulcanization on Rheological, Thermal, Mechanical, and Morphological Properties. *J Macromol Sci, Part B* .**2013**, *52* (8), 1142–1157. https://doi.org/10.1080/00222348.2012.756323.

Chapter

III

Spectroscopic Structural Analysis and Melt Rheological Properties

III.1 Introduction

Upon blending ENR with PP-g-MA, these two polymers react with each other through their functional groups. Therefore, and in order to check this possibility, Fourier-Transform Infrared Spectroscopy (FTIR) was carried out. In addition to FTIR spectroscopy, there is another technique namely Nuclear Magnetic Resonance (NMR) which was also used for structure analysis.

III.2 Fourier transform infrared spectroscopy of the CAs

Figure III.1 (**a, b, c**) shows the FTIR spectra of PP-g-MA, ENR, and ENR/PP-g-MA blend respectively. The spectrum of PP-g-MA exhibits three characteristic bands at **1854**, **1785**, and **1710 cm**$^{-1}$. The first two bands are due to the symmetric and asymmetric C=O stretching vibrations of maleic anhydride while the last one is attributed to the vibration of the C=O group of an acid function. These bands are justified by the opening of the maleic anhydride ring because of its susceptibility to undergo hydrolysis **[1]**. On the other hand, the spectrum of ENR (**Figure III. 1 b**) presents three main bands at **1250**, **875**, and **840 cm**$^{-1}$. The first two bands correspond to the stretching of the epoxide group. The band which appeared at **840 cm**$^{-1}$ corresponds to the C=C groups of the polyisoprene (NR) chain.

The spectrum of ENR/PP-g-MA indicates that all the bands assigned to anhydride groups have disappeared because of their reaction with the epoxide groups of ENR. However, the epoxy characteristic groups bands at **1250**, **875**, and **840 cm**$^{-1}$ are still present. This suggests that not all the epoxy functional groups have reacted. Moreover, a new absorption band appears at **1735 cm**$^{-1}$. This band is due to the stretching vibration of the carbonyl groups (C=O) and is attributed to the formation of an ester function. These findings demonstrate that a chemical reaction occurred between PP-g-MA and ENR.They are in accordance with the chemical reaction mechanism proposed by C. Nakason et al. **(Scheme III.1) [1]**. According to this mechanism, the maleic anhydride group in PP-g-MA undergoes ring opening under the presence of moisture (H_2O) to produce succinic acid which further reacts with the epoxy groups of ENR to form epoxidized natural rubber-grafted polypropylene characterized by an ester and acid-based crosslink. The FTIR analysis allowed therefore confirming that mixing PP-g-MA with ENR resulted in a blend which has a structure that would compatibilize the NR/PP thermoplastic elastomer.

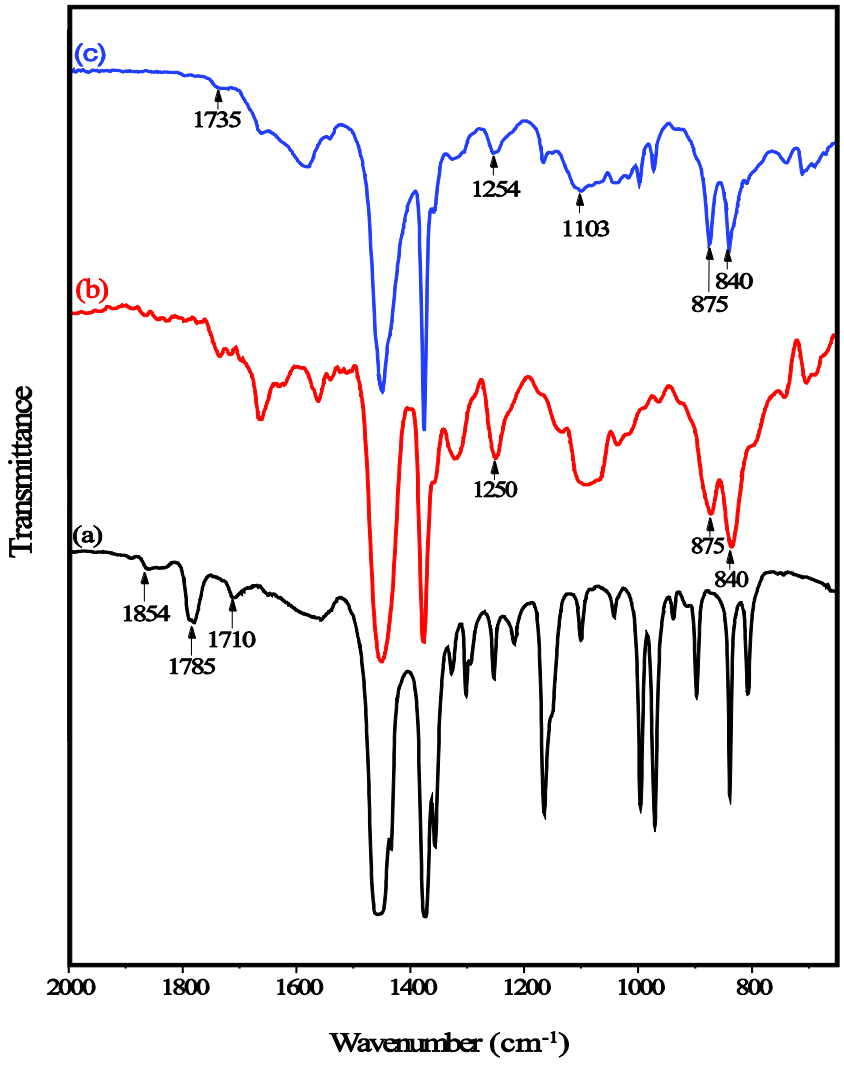

Figure III.1 FT-IR spectra of (a) PP-g-MA, (b) ENR_{25} and (c) ENR_{25}/PP-g-MA.

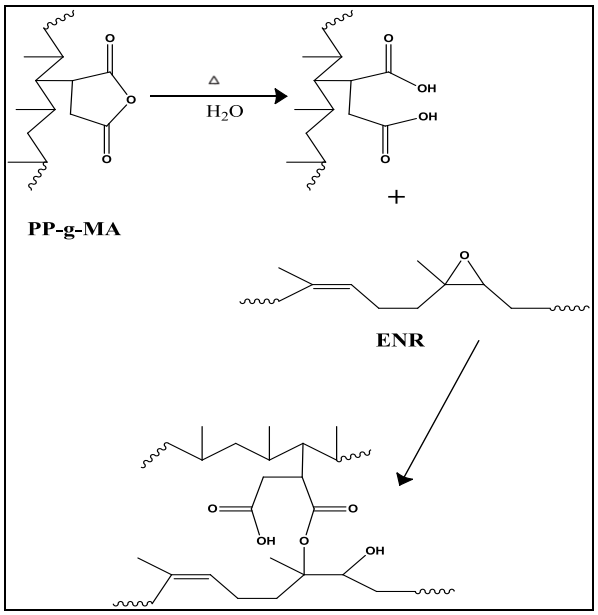

Scheme III.1 Possible mechanism of the chemical reaction between PP-g-MA and ENR molecules **[1]**.

III.3 Nuclear magnetic resonance spectroscopy of the raw materials

III.3.1 Characterization of the ENR structure

The ^{1}H-NMR technique was used to analyze the molecular structure and to determine the exact level of epoxide content in the ENRs. Deuterated chloroform ($CDCl_3$) was used to dissolve the ENR samples. The ^{1}H-NMR spectra of the ENRs are shown in **Figure III.2** and **Figure III.3** respectively. The integral values under these peaks at 2.7 and 5.1 ppm are taken to calculate the epoxide content in ENR according to Equation 2 **[2].**

$$Epoxide\ content\ (mol\%) = \frac{I_{2.7}}{I_{2.7}+I_{5.1}} \text{ x } 100 \text{..... (2)}$$

Where $I_{2.7}$ and $I_{5.1}$ are the integrals of the absorption peaks at the chemical shifts of 2.7and 5.1 ppm, respectively. In this experiment, the integrals at chemical shifts of 2.7 and 5.1 ppm were 0.44 and 1.00 for ENR_{25}; 1.26 and 1.00 for ENR_{50}, respectively.

Table III.1 presents the exact level of epoxide content that was determined by ^{1}H-NMR technique.

Table III.1 Exact level of epoxide content determined by ^{1}H-NMR technique.

Epoxidized Natural Rubber	Epoxide content (mol %)
ENR_{25}	30.55 mol% epoxide groups
ENR_{50}	55.75 mol% epoxide groups

The ^{1}H-NMR spectrum of ENR_{25} (**FigureIII.2**) shows the presence of signals at 5.1 and 2.7 ppm, assigned to the olefinic proton of cis-1,4-polyisoprenic structure and the methyne proton adjacent to the epoxide ring, respectively. The signal of methyl group adjacent to the epoxide unit was observed at 1.3 ppm. The residual unreacted unsaturation exhibited the signals of methyl and methylene protons next to the carbon– carbon double bond at 1.7 and 2.1 ppm, respectively. These results are in agreement with those of a recent work by Yokshan **[3]** and Hamzah et al **[4]**. The peak positions obtained from the ^{1}H-NMR spectrum of ENR are represented in **Table III.2**.

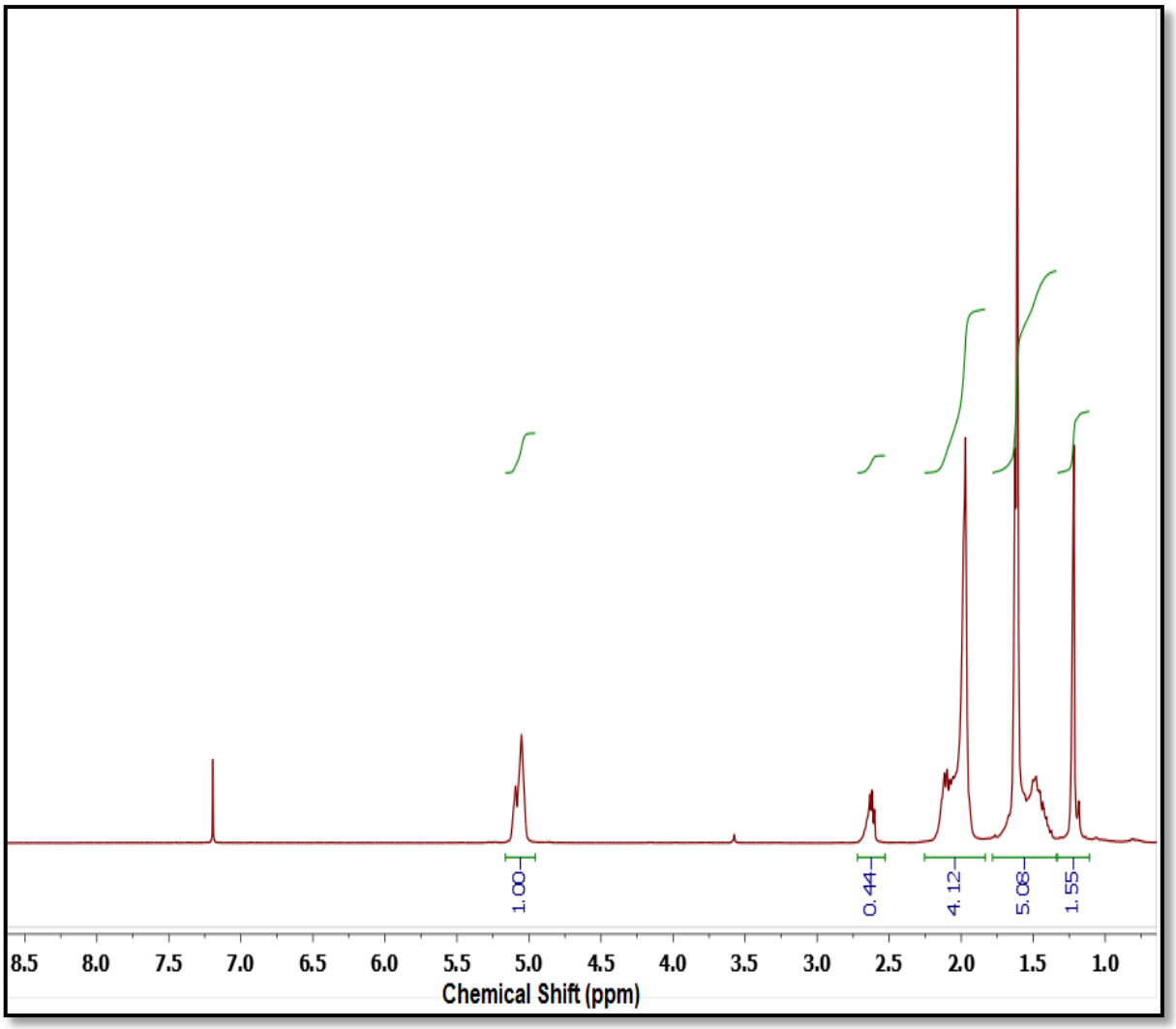

Figure III.2 ^{1}H-NMR spectrum of 25 mole% Epoxidized Natural Rubber in $CDCl_3$.

Table III.2 Peak assignments in the ^{1}H-NMR spectrum of ENR_{25}.

Peak position (ppm)	Characteristic group
1.3	Methyl of epoxy group
1.7	Methyl
2.1	Methylene
2.7	Methyne of epoxy group
5.1	Unsaturated methyne/olefinic hydrogen

The ^{1}H-NMR spectrum of the ENR_{50} which is presented in **Figure III.3**, shows the characteristic signals of methyl, methylene, and unsaturated methyne protons of cis-1,4-isoprene units appeared at 1.7, 2.1 and 5.1 ppm, respectively. It also shows two additional signals that appeared at 1.3 and 2.7 ppm which represent the methyl and methyne protons of the epoxy group, respectively.

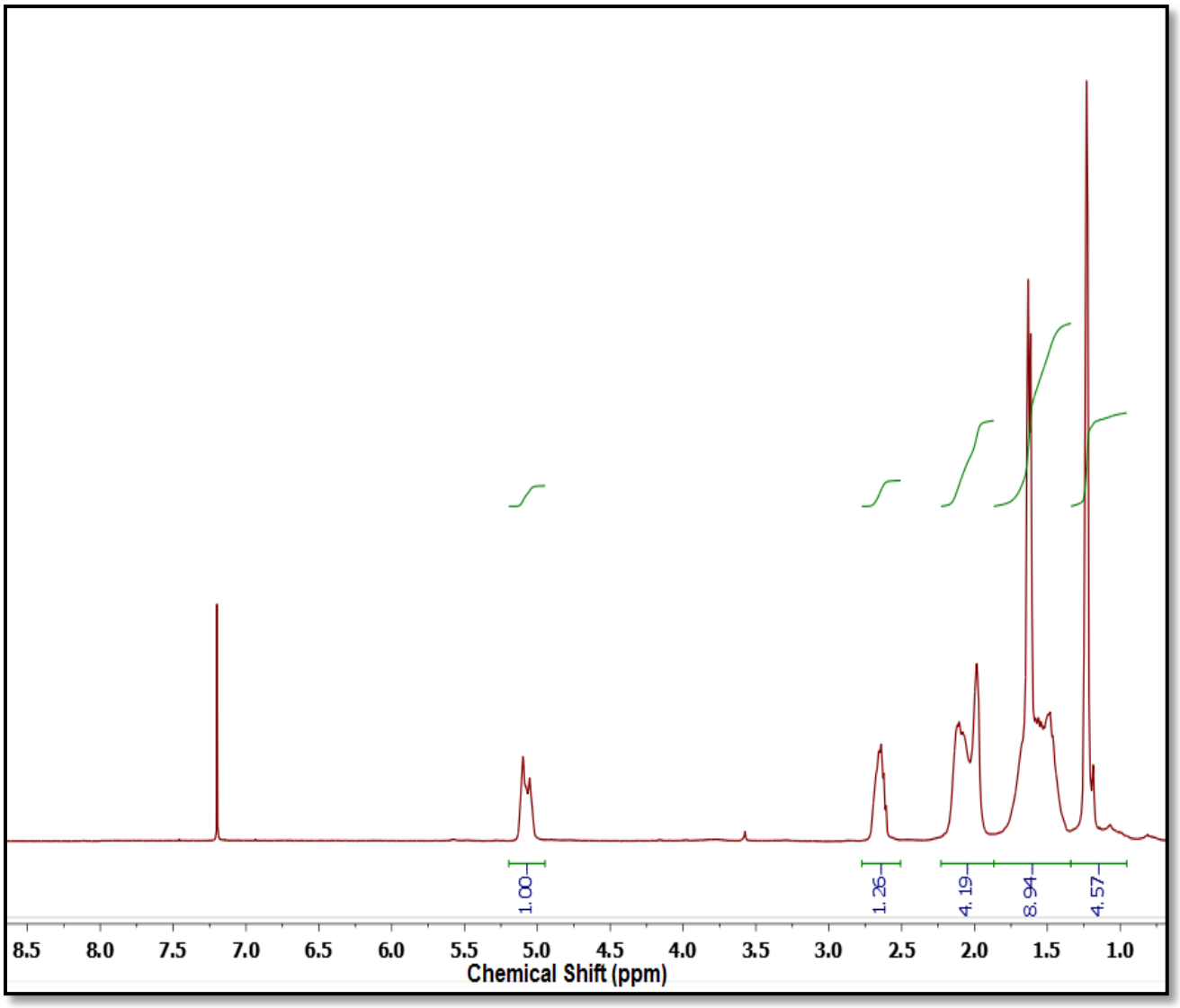

Figure III.3 ^{1}H-NMR spectrum of 50 mole% Epoxidized Natural Rubber in $CDCl_3$.

III.3.2 NMR analysis of maleic anhydride grafted polypropylene

Figure III.4 presents the ^{1}H-NMR spectrum of PP-g-MA. It shows a signal at about 7.00 ppm which is the characteristic of Toluene-d8.The succinyl functional groups of maleic anhydride are generally found in the region of 2-3 ppm. However, this peak appears in the spectrum in the region of (δ: 2.1-2.5 ppm) as a very tiny peak. In fact, it appears as a small shoulder (shown in the enlarged view) which confirms the grafting of MA on PP, but it is too small to be quantified in terms of MA grafting content. This confirms the low grafting content of 0.6 wt % reported by the PP-g-MA supplier **[5]**.

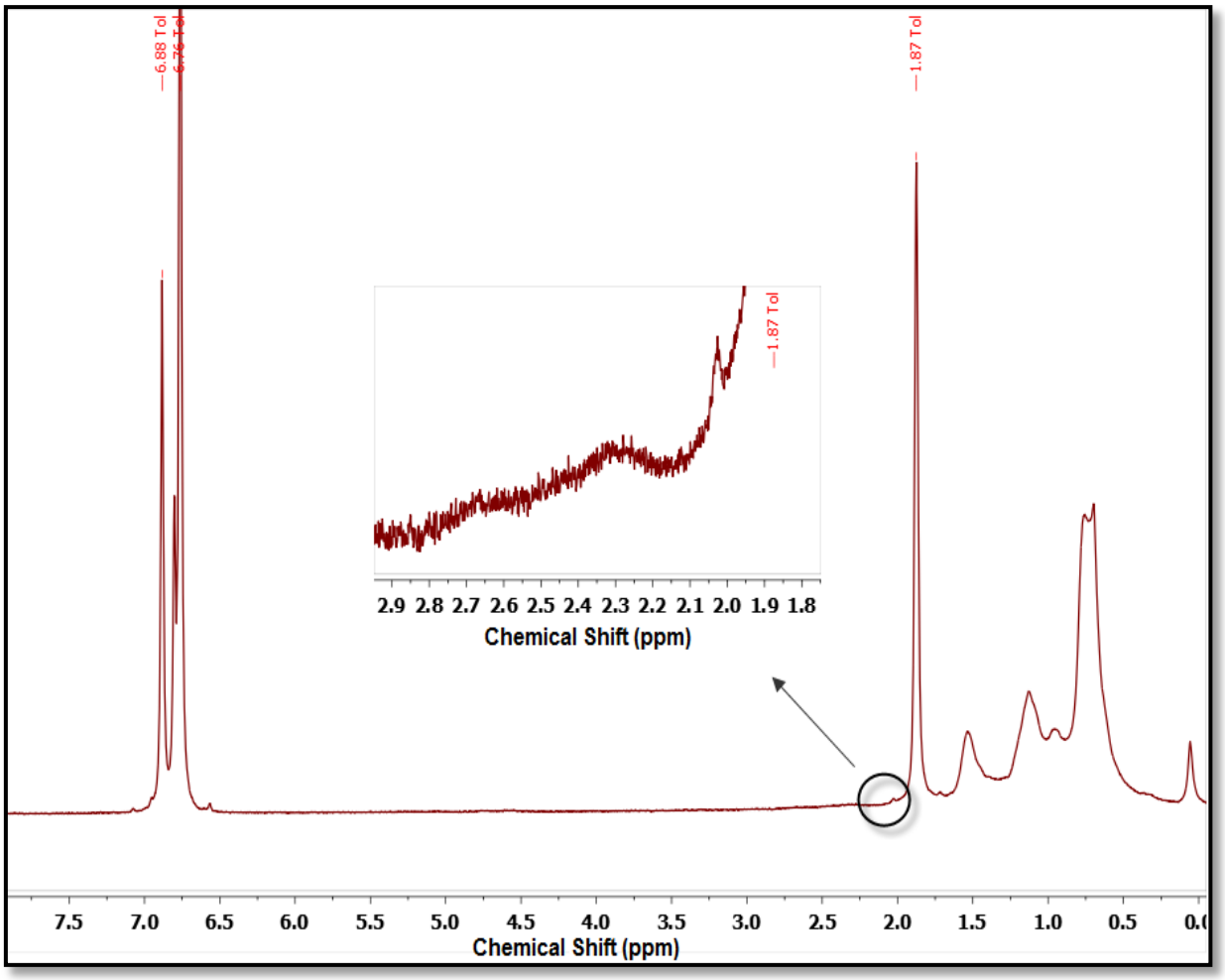

Figure III.4 ^{1}H-NMR spectra of maleic anhydride –grafted- Polypropylene in Deuterated Toluene-d8.

III.3.3 Characterization of the CAs structure

An attempt was made in order to characterize the CA structure by means of the ^{1}H-NMR analysis. However, upon the sample preparation, no solvent could dissolve this material. In fact, all the solvents including deuterated toluene-d8, deuterated chloroform-d8 ($CDCl_3$),that have been used failed to produce a single phase solution. Dissolving the CA in hot xylene (80°C) even for 48 hours produced only a swollen gel. This could confirm the fact that blending of ENR with PP-g-MA lead to a crosslinked structure.

III.4 Rheological characterization

Rheology has always been considered a strong characterization tool due to the existing highly reciprocal relationship between rheology and morphology. Generally several factors such as the intrinsic rheological properties of the constituent polymers, the interfacial properties, and eventually the presence of several additives such as compatibilizers drastically affect the rheological response of the polymeric materials **[6-17]**.

In this chapter, the results of the rheological characterization by means of the Brabender internal mixer, and the RPA will be discussed.

III.4.1 Study of the brabender plastograms

The progress of mixing and dynamic vulcanization can be appropriately followed by monitoring torque with mixing time. The variation of torque with mixing time for the unvulcanized and the dynamically vulcanized thermoplastic elastomer blends of 70/30 NR/PP are shown in the following plastograms.

III.4.1.1 Plastograms of unvulcanized NR/PP TPE blend

Figure III.5 presents the plots of the variation of the torque with mixing time for neat NR, neat PP and their 70/30 NR/PP TPE blend. The data points shown were selected from the actual Brabender plastograms. Each plastogram was obtained separately for the different blends studied. These plastograms are characterized by an initial sharp rise of the torque which corresponds to the time of the introduction of the polymer inside the mixing chamber. As the material is masticated and starts to melt the resistive torque decreases progressively until it reaches a constant level indicating a state of stabilization. It is shown that NR exhibited higher value of maximum torque than that of PP and would need a prolonged mixing time to reach a final stabilization torque, and that the plastograms of the 70/30 NR/PP blend exhibited intermediate values between those of PP and NR. This could be attributed to the fact that NR has a very high molecular weight and therefore requires mastication, compared to PP, especially the injection-molding grade used in this study with a high value of MFI, is more shear sensitive. This is reflected in the plastograms where it is observed that the decrease of the torque of neat PP, after its introduction in the mixing chamber, is much more pronounced than that of NR.

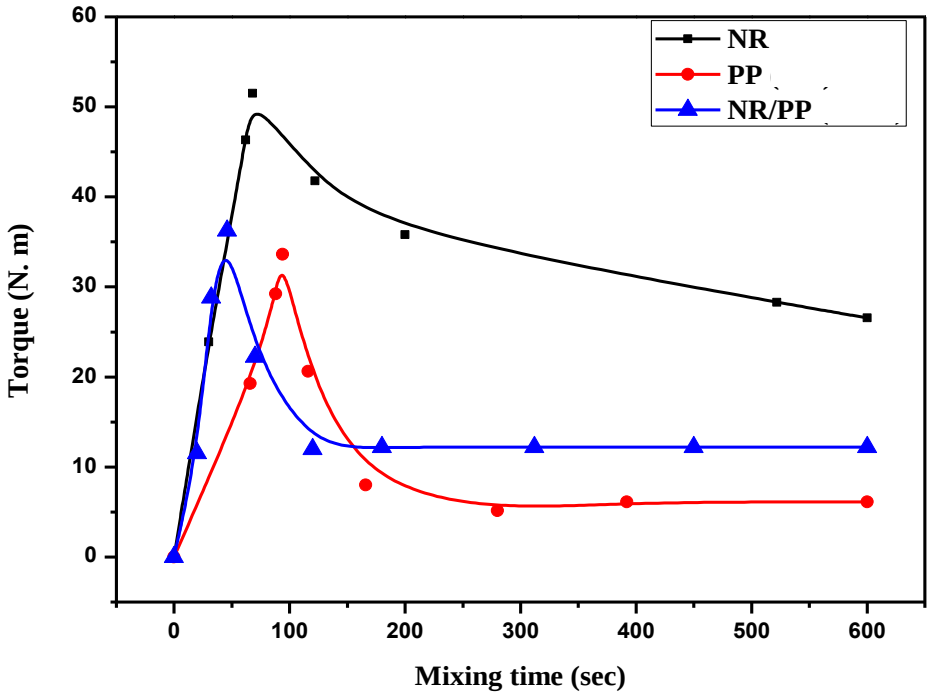

Figure III.5 Plastograms of neat NR, neat PP, and the control NR/PP TPE blend.

III.4.1.2 Plastograms of the compatibilizing agents (CA_{25}, and CA_{50})

Figure III.6 presents the plastograms for the two polymers used to prepare the compatibilizing agents CA_{25} and CA_{50}; i.e. the 50/50 blend of ENR with PP-g-MA, along with the plots of the temperature evolution that accompanies the variation of the torque with mixing time. These curves show also a similar general form as that noted for neat components (neat NR, and neat PP). That is an initial increase of the torque which corresponds to the time when PP-g-MA was first introduced in the mixing chamber, then as this polymer was sheared the torque decreased before levelling off. When ENR was added the plastograms exhibited a rapid increase followed by a slight reduction of the mixing torque. There is a second increase of the moment that follows and lasts for almost 1 min. The torque then further levels off indicating a final state of homogenization of the resulting blend. The increase of the torque that precedes the final plateau is attributed to the crosslinking reaction which took place between ENR and PP-g-MA. This means that the formation of crosslinks restricted the mobility of the polypropylene chains and those of epoxidized natural rubber and therefore increased the viscosity of the resulting CA_{25} and CA_{50} leading to a rise in the torque, which was accompanied by a rise of the temperature from 154 °C to 180 °C, and confirming hence the reaction mechanism proposed by C. Nackason and coworkers **[1]**.

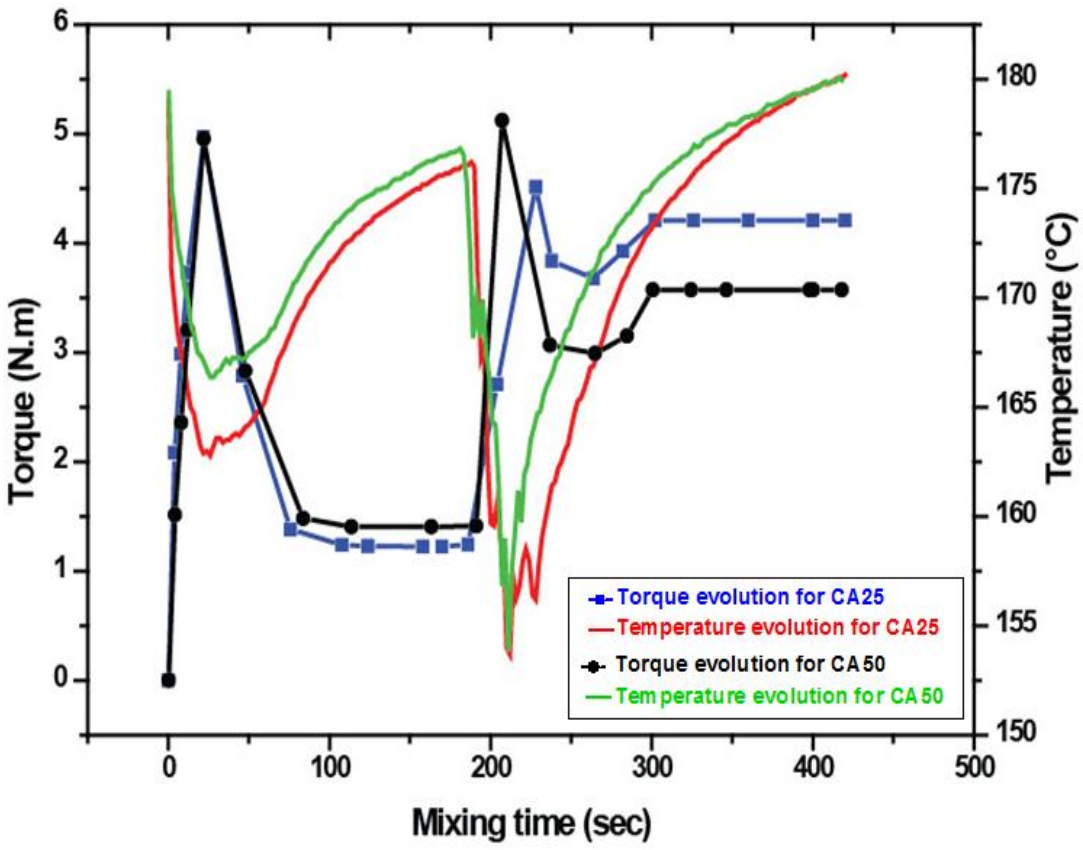

Figure III.6 Plastograms and evolution of temperature with mixing time for CA_{25}:ENR_{25}/PP-g-MA, and CA_{50}:ENR_{50}/PP-g-MA.

III.4.1.3 Plastograms of CA_{25} and CA_{50}-containing NR/PP TPE blends

Figure III.7 and Figure III.8 present the effects of the addition of CA_{25} and CA_{50} at concentrations of 5, 10, and 15 phr on the plastograms of the NR/PP/CA_{25} and NR/PP/CA_{50} respectively. We can observe that in addition to the first two peaks, which correspond to the introduction of PP, and the addition of NR respectively, there is a new third peak. Its portion where the torque increases reflects the interaction of CA_{25} and CA_{50} with PP and NR. This moderate increase could be explained by the fact that this interaction is inherent to only physical interactions that developed, on one hand between PP chains and those of the PP-g-MA present in the compatibilizing agent, and on the other hand between NR chains and those of ENR.We note also that the decrease that follows was milder in the case of CA_{50} than that in CA_{25}. This means that the higher the epoxidation level in the compatibilizing agent the softer the material gets causing a decrease of the viscosity. This behavior which is assimilated to a plastization effect is justified also by the lower value of the final torque (the plateau torque) in the case of the CA_{50}-based system compared to that in the CA_{25} modified one.

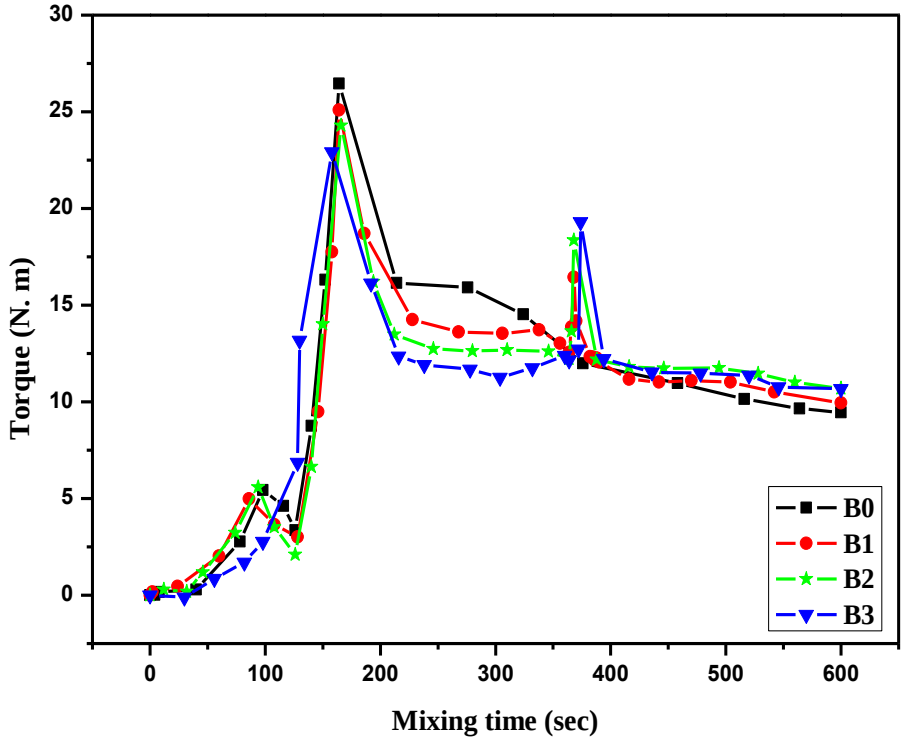

Figure III.7 Plastograms of B0: NR/PP, B1: NR/PP/CA_{25} (5 phr), B2: NR/PP/CA_{25} (10 phr), B3: NR/PP/CA_{25} (15 phr).

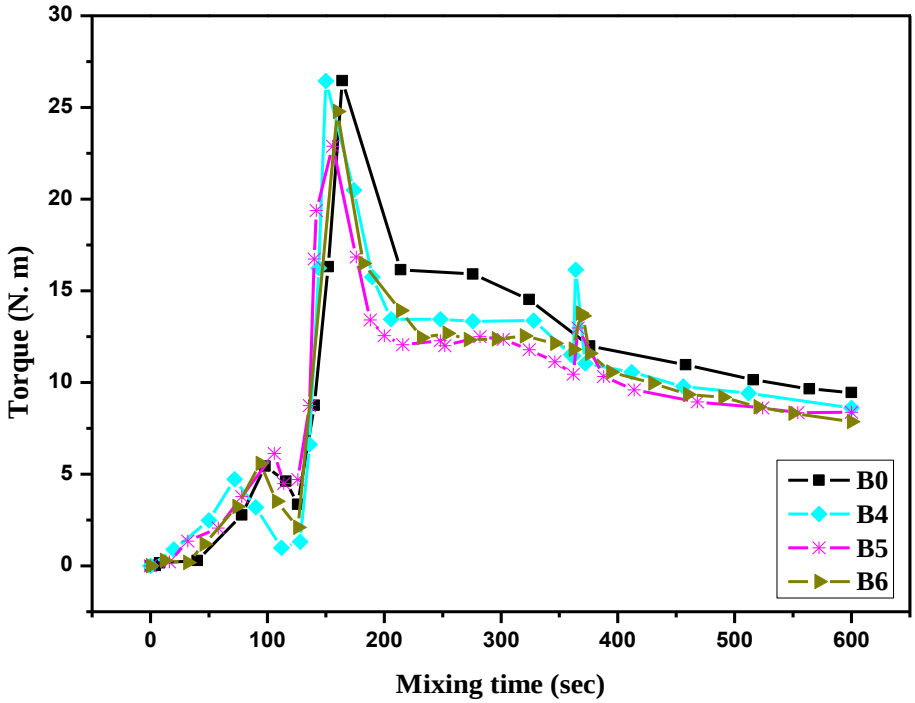

Figure III.8 Plastograms of B0: NR/PP, B4: NR/PP/CA_{50} (5 phr), B5: NR/PP/CA_{50} (10 phr), B6: NR/PP/CA_{50} (15 phr).

III.4.1.4 Plastograms of dynamically vulcanized NR/PP blends

The evolution of the torque-time curves of the dynamically vulcanized 70/30 NR/PP thermoplastic vulcanizates (TPVs) and those of the CA_{25} and CA_{50}-containing TPVs are presented in **Figures III.9, and Figure III.10**, respectively. It is to be recalled that a preliminary study was carried out in order to choose the best dynamic vulcanization system in terms of type and concentrations of the curative (See **Table II.3** in the second chapter).

These plastograms are denoted by the letters (A B C D E F G H I J K) in order to mark individual effects of the curatives and those of the CAs and taking into account the order of incorporation of each ingredient. It is to be recalled also that the different ingredients were incorporated according to the following sequence:

PP was first preheated for 5 minutes in the mixing chamber without rotation. It was then melted for 2 minutes at a rotor speed of 60 rpm. The compatibilizer was then incorporated (peak ABC) and mixed for 2 minutes. The NR compound, previously referred to as NR/VI was then added and mixing continued until a plateau mixing torque was reached. The blend products were finally pelletized.

The first peak (ABC) is due to the increase in the torque after the introduction of the cold CA into the mixer containing neat PP. Then as the CA is sheared inside the hot chamber it starts to melt and consequently the torque decreases. Upon the addition of NR/VI compound, the torque raises (CD). The torque thereafter decreases during the mixing of the whole ingredients (DE). However, with blends containing the curatives a substantial sharp increase in torque with increasing mixing time was observed (EF). This increase in torque is due to the formation of crosslinks inside the rubber phase (dynamic vulcanization) leading to greater resistance to rotation. A constant mixing torque was later observed and lasted for a mixing time of400 s (FG). A second rise of the torque (GH) was observed followed by a mild drop (HI) and another increase (IJ) before levelling off. It is clearly seen that the levels of the final mixing torque (JK) increased with increasing concentration of CAs in the compounds.

Taking into account the complexity of the system used with regard to possible chemical interactions that could take place through the functional groups present in the CA (epoxy of ENR, maleic anhydride of PP-g-MA, the ester and the acid which form upon mixing ENR with PP-g-MA), the first sharp rise of the torque (EF) could be attributed to a crosslinking reaction involving TMTD and/or DTDM. It is well established that TMTD can act as an ultra-accelerator for sulfur vulcanization as well as a sulfur donor and in this case would form

monosulfidic crosslinks. DTDM is also expected to play the same role owing to its structure which is similar to that of TMTD.

The second rather milder increase observed (GH) could be attributed to another crosslinking reaction. However, the fall of the torque (HI) that followed could be considered as a reversion, a phenomenon that indicates the instability of some of the crosslinks formed.

The last rise of the torque (IJ), which is more pronounced for the CA_{50}-based system, was observed only for the compatibilizing agent-containing blends.

Finally, it is clearly seen that the value of the final torque (JK) increased with increasing the concentration of the CA.

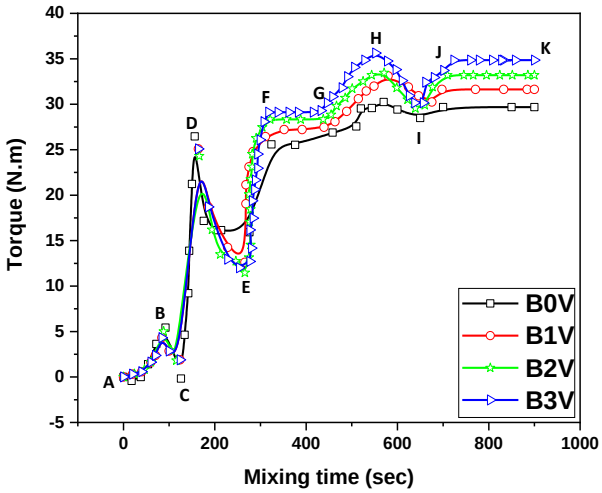

Figure III.9 Plastograms of vulcanized NR/PP, and those of theCA_{25}- containing blends with a sulfur donor-based crosslinking system.

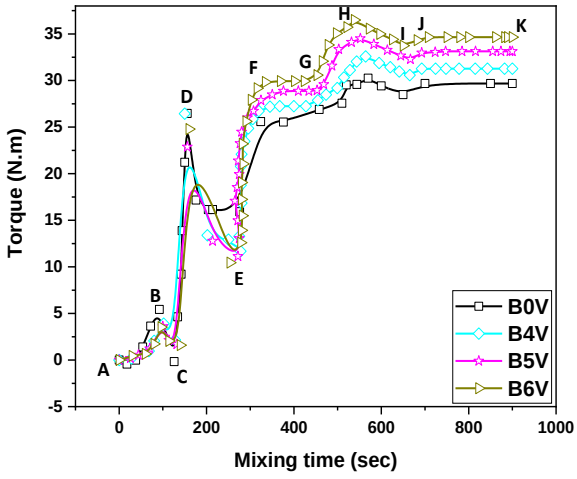

Figure III.10 Plastograms of vulcanized NR/PP, and those of the CA_{50}- containing blends with a sulfur donor-based crosslinking system.

Figure III.11, and **Figure III.12** which present the bargraphs of the final maximum torque for the CA_{25} and CA_{50} –based systems respectively, show that the TPVs exhibited higher values than those of the unvulcanized blends because of the increase of the viscosity imparted by the formation of the crosslink structure.

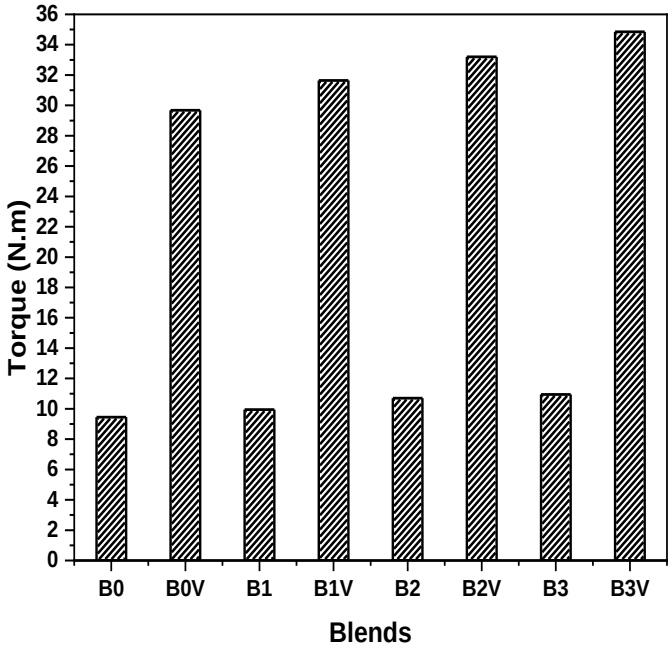

Figure III.11 Maximum torque values of vulcanized and unvulcanized blends containing the CA_{25}.

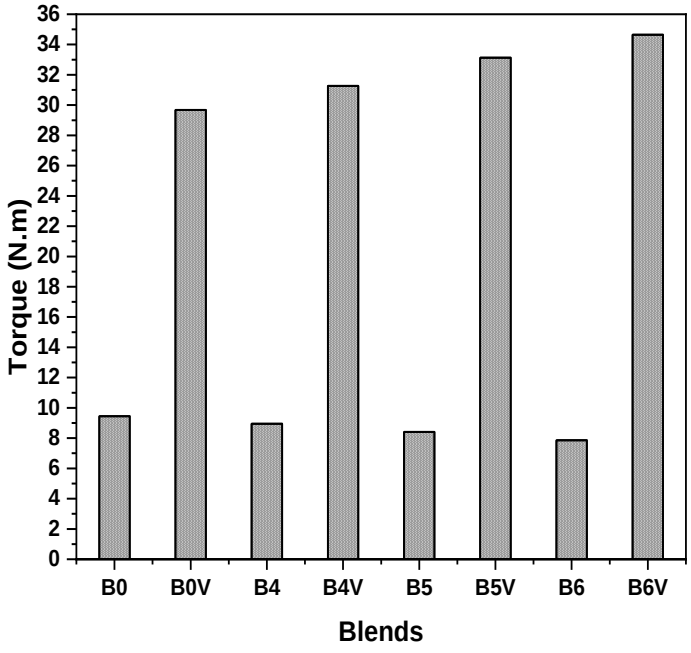

Figure III.12 Maximum torque values of vulcanized and unvulcanized blends containing the CA_{50}.

III.4.2 RPA viscoelastic properties

The RPA is a rheometer belonging to a new class of rheometers called dynamic mechanical rheological testing instruments (DMRTs). This type of rheometer allows analyzing the physical and dynamic properties of rubber compounds and monitoring the process of production of the compounds before, during and after vulcanization in versatile test configurations (wide ranges of temperatures, strains and frequencies). The measurements provide important information about processability, cure characteristics and final cured properties.

III.4.2.1 Frequency sweep of the compatibilizing agents

Figure III.13, and **Figure III.14** illustrate the complex viscosity (η*) and the storage modulus (G') of PP-g-MA, neat ENR_{25}, neat ENR_{50}, ENR_{25}/PP-g-MA and ENR_{50}/PP-g-MA at a temperature of 150°C. As shown in **Figure III.13**, it can be seen that the complex viscosity decreases continuously with increasing frequency for PP-g-MA, ENR_{25}, ENR_{50} and their blends. It is to be noted that at a given frequency, the viscosity of the 50/50 blend of either ENR_{25}/PP-g-MA or ENR_{50}/PP-g-MA is higher than that of the individual components. In addition, the values of the viscosity of ENR_{50}/PP-g-MA (CA_{50}) are higher than that of ENR_{25}/PP-g-MA (CA_{25}) indicating that the higher the epoxydation level in the CA, the higher the viscosity. This result is in favor of the crosslinking reaction which takes place between ENR and PP-g-MA as the crosslinks formed reduce the CA mobility confirming hence the previous results obtained through the brabender plastograms.

In **Figure III.14**, we can see that the storage modulus values of the parent polymers and those of the CA blends increased with the increase of the frequency. It is also clearly seen that the G' values of the CAs are higher than those of the PP-g-MA and those of ENRs at all the measured frequencies. It can be observed also that the plots of the storage modulus of the ENRs fell intermediately between those of PP-g-MA, and CAs.

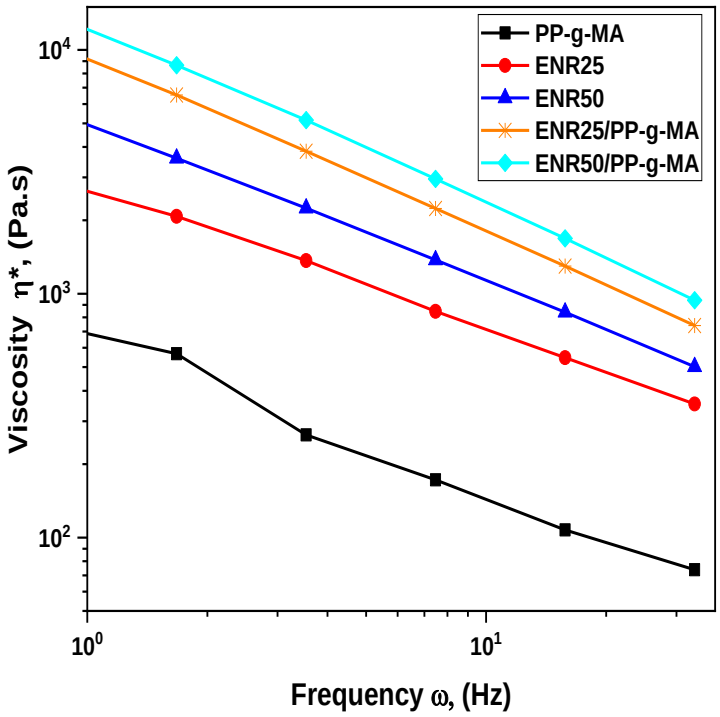

Figure III.13 Variation of complex viscosity (η*) as a function of frequency for PP-g-MA, ENR_{25}, ENR_{50} and their blends at 150°C.

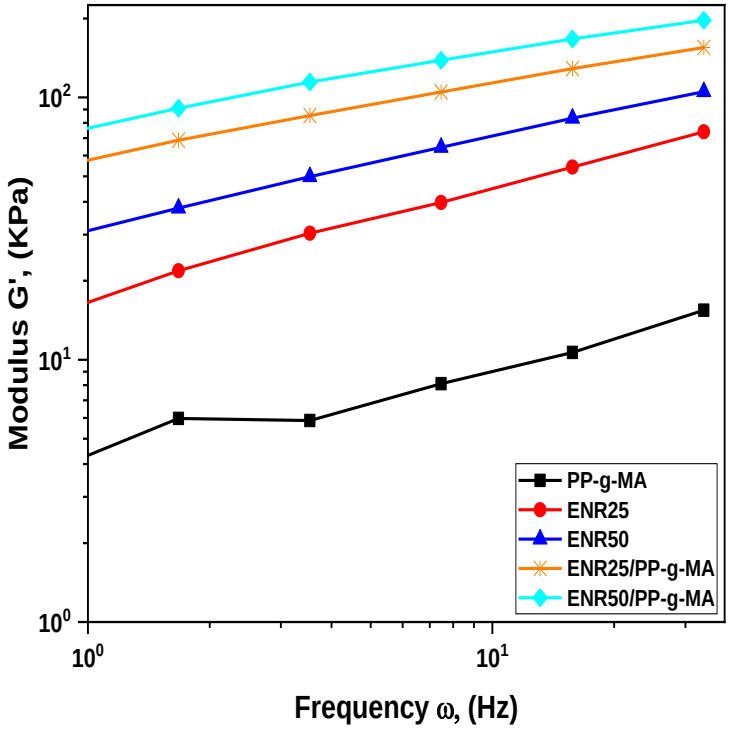

Figure III.14 Variation of storage modulus (G') as a function of frequency for PP-g-MA, ENR_{25}, ENR_{50} and their blends at 150°C.

III.4.2.2 Frequency sweep of NR/PP blend

Figure III.15 illustrates the complex viscosity of neat NR, neat PP and NR/PP blend at different temperatures (150°C, 170°C, and 190°C). As shown in **Figure III.15**, it can be seen that at a given temperature the complex viscosity decreases continuously with increasing frequency for NR, PP and their 70/30 blend. On the other hand, the plots also show that, for the three temperatures studied, the viscosity difference between the two polymers (NR, PP) narrows with increasing frequency. This is in fact a desired feature for mixing the two polymers composing the blend, for it contributes in reducing the interfacial tension between them. These results are in accordance with the observations reported by Souheng Wu **[18]**.

Figure III.16 shows the logarithmic plot of the variation of the shear storage modulus (G') with frequency for neat NR, neat PP and NR/PP blend at different temperatures (150°C,170°C, and 190°C). We can see that the G' values of NR, PP, and NR/PP blend increased with the increase of the frequency. It is also shown that the G' values of NR are higher than those of PP and 70/30 NR/PP blend at all the measured frequencies. This behavior could be attributed to the higher molecular weight of NR compared to that of PP, considering that the PP used in this study is an injection molding grade with a high value of the Melt Flow Index. It can be observed also that the plots of the storage modulus of the 70/30 NR/PP TPE blend fell intermediately between those of both polymers (NR, and PP).

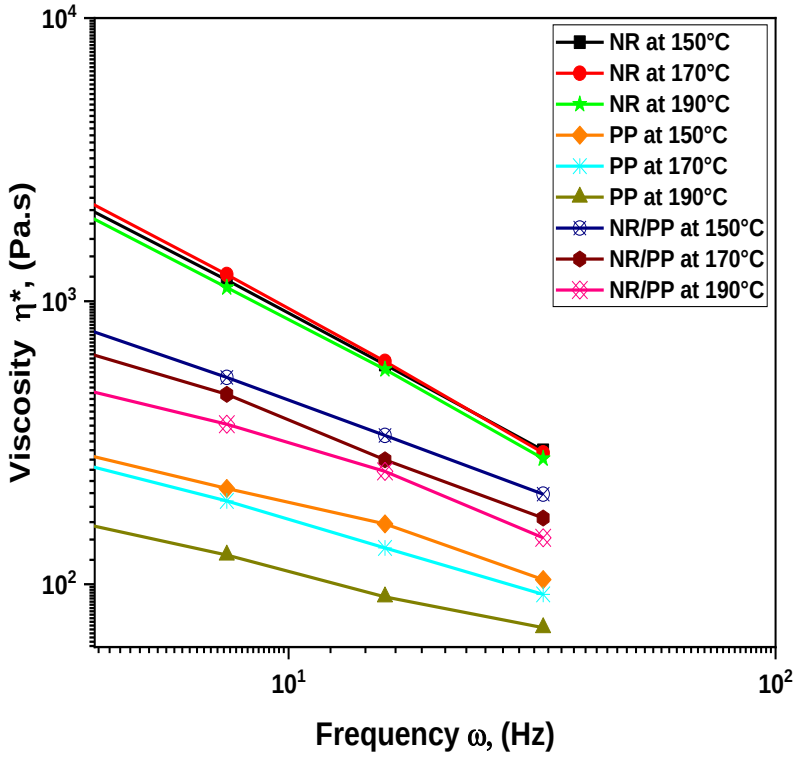

Figure III.15 Rheograph of the frequency sweep for complex viscosity (η*) of neat NR, neat PP and their 70/30 NR/PP TPE blend at different temperatures.

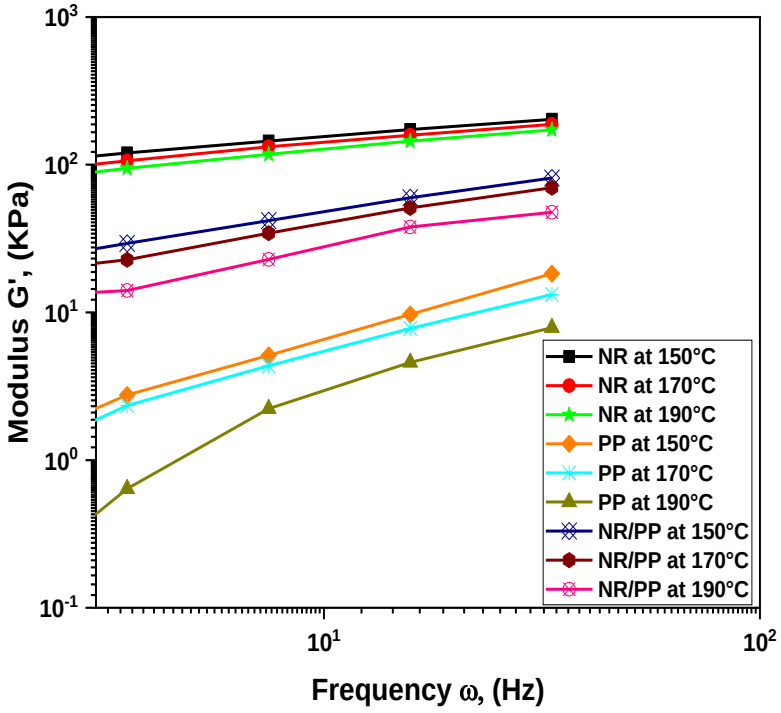

Figure III.16 Rheograph of the frequency sweep for storage modulus (G') of neat NR, neat PP and their 70/30 NR/PP TPE blend at different temperatures.

III.4.2.3 Frequency sweep of CA_{25} and CA_{50}-containing NR/PP blends

Figure III.17 through **Figure III.20** present the effects of the addition of CA_{25} and CA_{50} at concentrations of 5, 10, and 15 phr on the rheographs from the frequency sweep for the complex viscosity (η*) and the storage modulus (G') of the NR/PP/CA_{25} and NR/PP/CA_{50} at a temperature of 150°C, respectively. From **Figure III.17**, and Figure **III.19**, it is observed that for all the blends studied the same trend was obtained, i.e a decrease of the viscosity with increasing frequency. It was found that at a given frequency, the complex viscosity increases with increasing the concentration of the CA. These results are analogous to those reported in the literature by researchers who studied the effect of compatibilization on the rheological properties. It has been demonstrated that the addition of compatibilizers to polymer blends extensively affects their flow behaviour **[19-23]**. Chemical reaction occurring between the components of the blend upon compatibilization generally increases the viscosity of the system. For example, the viscosity of PP/PA blend was found to increase upon compatibilization using maleic anhydride grafted styrene-ethylene-co-butylene-styrene copolymer (SEBS-g-MA), due to the chemical reactions taking place between amine and anhydride groups **[19]**. George et al **[24]**, made a detailed investigation on the rheological behaviour of thermoplastic elastomers from PP and NBR. They have investigated the effect of blend ratio, dynamic vulcanization and compatibilization on the rheological behaviour of PP/NBR blends. They used modified PP as an effective compatibilizer which increased the viscosity of the system due to increased interaction between the phases as a result of compatibilization. The flow behaviour of PMMA/NR blends compatibilized with PMMA-g-NR was investigated by Thomas et al **[23]**. On compatibilization the viscosity of these blends was found to be increasing due to the high interfacial interaction. Joshi et al **[22]**, reported on the rheological aspects of poly (butylene terephthalate /high density polyethylene blends with a polyethylene based ionomers as the compatibilizer. Measurements showed that the shear viscosity increased for the blend with the addition of the compatibilizer.

Figure III.18, and **Figure III.20** which present the variation of the storage modulus with frequency, show that the storage modulus (G') increased with increasing frequency, and show also the same effects as those observed with the viscosity. In fact, it was found that at a given frequency, the storage modulus increases with increasing the concentration of the CA. This reflects the increased of physical interactions between NR and PP phases imparted by the compatibilizing agents.

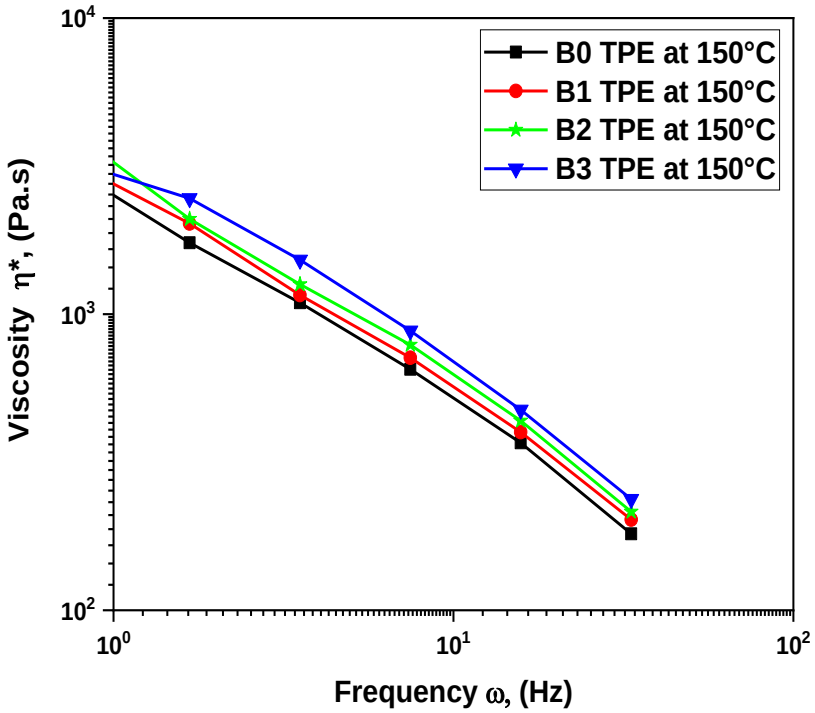

Figure III.17 Rheograph of the frequency sweep for complex viscosity (η*) of B0: NR/PP, B1: NR/PP/CA_{25} (5 phr), B2: NR/PP/CA_{25} (10 phr), B3: NR/PP/CA_{25} (15 phr) TPE blends at 150°C.

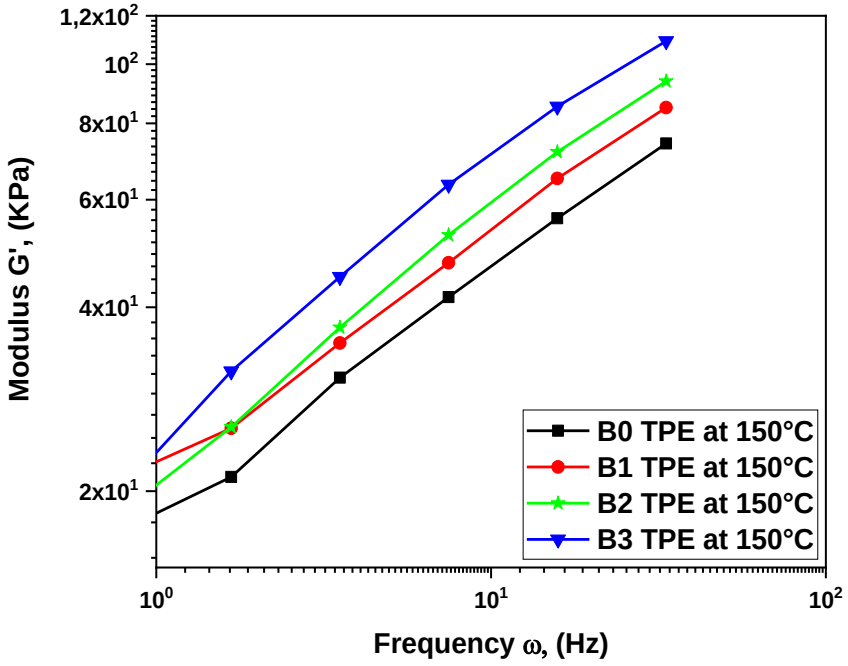

Figure III.18 Rheograph of the frequency sweep for storage modulus (G') of B0: NR/PP, B1: NR/PP/CA_{25} (5 phr), B2: NR/PP/CA_{25} (10 phr), B3: NR/PP/CA_{25} (15 phr) TPE blends at 150°C.

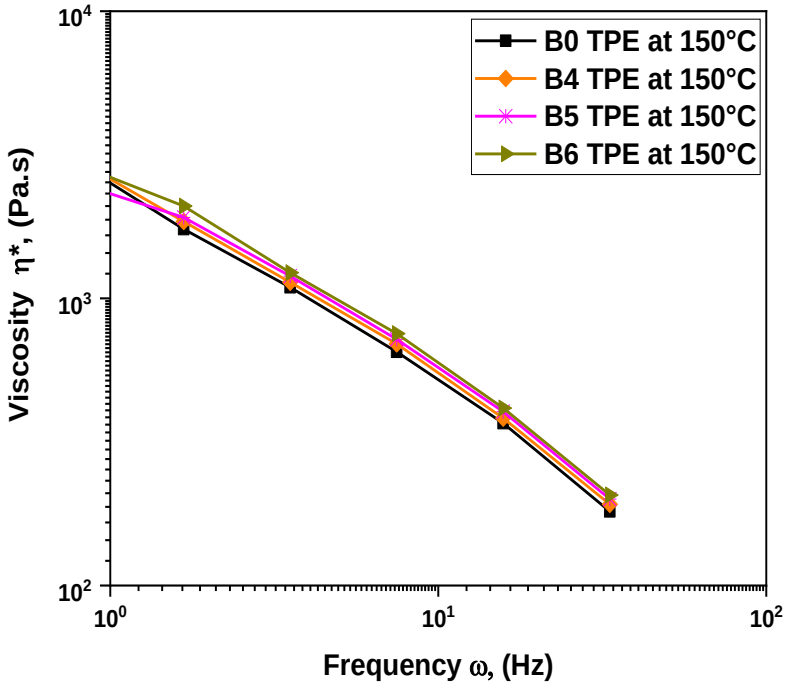

Figure III.19 Rheograph of the frequency sweep for complex viscosity (η*) of B0: NR/PP, B4: NR/PP/C_{50} (5 phr), B5: NR/PP/CA_{50} (10 phr), B6: NR/PP/CA_{50} (15 phr) TPE blends at 150°C.

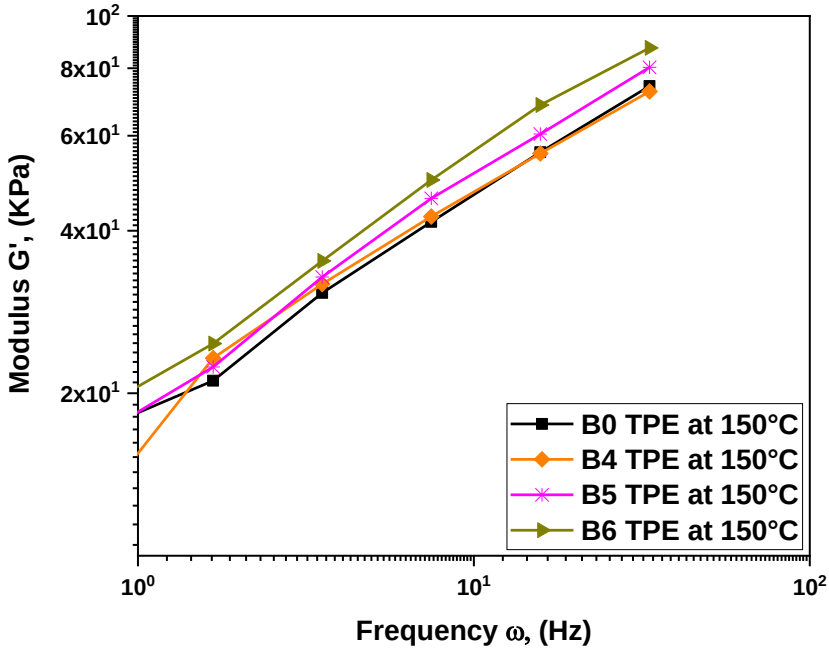

Figure III.20 Rheograph of the frequency sweep for storage modulus (G') of B0: NR/PP, B4: NR/PP/CA_{50} (5 phr), B5: NR/PP/CA_{50} (10 phr), B6: NR/PP/CA_{50} (15 phr) TPE blends at 150°C.

The variation of log (η*), log (G') versus frequency at three different temperatures for the CA_{25} and CA_{50}-containing blends is depicted in **Figure III.21** through **Figure III.24**. It is shown that at a given frequency and a given concentration of the CA, both complex viscosity and storage modulus decrease with increasing the temperature. This is due to the increase in the kinetic energy of the blend components, which arises from the thermal energy imparted from heating. But the extent of the decrease of the viscosity with increasing temperature is rather low. This suggests that the optimum processing temperature for the blend would be 190°C. Higher temperatures would lead to the thermal degradation of the major component.

Since the same trend was found when varying the concentration of the compatibilizing agent, only the plots of the viscosity and modulus as a function of frequency sweep for the CA concentration of 10 Phr are shown.

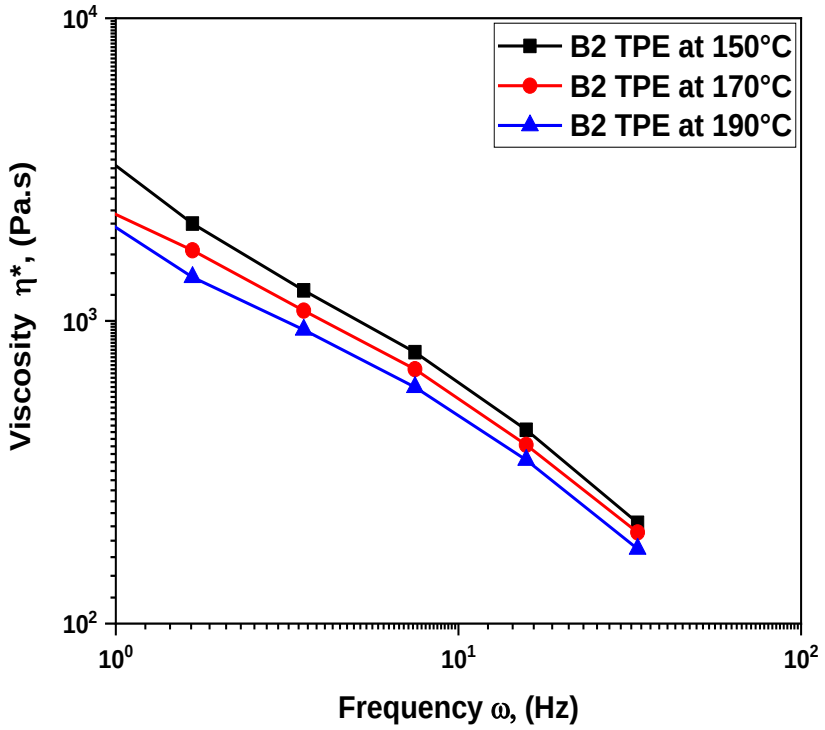

Figure III.21 Variation of log (η*) versus frequency of B2: NR/PP/CA_{25}(10 phr) TPE blend at different temperatures (150°C, 170°C, and 190°C).

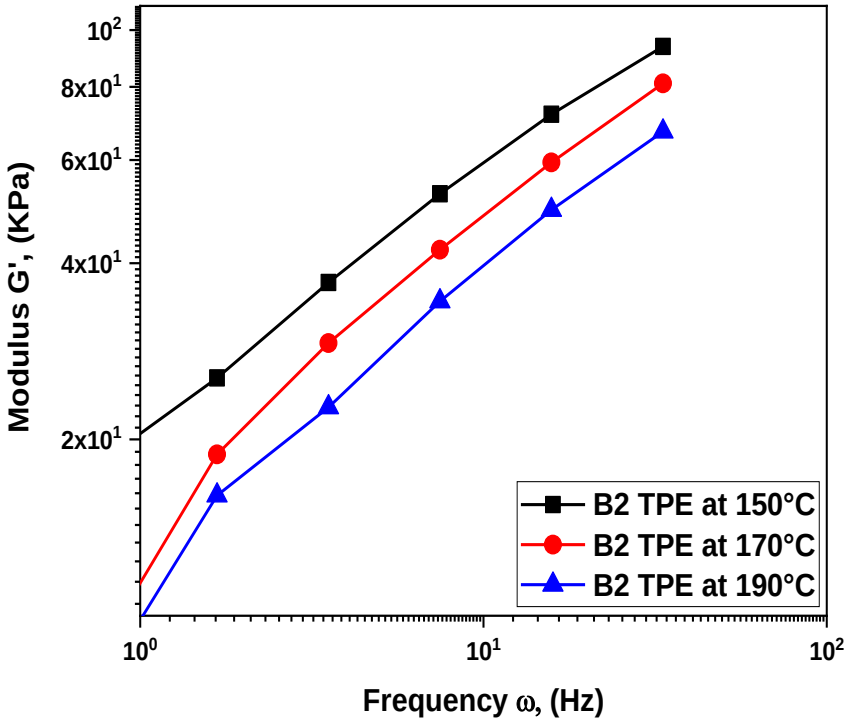

Figure III.22 Variation of log (G') versus frequency of B2: NR/PP/CA_{25}(10 phr) TPE blend at different temperatures (150°C, 170°C, and 190°C).

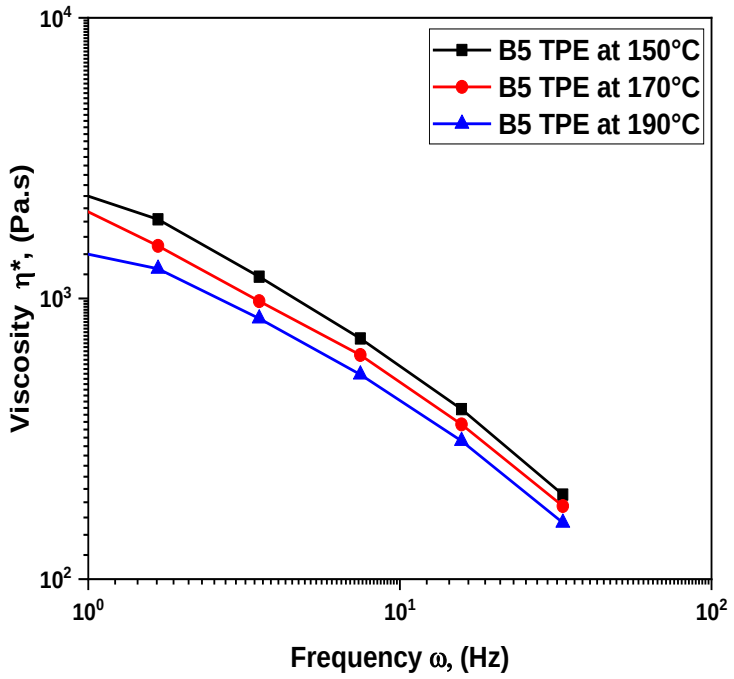

Figure III.23 Variation of log (η*) versus frequency of B5: NR/PP/CA $_{50}$(10 phr) TPE blend at different temperatures (150°C, 170°C, and 190°C).

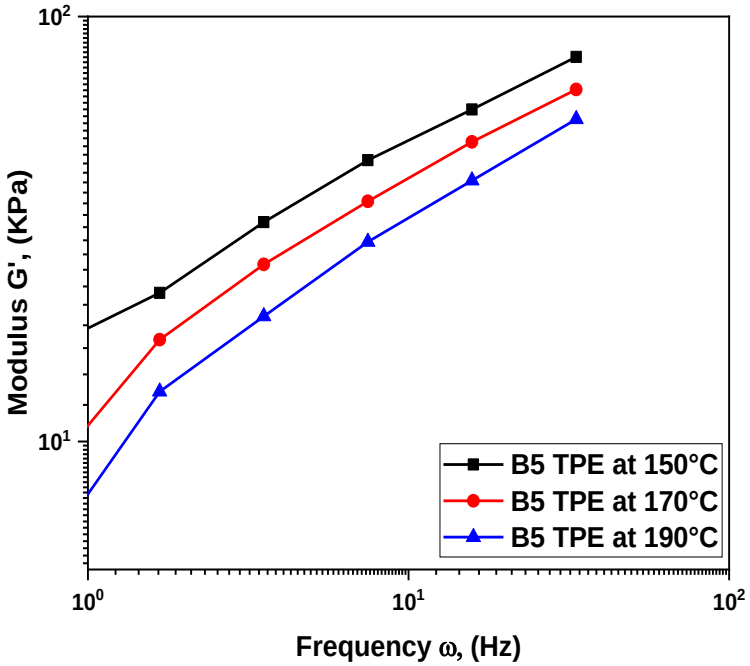

Figure III.24 Variation of log (G') versus frequency of B5: NR/PP/CA $_{50}$(10 phr) TPE blend at different temperatures (150°C, 170°C, and 190°C).

Similar effects of both CAs concentrations and those of temperatures were obtained for the dynamically vulcanized blends.

Figure III.25 through **Figure III.28** present the effect of dynamic vulcanization on viscosity and elastic modulus of the NR/PP/CAs (10Phr) at a temperature of 150°C. An enhancement of viscosity and elastic modulus were observed for the TPV, compared to the TPE blends.

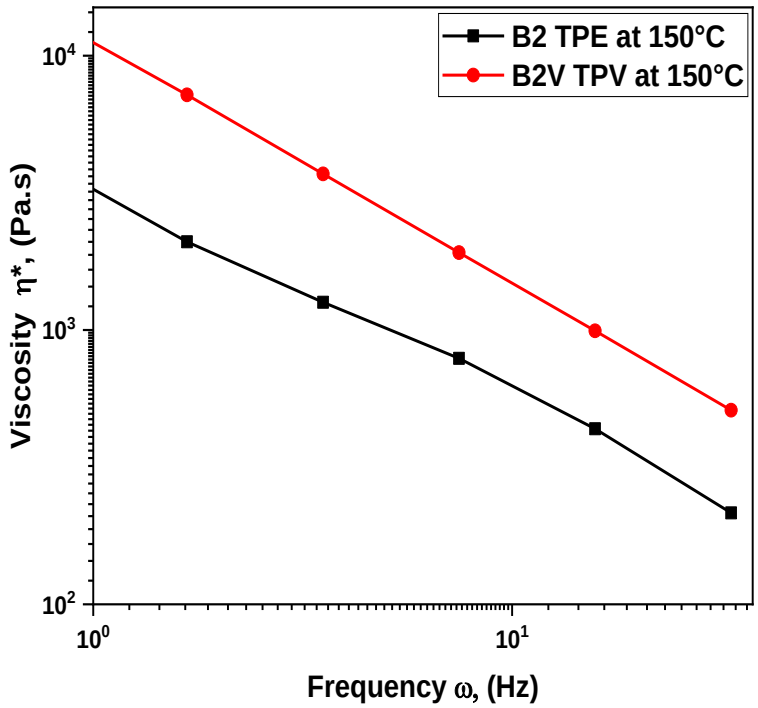

Figure III.25 Curves of viscosity (η*) response of frequency sweep for B2: NR/PP/CA $_{25}$ (10 phr), and B2V: NR/PP/CA $_{25}$(10 phr) blends at 150°C.

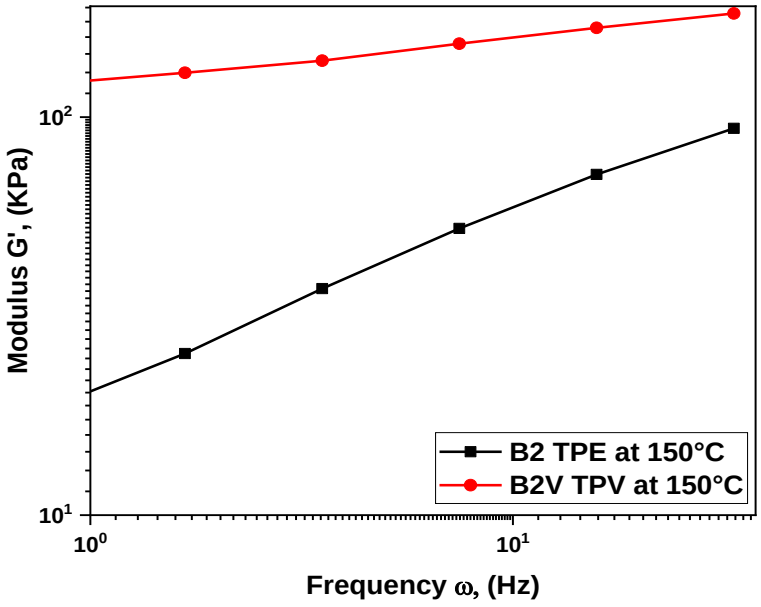

Figure III.26 Curves of elastic modulus (G') response of frequency sweep for B2: NR/PP/CA $_{25}$ (10 phr), and B2V: NR/PP/CA $_{25}$(10 phr) blends at 150°C.

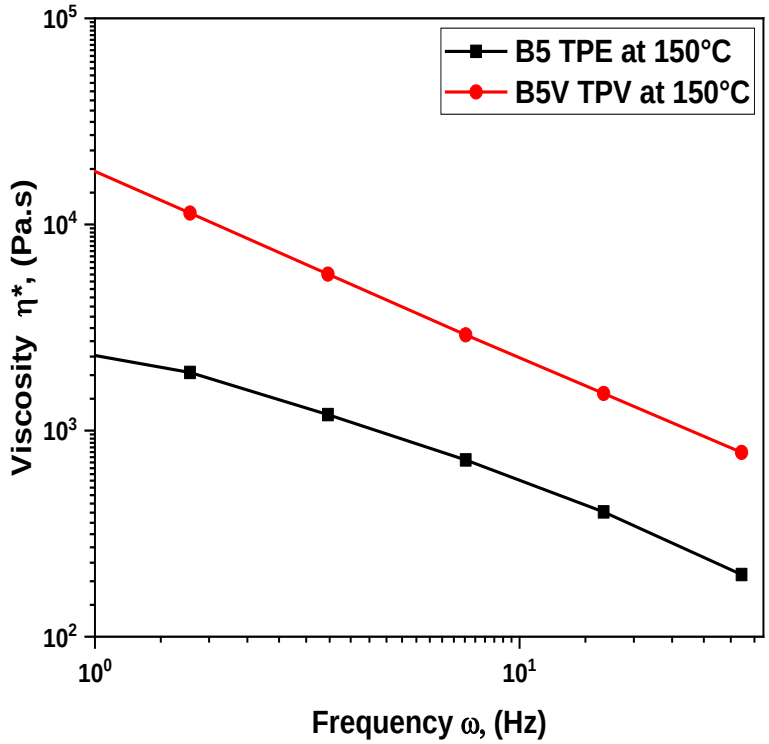

Figure III.27 Curves of viscosity (η*) response of frequency sweep for B5: NR/PP/CA $_{50}$ (10 phr), and B5V: NR/PP/CA $_{50}$(10 phr) blends at 150°C.

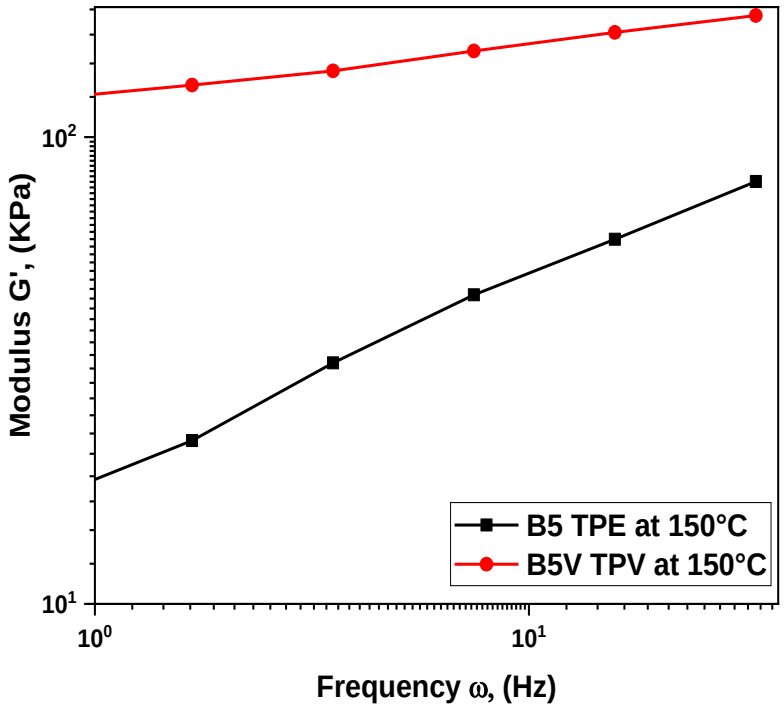

Figure III.28 Curves of elastic modulus (G') response of frequency sweep for B5: NR/PP/CA $_{50}$ (10 phr), and B5V: NR/PP/CA $_{50}$(10 phr) blends at 150°C.

III.5 Swelling Index for the dynamically vulcanized blends

The extent of crosslinking in vulcanized rubbers can be estimated from the swelling measurements based on the fact that crosslinked elastomers will not dissolve in a solvent but swell. The crosslink density for such materials is determined using Flory/Rehner equation **[25]**.

$$\rho_c = \left(\frac{1}{V_s}\right)\left[\frac{\log(1-V_r)+V_r+xV_r^2}{V_r^{\frac{1}{3}}-\frac{V_r}{2}}\right]$$

Where ρ_c is the crosslink density, V_s is the molar volume of the solvent, V_r the volume fraction of rubber in the swollen gel, and χ the interaction parameter which is dependent on the cohesive energy density of the polymer and solvent. Even though this equation is more precise for vulcanized elastomers since it takes into account both the extent of swelling and the interaction between the polymer and the particular solvent used, it is not valid for polymer blends or reinforced elastomers because blending or reinforcement modify their swelling behavior. Instead, the swelling index has rather been used to measure the extent of crosslinking for thermoplastic elastomers.

Figure III.29 shows the variation of the swelling index with the CA concentration for dynamically vulcanized NR/PP blend. It can be seen that the swelling index decreases continuously with increasing CAs concentration. It can be inferred therefore that changes down to the molecular level have taken place due to the interaction of CA_{25} and CA_{50} with PP and NR. This is due to the formation of crosslinks which restricted the mobility of the macromolecular chains. It is also clearly seen that this decrease of the swelling index is a result of the dynamic vulcanization meaning that the vulcanizates have been converted to a stiffer and less penetrable materials by the solvent. This result is in agreement with an analogous work on dynamically cured ENR/PVC blend **[26]**.

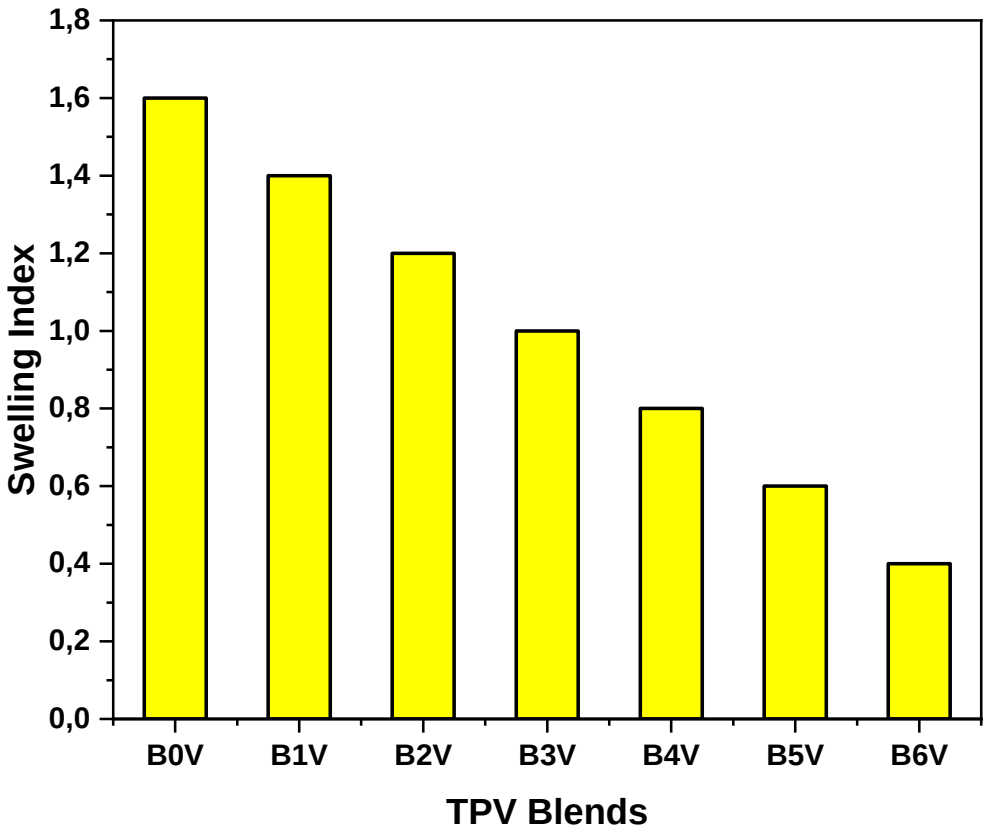

Figure III.29 Variation of the swelling index of vulcanized blends without and with compatibilizers.

III.6 Conclusions

In this chapter, the following conclusions were drawn:

1- The FTIR analysis revealed that upon blending, ENR reacted with PP-g-MA and produced ENR-grafted-PP with an ester and acid-based linkage. The results of ^{1}H-NMR revealed that the CA was insoluble and did not dissolve in the different solvents but swelled only. This could confirm the fact that blending of ENR with PP-g-MA lead to a crosslinked structure.

2- The brabender plastograms of the NR/PP blends containing the compatibilizers showed a moderate increase of the torque when the CAs were added. This increase was attributed to the interactions that developed with the blend constituents through the functional groups of ENR and PP-g-MA. The Brabender plastograms of the dynamically vulcanized blends also showed the same general trend as that of the control NR/PP TPV formulation which was cured with a mixture of TMTD/DTDM/CBS. It was found that higher torque levels were obtained with a higher extent of the CA concentration.

3- The RPA measurements indicated that the viscosity of both types of the compatibilizing agents was higher than that of their respective individual values, confirming hence the crosslinking reaction which results upon blending ENR with PP-g-MA. Moreover, the RPA results revealed that, the viscosity of both TPEs and that of TPVs increased with increasing the concentration of both types of the CAs. The same trends were observed for the effects on the storage modulus.

4- Measurements of the swelling index, pointed out that it decreases continuously with increasing CAs concentration for the dynamically vulcanized NR/PP blend. This is due to the formation of crosslinks which restricted the mobility of the macromolecular chains and meaning that the vulcanizates have been converted to a stiffer and less penetrable material by the solvent.

References

[1] Nakason, C.; Wannavilai, P.; Kaesaman, A. Thermoplastic Vulcanizates Based on Epoxidized Natural Rubber/Polypropylene Blends: Effect of Compatibilizers and Reactive Blending. *J. Appl. Polym. Sci.***2006**, *100* (6), 4729–4740. https://doi.org/10.1002/app.23260.

[2] Taranamai, P.; Phinyocheep, P.; Panbangred, W.; Janhom, M.; Daniel, P. Antibacterial Activity of Sustainable Composites Derived from Epoxidized Natural Rubber/Silver-Substituted Zeolite/Poly(Lactic Acid) Blends. *J Mater Sci.***2019**, *54* (14), 10389–10409. https://doi.org/10.1007/s10853-019-03599-1.

[3] Yokshan, R, Kasetsart. Epoxidized Natural Rubber for Adhesive Applications. *J.Nat. Sci*.**2008**, *42(5)*, 325-332.

[4] Hamzah, R.; Bakar, M. A.; Khairuddean, M.; Mohammed, I. A.; Adnan, R. A Structural Study of Epoxidized Natural Rubber (ENR-50) and Its Cyclic Dithiocarbonate Derivative Using NMR Spectroscopy Techniques. *Molecules.***2012**, *17* (9), 10974–10993. https://doi.org/10.3390/molecules170910974.

[5] Polypropylene-graft-maleic anhydride maleic anhydride ~0.6 wt. %; Compatibilizer in polymer blends and alloys. https://www.sigmaaldrich.com/catalog/product/aldrich.

[6] Utracki, L. A.; Kanial, M. R. Melt Rheology of Polymer Blends. *Polym. Eng. Sci.***1982**, *22* (2), 96–114. https://doi.org/10.1002/pen.760220211.

[7] Kim YJ, Shin GS, Lee IT, Kim BK. Miscible and Immiscible Blends of ABS with PMMA. I. Morphology and Rheology. *J. Appl. Polym. Sci*.**1993**, 47, 295-304. https://doi.org/10.1002/app.1993.070470209.

[8] Koshy, A. T.; Kuriakose, B.; Thomas, S.; Premalatha, C. K.; Varghese, S. Melt Rheology and Elasticity of Natural Rubber—Ethylene–Vinyl Acetate Copolymer Blends. *J. Appl. Polym. Sci.***1993**, *49* (5), 901–912. https://doi.org/10.1002/app.1993.070490516.

[9] Varghese H, Ramamurthy K, Janardhan R, Bhagawan SS, Thomas S. *Polym Plast Technol En* (in press).

[10] Varughese, K. T.; De, P. P.; Nando, G. B.; De, S. K. Melt Flow Behavior of Blends from Poly(Vinyl Chloride) and Epoxidized Natural Rubber. *J. Vinyl Addit. Technol.***1987**, *9* (4), 161–167. https://doi.org/10.1002/vnl.730090406.

[11] Varughese, K. T. Melt Rheology of Plasticized Poly(Vinyl Chloride)/Epoxidized Natural Rubber Miscible Blends. *J. Appl. Polym. Sci.***1990**, *39* (2), 205–223. https://doi.org/10.1002/app.1990.070390201.

[12] Akhtar S, Kuriakose B, De PP, De SK.Rheological Behaviour and Extrudate Morphology of Thermoplastic Elastomers From Natural Rubber and High Density Polyethylene. *Plast Rubber Process Applic*, **1987**,7, 11.http://pascal-francis.inist.fr/vibad/index.php?action=getRecordDetail&idt=7594175

[13] Kuriakose B. Kaustschuk Gummi Kunststoffe;**1984**,37,1044.

[14] Duvdevani, I.; Agarwal, P. K.; Lundberg, R. D. Blends of EPDM and Sulfonated Ethylene-Propylene-Diene (EPDM) Rubber with Polypropylene: Structure, Physical, and Rheological Properties. *Polym. Eng. Sci.***1982**, *22* (8), 499–506. https://doi.org/10.1002/pen.760220808.

[15] Kim, B. K.; Jeong, H. M.; Lee, Y. H. Melt Rheology of Poly(Ethylene Terephthalate), Polyarylate, and Their Blends. *J. Appl. Polym. Sci.***1990**, *40* (1112), 1805–1818. https://doi.org/10.1002/app.1990.070401101.

[16] Brostow, W.; Sterzynski, T.; Triouleyre, S. Rheological Properties and Morphology of Binary Blends of a Longitudinal Polymer Liquid Crystal with Engineering Polymers. *Polymer.***1996**, *37* (9), 1561–1574. https://doi.org/10.1016/0032-3861(96)83704-9.

[17] Zhuang, P.; Kyu, T.; White, J. L. Characteristics of Hydroxybenzoic Acid-Ethylene Terephthalate Copolymers and Their Blends with Polystyrene, Polycarbonate, and Polyethylene Terephthalate. *Polym. Eng. Sci.***1988**, *28* (17), 1095–1106. https://doi.org/10.1002/pen.760281704.

[18] Wu, S. Formation of Dispersed Phase in Incompatible Polymer Blends: Interfacial and Rheological Effects. *Polym. Eng. Sci.***1987**, *27* (5), 335–343. https://doi.org/10.1002/pen.760270506.

[19] Holsti-Miettinen, R. M.; Seppälä, J. V.; Ikkala, O. T.; Reima, I. T. Functionalized Elastomeric Compatibilizer in PA 6/PP Blends and Binary Interactions between Compatibilizer and Polymer. *Polym. Eng. Sci.***1994**, *34* (5), 395–404. https://doi.org/10.1002/pen.760340504.

[20] Germain, Y.; Ernst, B.; Genelot, O.; Dhamani, L. Rheological and Morphological Analysis of Compatibilized Polypropylene/Polyamide Blends. *J Rheol*.**1994**, *38* (3), 681-697.https://doi: 10.1122/1.550602.

[21] Valenza, A.; Acierno, D. Ternary Blends of Nylon 12/Polypropylene/Modified Polypropylene: Influence of Functional Groups of the Modified Polypropylene. *Eur Polym J*.**1994**, *30* (10), 1121–1126. https://doi.org/10.1016/0014-3057(94)90248-8.

[22] Joshi, M.; Maiti, S. N.; Misra, A. Poly(Butylene Terephthalate)/High Density Polyethylene Alloys. II. Mechanical Properties and Rheology. *J. Appl. Polym. Sci.***1992**, 45 (10), 1837–1847. https://doi.org/10.1002/app.1992.070451018.

[23] Thomas, S.; Oommen, Z.; Premalatha, C. K.; Kuriakose, B. Melt Rheological Behaviour of Natural Rubber/Poly(Methyl Methacrylate)/Natural Rubber-g-Poly(Methyl Methacrylate) Blends. *Polymer*.**1997**, *38* (22), 5611–5621. https://doi.org/10.1016/S0032-3861(97)00120-1.

[24] George, S.; Ramamurthy, K.; Anand, J. S.; Groeninckx, G.; Varughese, K. T.; Thomas, S. Rheological Behaviour of Thermoplastic Elastomers from Polypropylene/Acrylonitrile–Butadiene Rubber Blends: Effect of Blend Ratio, Reactive Compatibilization and Dynamic Vulcanization. *Polymer*.**1999**, *40* (15), 4325–4344. https://doi.org/10.1016/S0032-3861(98)00681-8.

[25] Flory, P. J.; Rehner, J. Statistical Mechanics of Crosslinked Polymer Networks I. Rubberlike Elasticity.*J Chem Phys*.**1943**, *11* (11), 512–520. https://doi.org/10.1063/1.1723791.

[26] Abdul Majid, R.; Ismail, H.; Mat Taib, R. Effects of Polyethylene Grafted Maleic Anhydride on the Mechanical, Morphological, and Swelling Properties of Poly (Vinyl Chloride) / Epoxidized Natural Rubber / Kenaf Core Powder Composites. *Bio Resources.***2014**, *9* (4), 7059–7072. https://doi.org/10.15376/biores.9.4.7059-7072.

Chapter IV

Mechanical, Dynamic Mechanical, Morphological and Thermal Properties

The addition of ENR/PP-g-MA as a compatibilizer for NR/PP blend is expected to affect the mechanical, dynamic mechanical as well as the morphological and thermal properties of the resulting TPE and TPV blends. In this chapter the effects of varying the concentration of the CA used on various properties will be discussed for both unvulcanized and the dynamically vulcanized blends.

IV.1 Tensile properties

The stress–strain curves of the control NR/PP blend and those of the unvulcanized and dynamically vulcanized blends containing different quantities of CA_{25} and CA_{50} are presented in **Figure IV.1**, **and Figure IV.2**, respectively. These curves show that the blends containing the CAs exhibit a shape typical of a soft material with moderate values of the modulus. We can also observe that the higher the epoxidation content in the CA, the higher is the ultimate stress at break (B4 > B1, B5 > B2, B6 > B3) for TPE blends and (B4V > B1V, B5V > B2V, B6V > B3V) for TPV blends; and the lower is the elongation at break. For the blend containing 15 phr CA_{50} (**Figure IV.1**), it appears that the stress–strain curve tends to follow an upward shift suggesting that above this dosage the rigidity of the material would increase more. This is linked to the crosslinked structure of the CA which contributed to rendering the blend more rigid by imparting a reinforcing effect.

Figure IV.3 and **Figure IV.4**, which present the mechanical properties in terms of tensile strength, Young's modulus, and elongation at break, show a trend of increased tensile strength and modulus and a decrease of the elongation at break. This means that the addition of CA_{25} and CA_{50} increased the capacity of the blends to withstand the tensile load and therefore led to an enhanced mechanical resistance.

Taking into account the chemical reaction mechanism initially proposed by C Nakason et al [**1],** and also reported by Balakrishnan et al. **[2],** it is proposed to associate this improvement of the mechanical properties to the interactions that developed between the PP chains and those of the PP-g-MA in the CA, and at the same time between the NR backbone with the ENR chains also present in the compatibilizer.

On the other hand, it is noted that the increase of tensile strength and modulus increased with increasing the ENR content as there are more functional groups in CA_{50} than those in CA_{25}. In addition, the hydroxyl group in both CA_{25} and CA_{50} participated also in improving the interactions, diminishing hence the interfacial tension between the blend constituents. Another plausible interpretation of these results is that the crosslinked structure in the CA imparted a

reinforcing effect. This correlates well with the mixing behavior discussed earlier where it was observed that the torque increased after the addition of CA_{25} for TPE blends, and CA_{25} as well as CA_{50} for TPV blends.

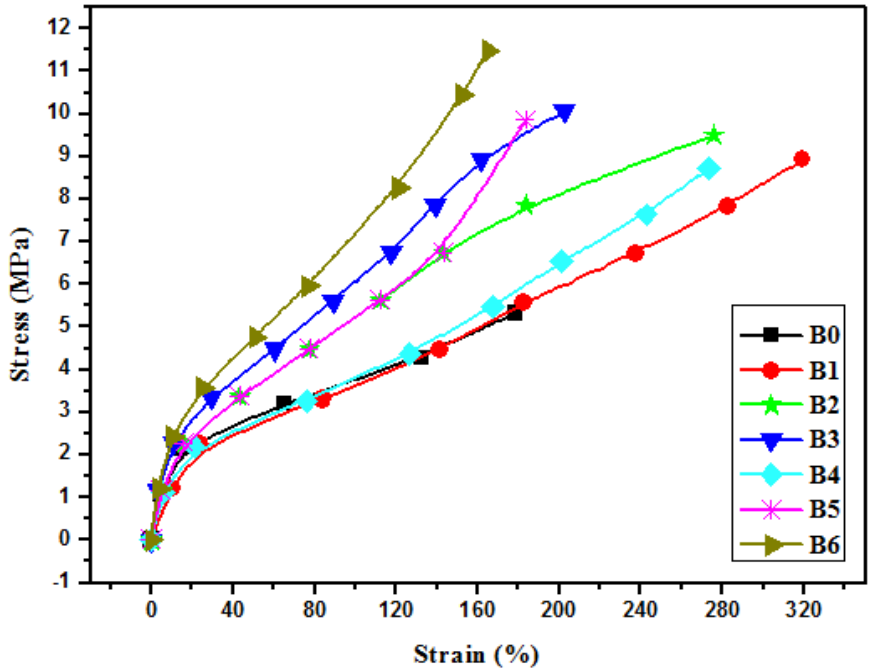

Figure IV.1 Stress/strain curves of the control NR/PP blend, and those of the CA_{25}, and CA_{50}-containing TPE blends.

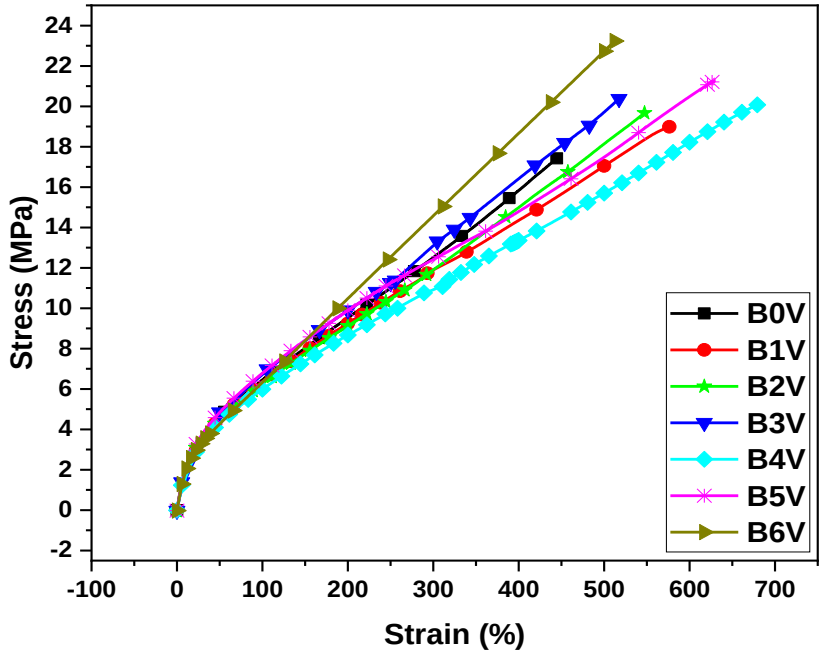

Figure IV.2 Stress/strain curves of the control NR/PP blend, and those of the CA_{25}, and CA_{50}-containing TPV blends.

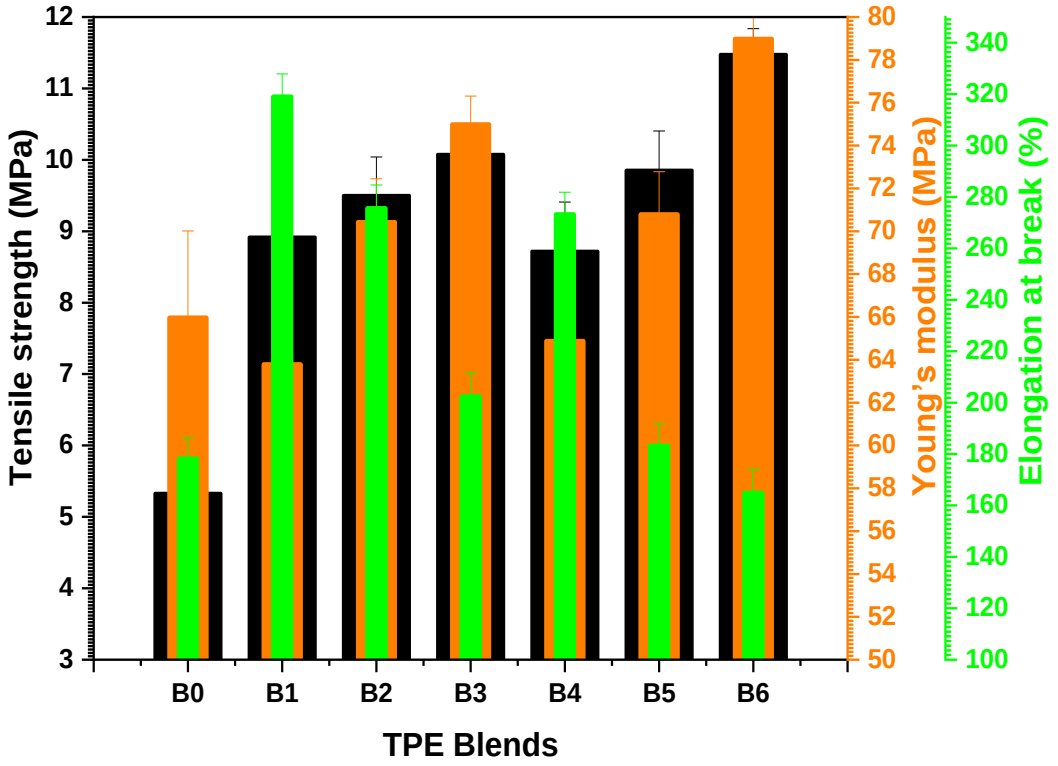

FigureIV.3 Tensile strength, Young's modulus, and elongation at break of the control NR/PP blend, and those of the CA_{25}, and CA_{50}-containing TPE blends.

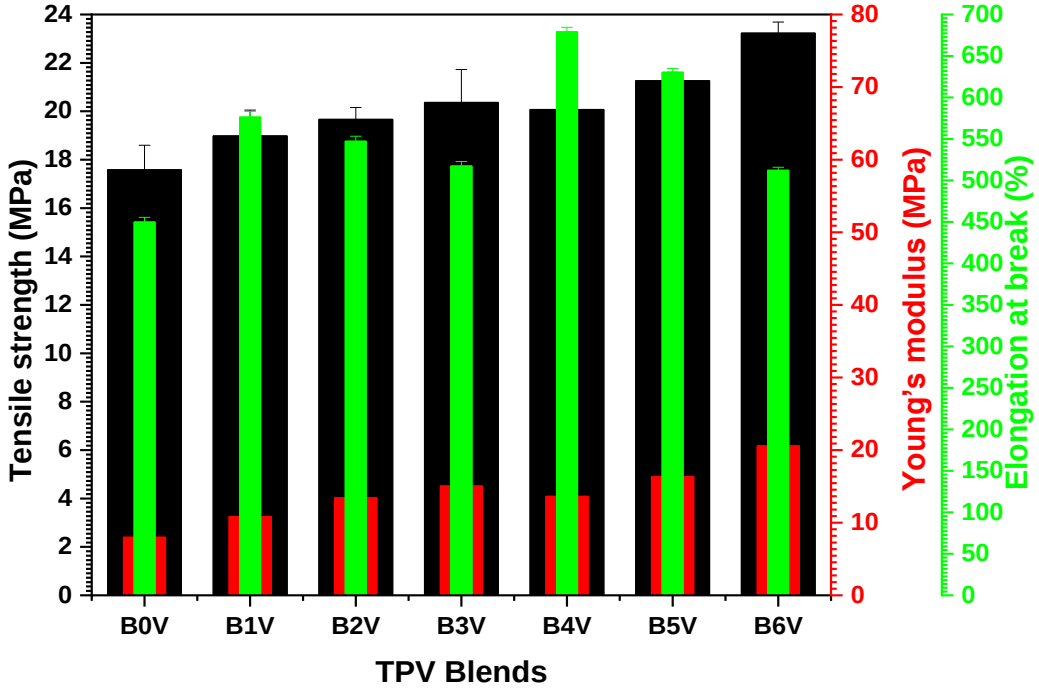

Figure IV.4 Tensile strength, Young's modulus, and elongation at break of the control NR/PP blend, and those of the CA_{25}, and CA_{50}-containing TPV blends.

Figure IV.5 and **FigureIV.6** show the stress-strain curves of the CA_{25} and CA_{50} containing NR/PP along with those of the dynamically vulcanized blends, respectively.

The stress-strain curves of unvulcanized and vulcanized blends show distinct elastic and inelastic regions. These figures show that the unvulcanized blends behave as a weak and brittle material with a low resistance to deformation and a low value of the elongation at break in contrast to the dynamically vulcanized blends which exhibit a deformation behaviour akin to strong and tough materials. Their deformation pattern was characterized by a sharp increase in the stress with strain in the linear region, then after passing through a yield point, this increase become gradual.

The respective values of Tensile strength, Young's modulus and Elongation at break are presented in the bargraphs of **Figure IV.7 and Figure IV.8**.

For the CA-containing blends, the improvement of the mechanical properties is reflected by the increase of the values of tensile strength when increasing the concentration of the CA, especially for the dynamically vulcanized blends compared to the unvulcanized ones (B0 vs B0V),(B1 vs B1V, B2 vs B2V, B3 vs B3V for the CA_{25}-based systems) and (B4 vs B4V, B5 vs B5V, B6 vs B6V for the CA_{50}-based systems).

These bargraphs show the combined effects of the addition of the compatibilizers with those of the dynamic vulcanization, which resulted in higher values of tensile strength and elongation at break, and lower values of young's modulus of the TPV than those of the TPE blends.

The above results are analogous to those reported in literature by many researchers who studied the effects of compatibilization and dynamic vulcanization on the mechanical properties. For example, A. Thitithammawong et al. **[3]** have studied the influence of two types of blend compatibilizers (PP-g-MA and Ph-PP) on the mechanical properties of epoxidized natural rubber/polypropylene thermoplastic vulcanizates. They have found that the mechanical properties improved in a range of loading levels of compatibilizers at 0–7.5 wt %. This was attributed to a chemical interaction between the different phases caused by the functionalized compatibilizers. In another publication, N. Mohamad et al. **[4]** investigated the mechanical properties of thermoplastic vulcanizates based on polypropylene/epoxidized natural rubber (PP/ENR) when treated with maleic anhydride-grafted polypropylene. It was found that the tensile properties of the vulcanizates improved with the addition of MA-g-PP compatibilizer into the blend during the compounding process. This was attributed to the

enhancement of the compatibility between the thermoplastic and the rubber molecules with the presence of the compatibilizer.

In another study, I. P Mahendra et al.**[5]**investigated the influence of maleic anhydride-grafted polypropylene and maleic anhydride-grafted-cyclic natural rubber (CNR-g-MA) as compatibilizers on the properties of polypropylene/ cyclic natural rubber (PP/CNR)blends. Thermogravimetry analysis confirmed that the addition of compatibilizers improved the thermal stability of blends. The DSC curve shows that the glass transition temperature was significantly decreased due to the maleic anhydride-grafted polymers incorporation. The decrease of CNR's Tg value implies that the incorporation of maleic anhydride-grafted polymer into PP/CNR blends can improve blend compatibility. The compatibilization was further confirmed by an increase in tensile strength of the compatibilized blends.

Nakason C et al.**[6]** investigated the effect of blend compatibilizers (a graft copolymer of HDPE and maleic anhydride (MA; i.e., HDPE-g-MA) and two types of phenolic modified HDPEs using phenolic resins SP-1045 and HRJ-10518 (i.e., PhSP-PE and PhHRJ-PE) on the mechanical properties of thermoplastic elastomers based on epoxidized natural rubber and high-density polyethylene blends. They found that the blend with compatibilizer exhibited superior tensile strength, hardness, and set properties to that of the blend without compatibilizer. The ENR and HDPE interaction via the link of compatibilizer molecules was the polar functional groups of the compatibilizer with the oxirane groups in the ENR molecules. Also, another end of the compatibilizer molecules (i.e., HDPE segments) was compatibilizing with the HDPE molecules in the blend components.

In another publication, Nakason C et al. **[7]** have studied the effect of epoxide levels in ENR molecules of thermoplastic vulcanizates based on epoxidized natural rubber/polypropylene blends. Thermoplastic vulcanizates based on 75/25 ENRs/PP blends with Ph-PP compatibilizer were later prepared by dynamic vulcanization using sulfur curing system. Influence of various levels of epoxide groups on the mechanical properties was investigated. It was found that the tensile strength and hardness properties increased with increasing levels of epoxide groups in the ENR molecules. This may be attributed to increasing level of chemical interaction between the methylol groups of the Ph-PP molecules and the polar functional groups of the ENR molecules. Also, the PP segments in the Ph-PP molecules are capable of compatibilizing with the PP molecules used as a blend composition.

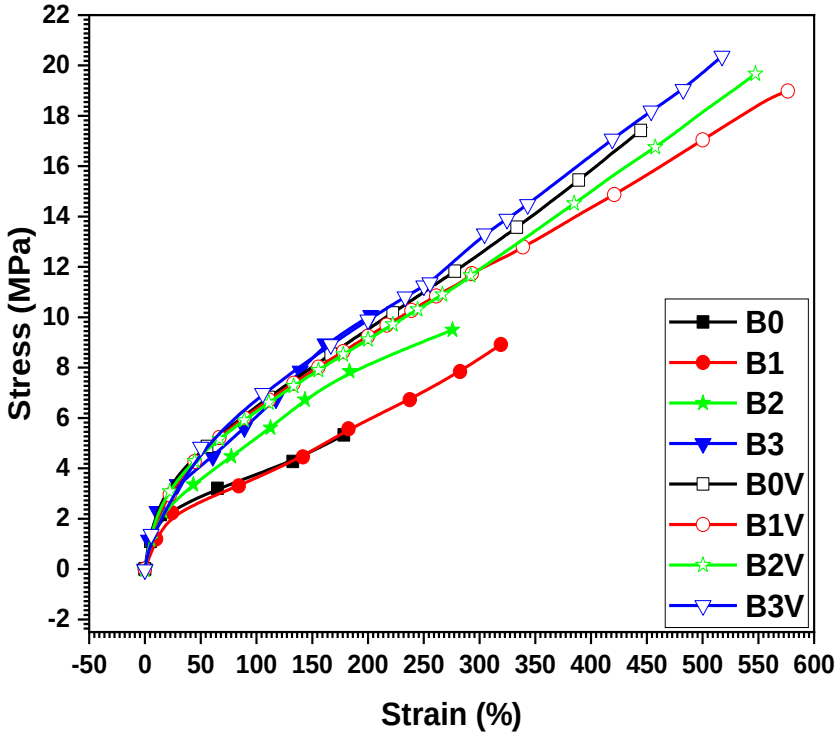

Figure IV.5 Tensile stress-strain curves of the control NR/PP blend, and those of CA_{25}- containing TPE and TPV blends.

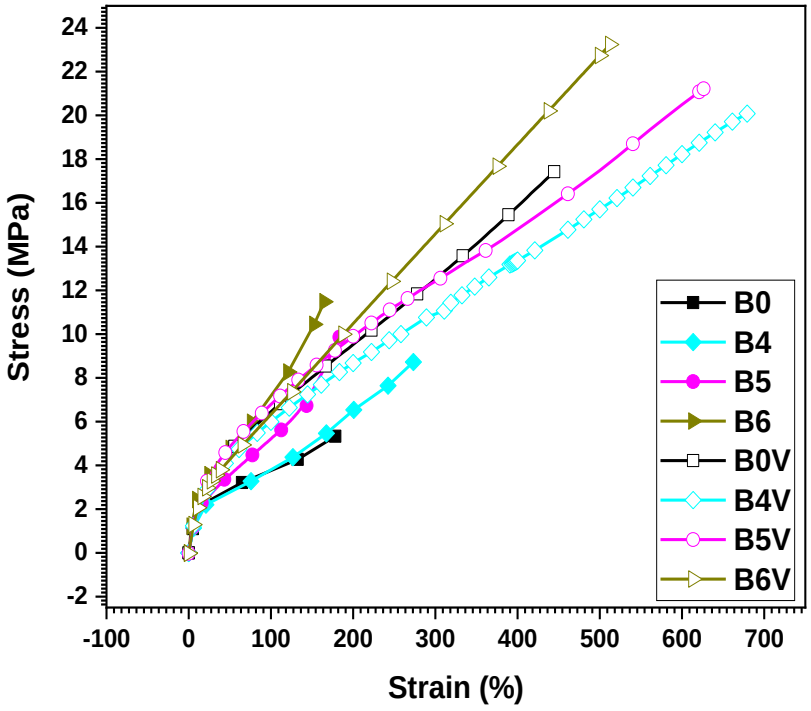

Figure IV.6 Tensile stress-strain curves of the control NR/PP blend, and those of CA_{50} -containing TPE and TPV blends.

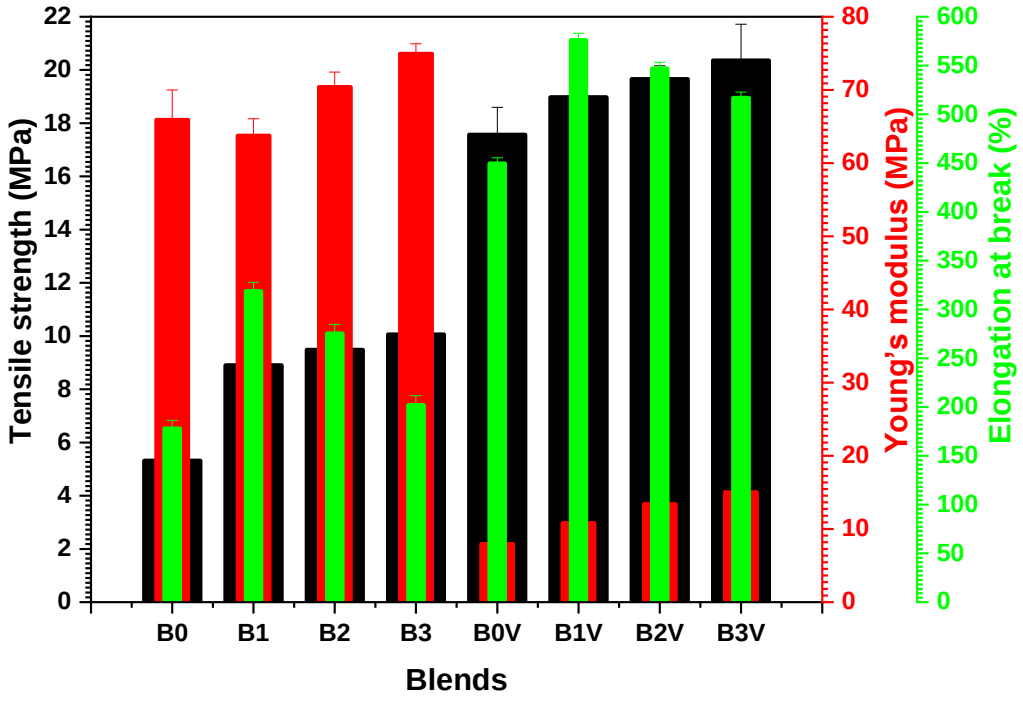

Figure IV.7 Tensile strength, Young's modulus, and elongation at break of the control NR/PP blend, and those of the CA_{25}- containing TPE and TPV blends.

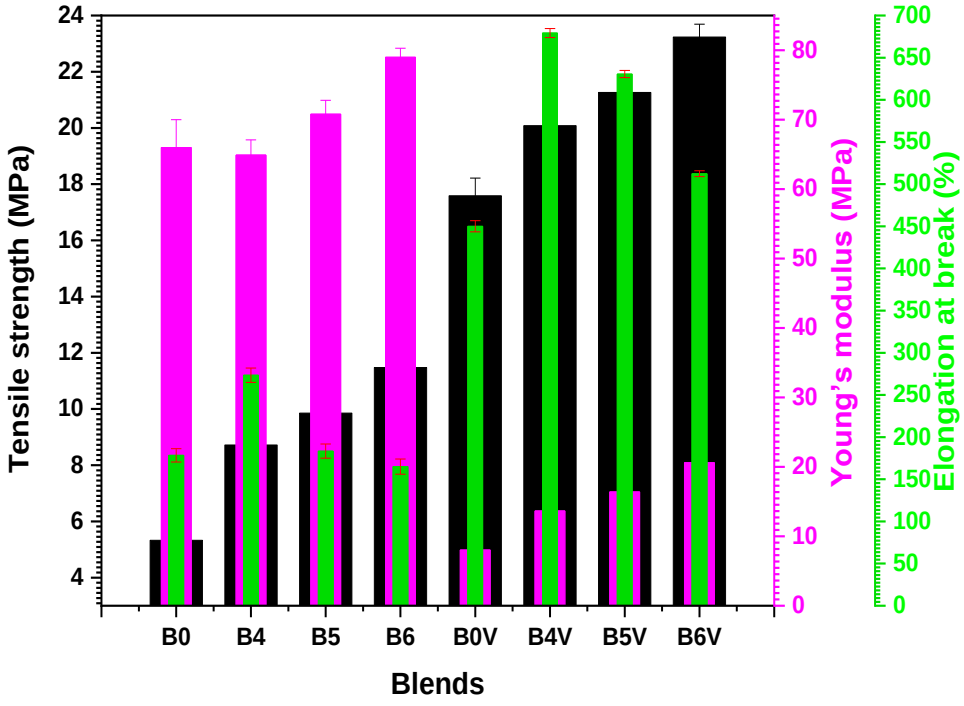

Figure IV.8 Tensile strength, Young's modulus, and elongation at break of the control NR/PP blend, and those of the CA_{50}-containing TPE and TPV blends.

IV.2 Dynamic mechanical properties

The miscibility and phase behavior of polymer blends are of crucial importance in many applications. Dynamic mechanical thermal analysis (DMTA) is a widely accepted method for studying the structure-property relations in polymers. The viscoelastic data can be successfully used to study the miscibility in polymer blends in terms of changes in Tg (glass transition temperature) of the components of the blends. Miscible blends will have a single sharp glass transition temperature intermediate between those of the individual polymers. In the case of borderline miscibility, the broadening of the transitions will occur, whereas two separate transitions corresponding to the constituents may occur in the case of completely immiscible blends. Generally, the dynamic mechanical properties are expressed in terms of storage modulus, loss modulus, and damping factor and these depend on crystallinity, structure, and extent of crosslinking. The performance of most of the rubber products is related to their dynamic properties which are a very important consideration when rubber compounds are designed for components to be used in dynamic applications **[8].**

The dynamic mechanical properties of NR/PP blends are reported in this chapter. The properties including storage modulus (E'), loss modulus (E") and damping factor (tan δ) were investigated as a function of temperature. The effects of compatibilizer and dynamic vulcanization on the dynamic mechanical properties have been investigated.

IV.2.1 Dynamic mechanical properties of NR and ENRs

Figures IV.9, **Figure IV.10**, and **Figure IV.11** show the variation of the storage modulus, loss modulus, and damping factor as a function of temperature, for neat NR, neat ENR_{25}, and neat ENR_{50}. It can be seen that the storage modulus shows three distinct regions: a glassy high modulus region where the segmental mobility is restricted, a transition region with substantial decrease in E' as the temperature increases, and a rubbery region with increasing chain mobility and drastic loss of modulus with increasing temperature. In **Figure IV.9**, it is seen that E' of neat NR is higher than those of ENR_{25} and ENR_{50}. It is also clearly seen that the E' of ENR_{50} is higher than that of ENR_{25} in the glassy region. This is due to the epoxidation level of the NR.

Figure IV.10 shows that E" which expresses the viscous component and the capacity of the material to dissipate energy, passes through a maximum that corresponds to Tg. It can be observed that below their respective Tgs, the loss modulus of neat NR is higher than that of

ENR_{25} and ENR_{50}. At temperatures below Tg the loss modulus of ENR_{25} is lower than that of ENR_{50} and the intensity of the corresponding peak is also lower.

In **Figure IV.11**, it is seen that the three types of NR have larger areas underneath the tan δ curve compared to those of the E" peaks. It is clear that neat NR has the largest area, followed in rank order by ENR_{25} and ENR_{50}. This matches the elasticity and damping properties of these materials. The chemical differences between NR and its modified forms are important determinants of elasticity and damping properties. In **Figure IV.11**, the glass transition temperature (Tg) was determined from the maximum peak of the tan delta–temperature curve, it is seen that NR, ENR_{25}, and ENR_{50} had their Tgs at −53°C,−27°C, and−3°C, respectively. That is, the Tg shifted to higher temperatures with increasing epoxidation level. This is caused by chain stiffening and the chemical interactions of epoxide functional groups in ENR restricting molecular mobility.

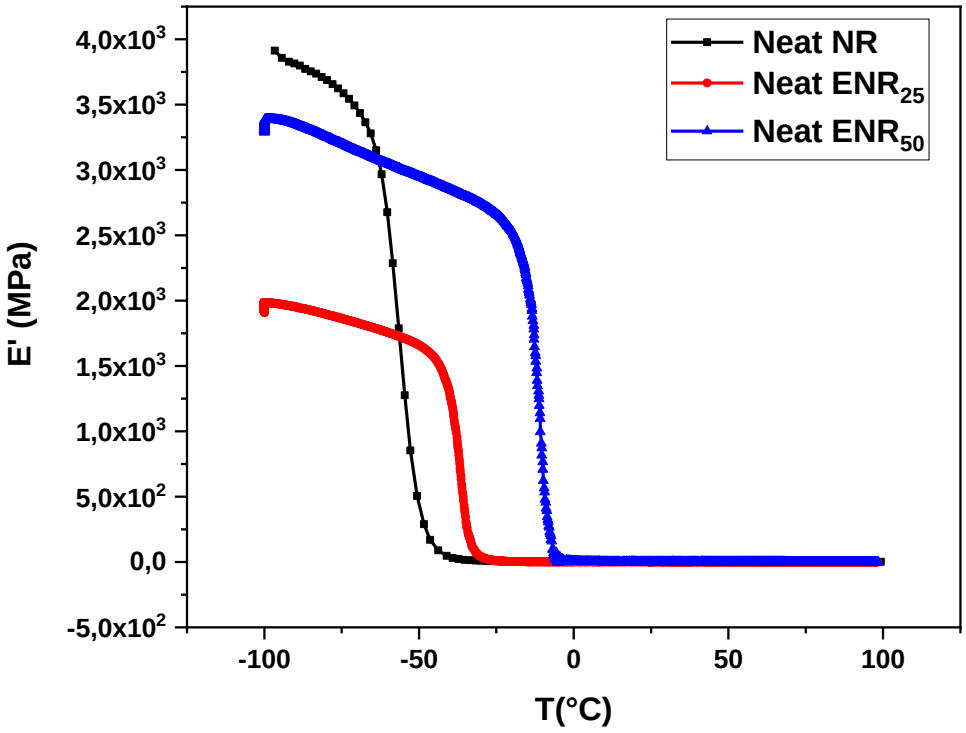

Figure.IV.9 Variation of the storage modulus E' as a function of temperature for neat NR, neat ENR_{25}, and neat ENR_{50}.

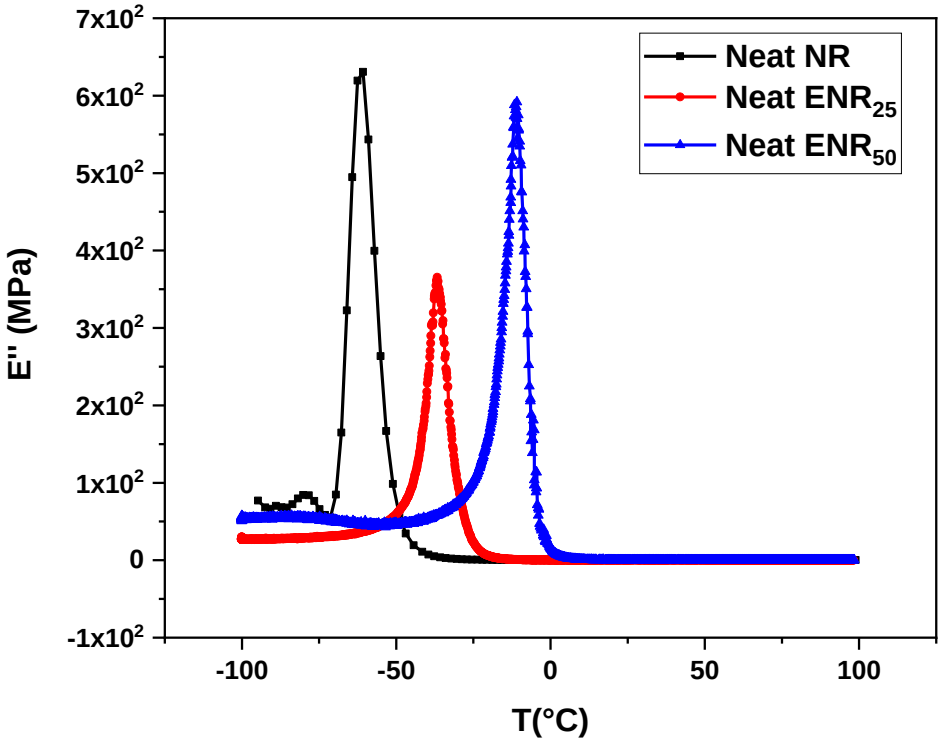

Figure IV.10 Variation of the loss modulus E" as a function of temperature for neat NR, neat ENR_{25}, and neat ENR_{50}.

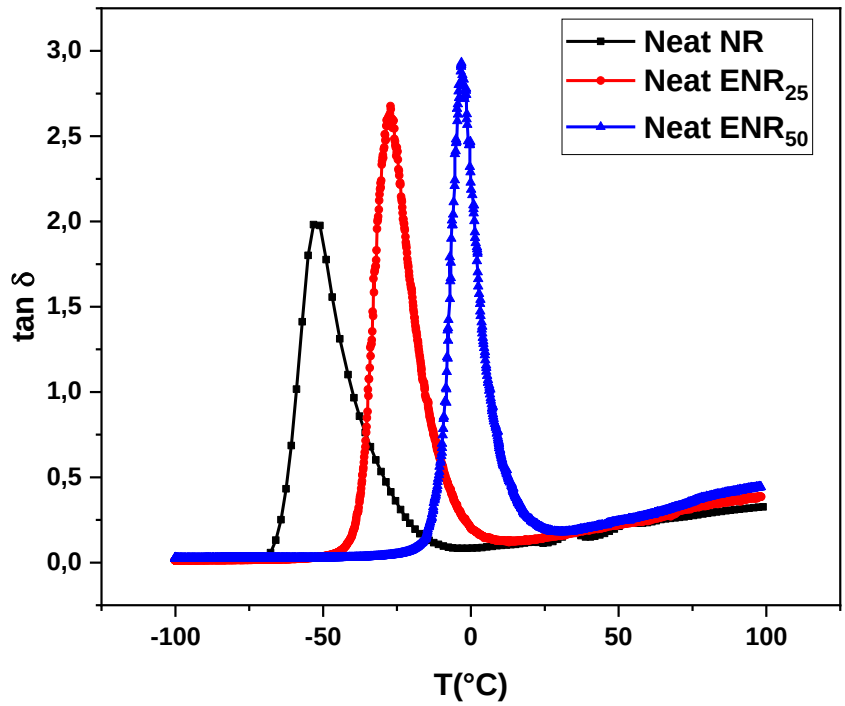

Figure IV.11 Variation of the damping factor tan δ as a function of temperature for neat NR, neat ENR_{25}, and neat ENR_{50}.

IV.2.2 Dynamic mechanical properties of the compatibilizing agents

The main goal of compatibilization is to improve the dynamic mechanical properties of the blends which determine the use of the material. These properties depend on many factors, including the concentrations of the CAs and their adhesion at the blend interface.

Figure IV.12 presents the temperature dependence of the storage modulus E' of PP-g-MA, ENR_{25}, ENR_{50}, and compatibilizing agents (CA_{25}: ENR_{25}/PP-g-MA, and CA_{50}: ENR_{50}/PP-g-MA). It is observed that the storage modulus curves of the CA_{25} and CA_{50} is divided into three regions. In the first region, at low temperature, the molecular chains are frozen in a rigid network with a high value of the modulus (glassy state). Then a sharp decrease of the storage modulus by three folds is observed at the glass transition region. In the third region, the storage modulus exhibits a plateau curve which corresponds to the rubbery state. According to **Figure IV.12**, it was found that the storage modulus of either ENR_{25}/PP-g-MA or ENR_{50}/PP-g-MA is higher than that of the individual components (i.e: ENR_{25}, andENR_{50}).confirming hence the crosslinking reaction which results upon blending ENR with PP-g-MA. In addition, the values of the storage modulus of ENR_{50}/PP-g-MA (CA_{50}) are higher than that of ENR_{25}/PP-g-MA (CA_{25}) indicating that the higher the epoxydation level in the CA, the higher the elastic modulus.

Figure IV.13 which presents the variation of the loss modulus E" as a function of temperature shows that the Tg value of CA_{50} is higher than that of CA_{25} (from -19°C to+9°C). This is attributed to the fact that upon blending ENR with PP-g-MA, the higher epoxidation level in CA_{50} resulted in a stiffer material owing to higher level of crosslinking.

The variation of the damping factor tan δ, which is the ratio of the loss modulus to the storage modulus, as a function of temperature is shown in **Figure IV.14**. The maximum position of tan δ peak is also commonly taken to determine the glass transition temperature (Tg) of polymers **[9].** The transition region of the storage modulus and the position of tan δ peak shifted to higher temperatures with increasing the epoxide level in the CA as shown in **Figure IV.12 and Figure IV.14**. The relative high Tg of ENR is mainly caused by the steric interference of the epoxide group, resulting in restriction of the chain mobility of the ENR molecules **[10, 11].** The intensity of the intermolecular forces depends on the concentration of the polar groups in the ENR molecules; higher epoxide contents cause lower chain mobility and hence a higher Tg. Gelling **[12]** reported that for every mole percent increase in epoxidation, the glass transition temperature increases by 0.93°C.

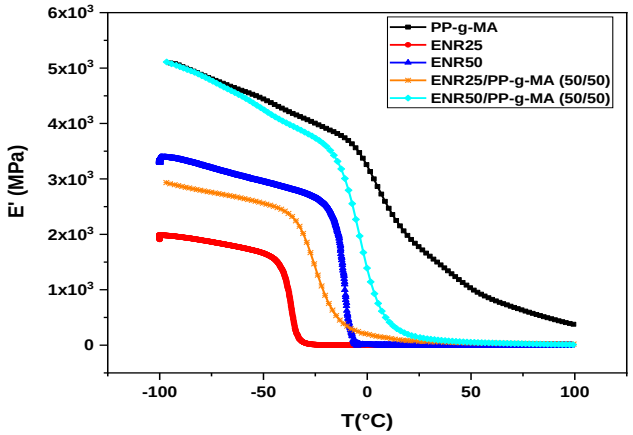

Figure IV.12 Variation of the storage modulus E' as a function of temperature for PP-g-MA, ENR_{25}, ENR_{50}, ENR_{25}/PP-g-MA and ENR_{50}/PP-g-MA.

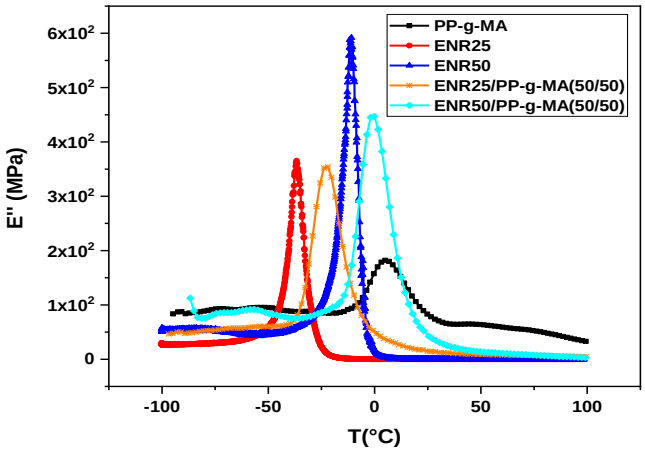

FigureIV.13 Variation of the loss modulus E'' as a function of temperature for PP-g-MA, ENR_{25}, ENR_{50}, ENR_{25}/PP-g-MA and ENR_{50}/PP-g-MA.

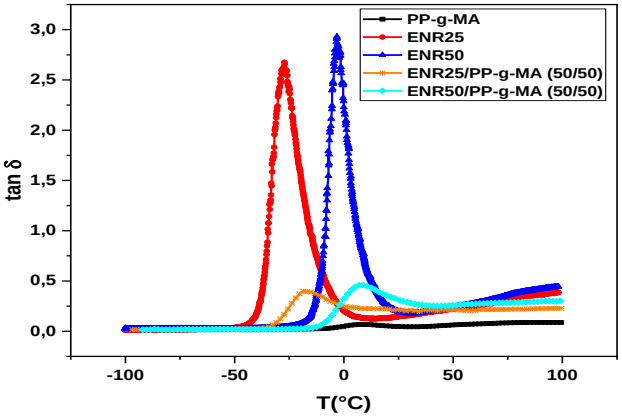

Figure IV.14 Variation of the damping factor tan δ as a function of temperature for PP-g-MA, ENR_{25}, ENR_{50}, ENR_{25}/PP-g-MA and ENR_{50}/PP-g-MA.

IV.2.3 Dynamic mechanical properties of uncompatibilized NR/PP blend

The variation of the storage modulus E', the loss modulus E", and the damping factor tan δ with temperature for neat NR, neat PP, and their 70/30 NR/PP blend is shown in **Figure IV.15**, **Figure IV.16**, and **Figure IV.17**, respectively.

For neat PP, the elastic modulus decreases gradually with increasing temperature. In the plot of the variation of the loss modulus, a transition was observed as a broad peak at + 18°C. This transition is similar to that reported by S.Thomas **[13]** and by Choudhury et al. **[14],** and for whom it is due to a β-relaxation process which is associated with the unfreezing of segmental motion of the main chains in the amorphous region. This transition appears also as a broad peak at + 21°C in the tan δ curve (**Figure IV.17**).

For neat NR, the glass transition temperature, which was taken as the peak position of the tan δ curve, was detected at -53°C.

As shown in **Figure IV.15**, the storage modulus of NR/PP in the glassy region is lower than that of neat NR and neat PP. The gap narrows down and disappears above Tg where the curves of NR, and NR/PP superimpose.

Figure IV.16 represents the temperature dependence of E" for neat NR, neat PP and NR/PP blend. The loss modulus curves are similar for NR and NR/PP except for neat PP which exhibits the β transition peak at +18°C.

Figure IV.17 presents the variation of the damping factor tan δ as a function of temperature for neat NR, neat PP and NR/PP blend. It can be seen that for NR/PP blend, two peaks were observed at about -52 and +13°C, representing the glass transition temperature of the NR phase and the β transition peak of the PP phase, respectively. The latter peak corresponding to the PP phase is zoomed out (**Figure IV.17**) and appears as a broad peak extending from approximately -3°C to +18°C. The presence of these two peaks indicates the existence of two separate phases in the 70/30 NR/PP TPE blend.

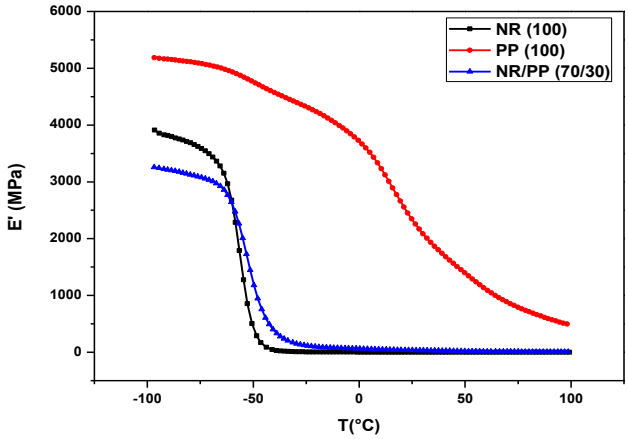

Figure IV.15 Variation of the storage modulus E' as a function of temperature for neat NR, neat PP and NR/PP blend.

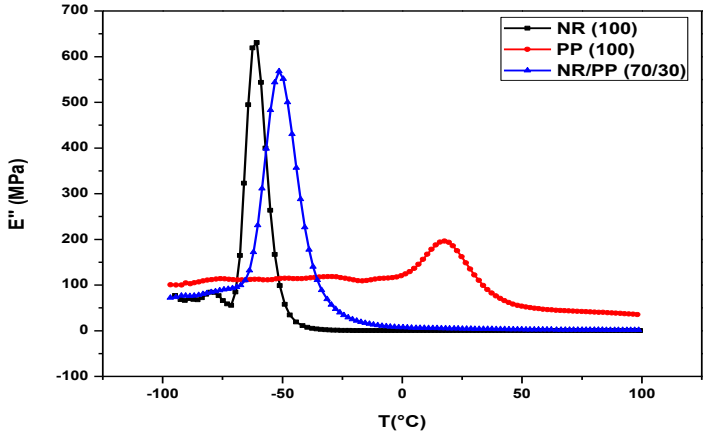

Figure IV.16 Variation of the loss modulus E" as a function of temperature for neat NR, neat PP and NR/PP blend.

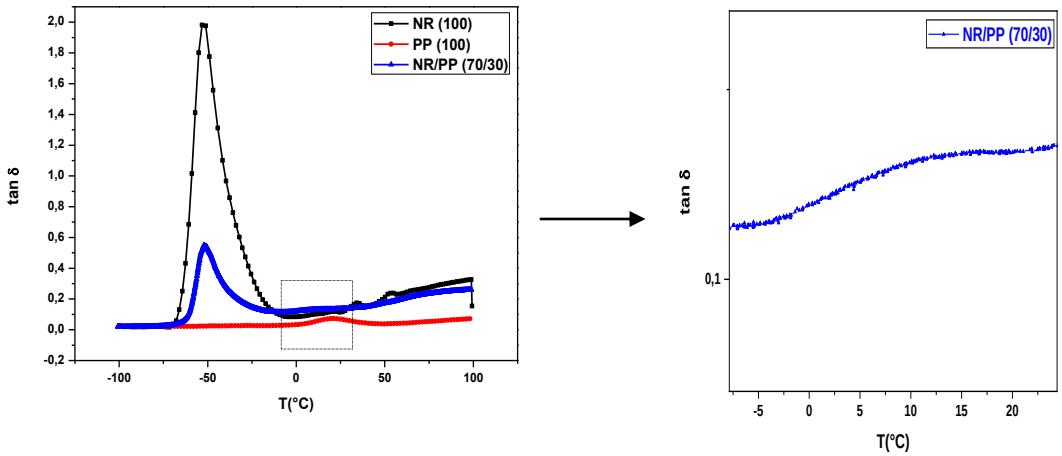

Figure IV.17 Variation of the damping factor tan δ as a function of temperature for neat NR, neat PP and NR/PP blend.

IV.2.4 Dynamic mechanical properties of the CA-containing TPE blends

The variation of the storage modulus E', loss modulus E", and damping factor tan δ as a function of temperature for the CA_{25}-containing blends: (NR/PP/ENR_{25}/PP-g-MA) at different concentrations are presented in **Figure IV.18**, **Figure IV.19**, and **Figure IV.20**. Those for the CA_{50}-containing blends are presented in **Figure IV.21**,**Figure IV.22**, and **Figure IV.23**, respectively.

Figure IV.18, and **Figure IV.21**, show that in the glassy region (below Tg), as the concentration of the CA increases, the storage modulus increases. However, these differences disappear in the flow region where all the curves superimpose. On the other hand, as shown in **Figure IV.19**, and **Figure IV.22**, it is observed that as the concentration of the CA increases the maximum E" position decreases and the corresponding Tgs shift to higher values.

These effects are reflected in the plots of tan δ as a function of temperature (**Figure IV.20**, and **Figure IV.23**) where it is observed that the higher the concentration of the compatibilizing agent the broader is the tan δ peak and the higher is the shift in the Tg value.

The respective values of Tg are summarized in **Table IV.1**. In fact, the glass transition temperature shifted by 11°C, 17°C, and 18°C when increasing the concentration of CA_{25} by 5, 10, and 15 Phr, respectively. However, these shifts (maximum E" position, and Tg value from tanδ peak) were not to the same extent for the CA_{50}–based systems. For example, the Tg value differences was only 1°C when increasing the CA_{50} concentration from 5 to 15 Phr (Tg B4 (5Phr)CA_{50}= -38°C,Tg B5 (10Phr)CA_{50} = -38°C , Tg B6 (15Phr)CA_{50} = -39°C). This means that the concentration of the CA_{50} did not seem to affect much the extent of the Tg values.

Moreover, these shifts were accompanied by a disappearance of the β transition peak (relative to the PP phase) with respect to the control NR/PP blend (B0).

An analogous improvement of the storage modulus in compatibilized blends has been described in the literature. For instance, Zachariah Oommen et al. **[15]** studied the effect of NR-g-PMMA as a compatibilizer on the dynamic mechanical and thermal properties of NR/PMMA blends. They have found that the addition of a compatibilizer increased the interfacial adhesion and improved the storage modulus of the blend at lower temperature.

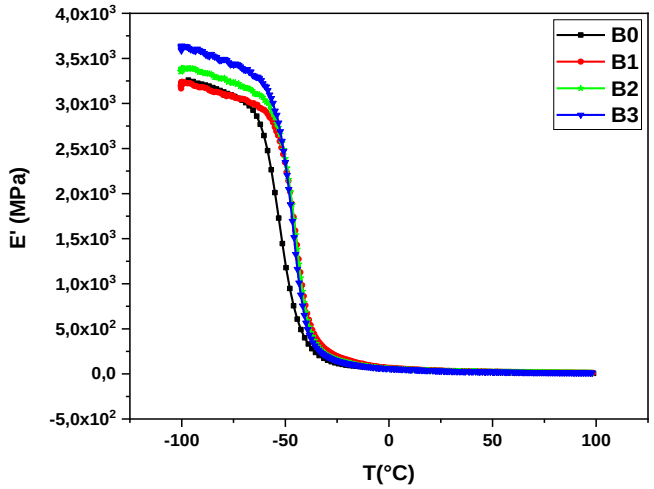

Figure IV.18 Variation of the storage modulus E' as a function of temperature for B0: NR/PP, B1: NR/PP/CA_{25} (5 phr), B2: NR/PP/CA_{25} (10 phr), B3: NR/PP/CA_{25} (15 phr).

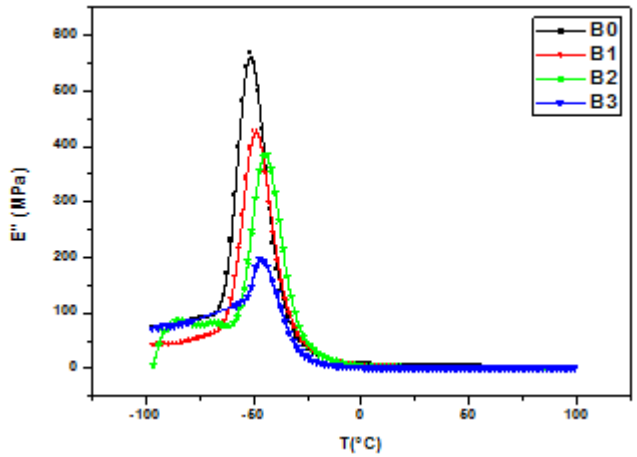

Figure IV.19 Variation of the loss modulus E'' as a function of temperature for B0: NR/PP, B1: NR/PP/CA_{25} (5 phr), B2: NR/PP/CA_{25} (10 phr), B3: NR/PP/CA_{25} (15 phr).

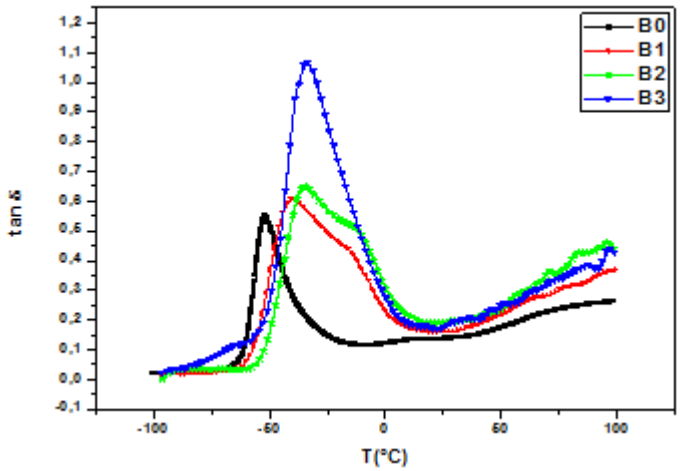

Figure IV.20 Variation of the damping factor tan δ as a function of temperature for B0: NR/PP, B1: NR/PP/CA_{25} (5 phr), B2: NR/PP/CA_{25} (10 phr), B3: NR/PP/CA_{25} (15 phr).

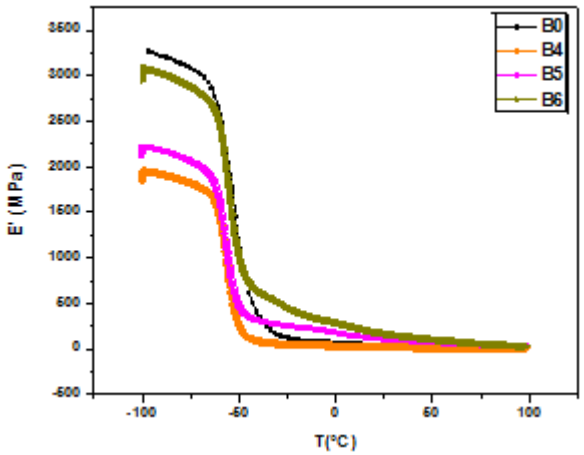

Figure IV.21 Variation of the storage modulus E' as a function of temperature for B0: NR/PP, B4: NR/PP/CA_{50} (5 phr), B5: NR/PP/CA_{50}(10 phr), B6: NR/PP/CA_{50} (15 phr).

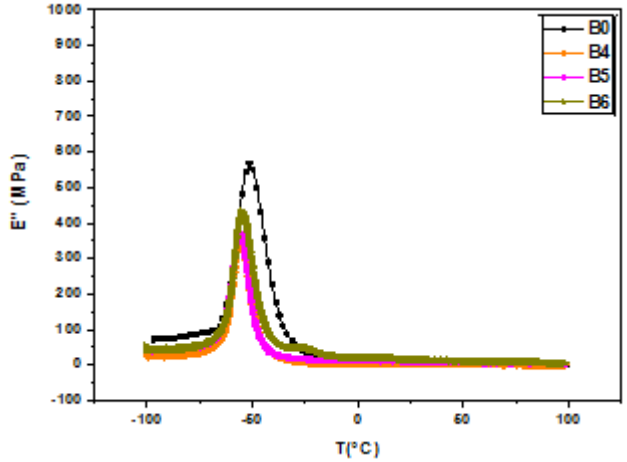

Figure IV.22 Variation of the loss modulus E" as a function of temperature for B0: NR/PP, B4: NR/PP/CA_{50} (5 phr), B5: NR/PP/CA_{50}(10 phr), B6: NR/PP/CA_{50} (15 phr).

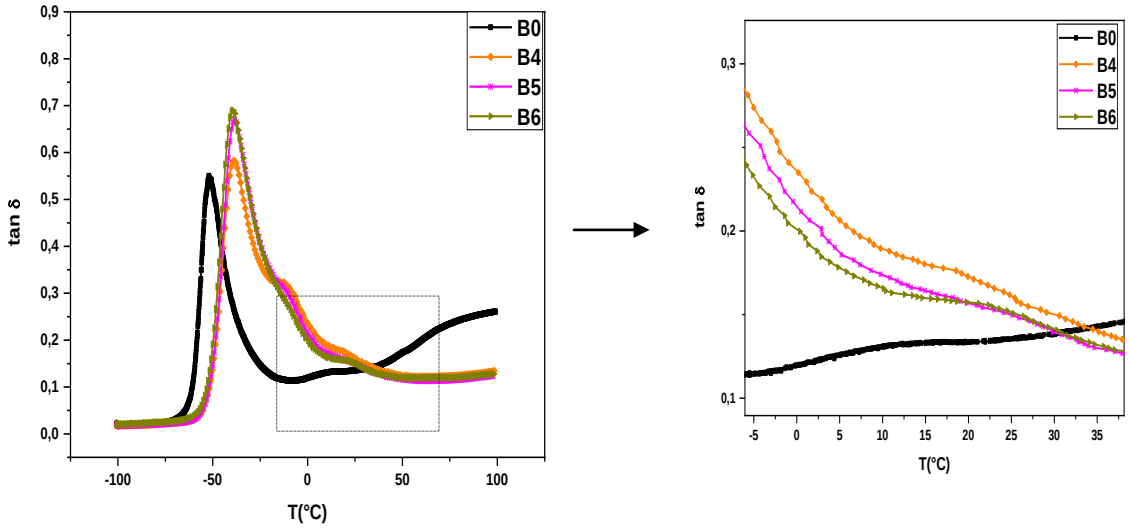

Figure IV.23 Variation of the damping factor tan δ as a function of temperature for B0: NR/PP, B4: NR/PP/CA_{50} (5 phr), B5: NR/PP/CA_{50}(10 phr), B6: NR/PP/CA_{50} (15 phr).

Table IV.1 Values of the different transitions (T_g, T_β) for the different polymers and those of the CA-containing TPE blends.

Blends	T_g (°C)	T_β (°C)
NR	-53	-
ENR_{25}	-27	-
ENR_{50}	-3	-
PP	-	21
PP-g-MA	-	8
CA_{25}	-19	-
CA_{50}	9	-
B0	-52	13
B1	-41	-
B2	-35	-
B3	-34	-
B4	-38	-
B5	-38	-
B6	-39	-

IV.2.5 Dynamic mechanical properties of the CA-containing TPV blends

The plots of the storage modulus (E'), the loss modulus (E''), and the damping factor (tan δ) as a function of temperature for the dynamically vulcanized blends are presented in **Figure IV.24**, **Figure IV.25**, and **Figure IV.26** for the CA_{25}-based systems and in **Figure IV.27**, **Figure IV.28**, and **Figure IV.29** for the CA_{50}- based blends.

To examine the contribution of the dynamic vulcanization, the variation of E', E'', and tanδ as a function of temperature for a constant concentration of the compatibilizing agent (10 Phr) were gathered along with those of the control blend and are presented in **Figure IV.30**, **Figure IV.31**, and **Figure IV.32**.

Overall, the same effects which were noted for the unvulcanized blends were also observed for the dynamically vulcanized systems. That is:

1- An increase of the storage modulus E' with increasing the concentration of the compatibilizing agent (CA_{25} or CA_{50}),
2- A decrease of the loss modulus E'' and the maximum tan δ peak position with increasing the concentration of the compatibilizing agents.

However, a particular result which is worth to be emphasized is the fact that the dynamic vulcanization did not affect much the Tg value of the vulcanized blends compared to the

control TPV blend. For example as shown in **Table IV.2**, the Tg decreased only by 1°C when increasing the concentration of the CA_{25} from 5 to 15 Phr and remained unchanged for the CA_{50} at the three concentrations studied.

It is to be noted that contrarily to the unvulcanized blends (**Figure IV.20,** and **Figure IV.23**), increasing the concentration of the CA_{50} decreased much the value of the T_β transition. For instance, T_β decreased from 12°C for the control NR/PP TPV blend to 8°C for the 5 Phr of CA_{50}-containing blend. It decreased further to 4°C for the 10 Phr CA_{50}-containing blend.

In fact, while the T_β peak disappeared for the unvulcanized CA_{25} or CA_{50} –containing blends (See **Figure IV.20**, and **Figure IV.23**), it shifted by almost 9°C for the CA_{50}TPV (T_β= 3°C for 15Phr of CA_{50})with respect to the control blend (T_β=12°C) (an amplification of these transition is shown in **Figure IV.26**, and **Figure IV.29**, respectively.

A similar effect was found by Benmesli et al. **[16],** who reported a shift by 10°C of this transition as a result of the functionalization of the NR phase and that of the PP phase. It can therefore be stated that the incorporation of the ENR/PP-g-MA as a compatibilizing agent resulted in an alteration of the NR/PP interphase.

These conflicting effects, i.e the fact that the β transition disappeared for the unvulcanized blend, but was more pronounced for the dynamically vulcanized system, reflect also the complexity of the blend studied owing to the contribution of many factors which are the epoxy group in ENR, the maleic anhydride group in PP, the ester and acid based linkage formed after mixing ENR with PP-g-MA and the vulcanization system.

Table IV.2 Values of the different transitions (T_g, T_β) for TPV blends with and without compatibilizers.

TPV Blends	T_g (°C)	T_β(°C)
B0V	-48	12
B1V	-47	13
B2V	-48	13
B3V	-49	13
B4V	-48	8
B5V	-48	3
B6V	-48	3

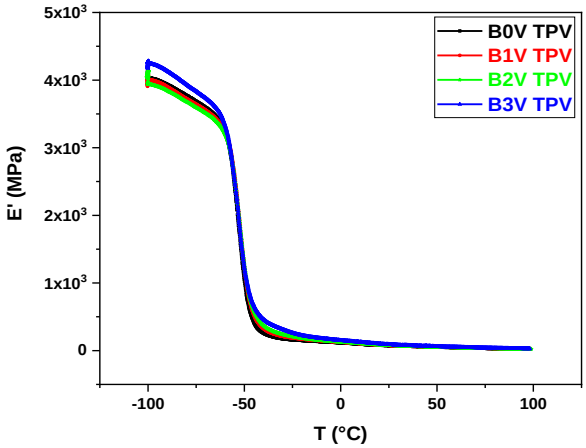

Figure IV.24 Variation of the storage modulus E' as a function of temperature for B0V: NR/PP, B1V: NR/PP/CA_{25} (5 phr), B2V: NR/PP/CA_{25} (10 phr), B3V: NR/PP/CA_{25} (15 phr) TPV blends.

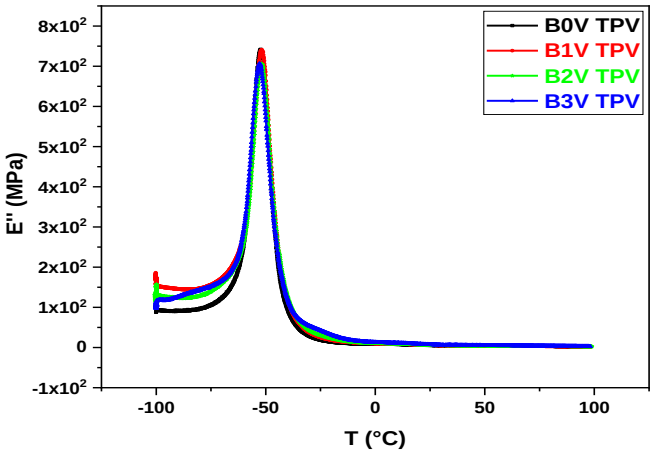

Figure IV.25 Variation of the loss modulus E'' as a function of temperature for B0V: NR/PP, B1V: NR/PP/CA_{25} (5 phr), B2V: NR/PP/CA_{25} (10 phr), B3V: NR/PP/CA_{25} (15 phr) TPV blends.

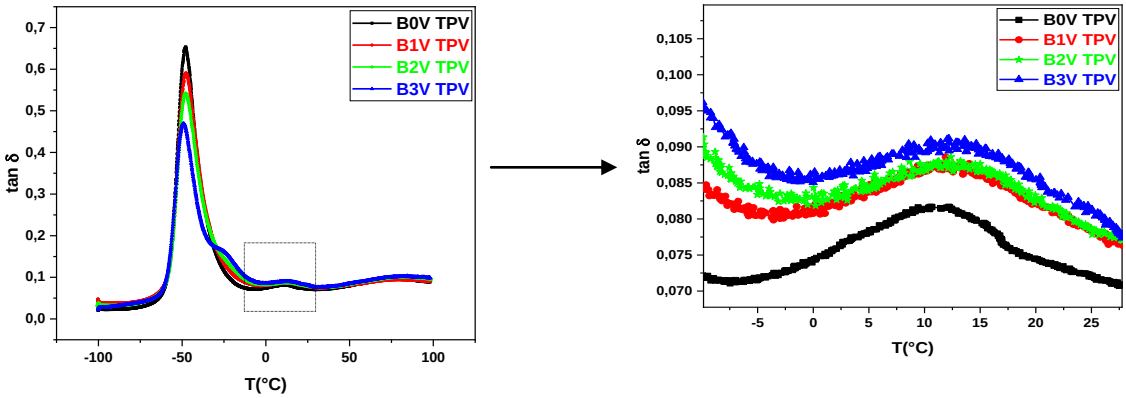

Figure IV.26 Variation of the damping factor tan δ as a function of temperature for B0V: NR/PP, B1V: NR/PP/CA_{25} (5 phr), B2V: NR/PP/CA_{25} (10 phr), B3V: NR/PP/CA_{25} (15 phr) TPV blends.

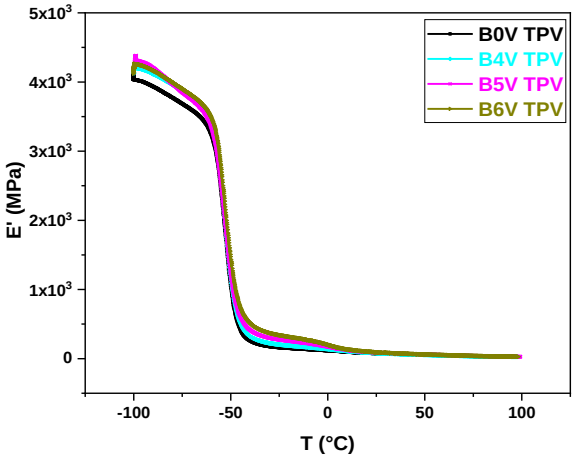

Figure IV.27 Variation of the storage modulus E' as a function of temperature for B0V: NR/PP, B4V: NR/PP/CA_{50} (5 phr), B5V: NR/PP/CA_{50} (10 phr), B6V: NR/PP/CA_{50} (15 phr) TPV blends.

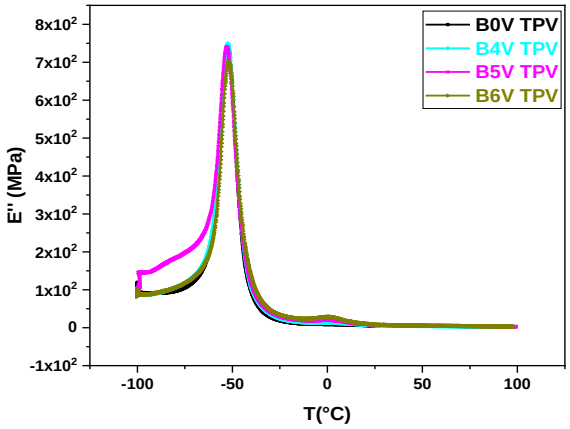

Figure IV.28 Variation of the loss modulus E'' as a function of temperature for B0V: NR/PP, B4V: NR/PP/CA_{50} (5 phr), B5V: NR/PP/CA_{50} (10 phr), B6V: NR/PP/CA_{50} (15 phr) TPV blends.

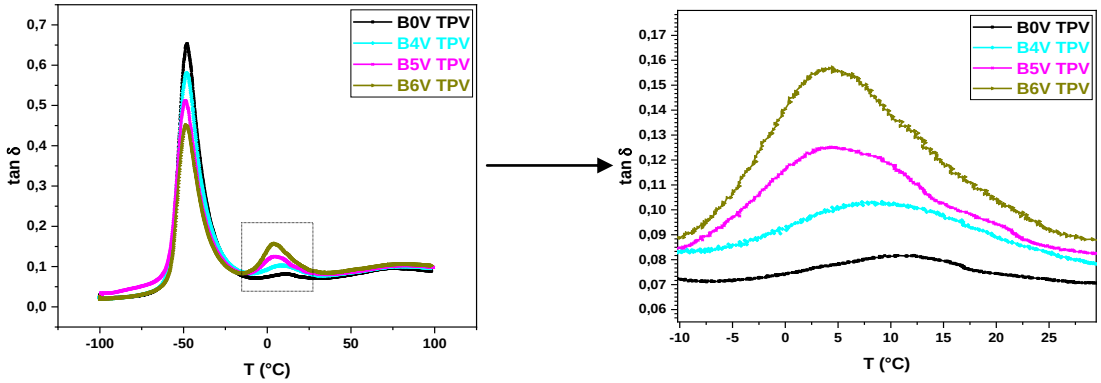

Figure IV.29 Variation of the damping factor tan δ as a function of temperature for B0V: NR/PP, B4V: NR/PP/CA_{50} (5 phr), B5V: NR/PP/CA_{50} (10 phr), B6V: NR/PP/CA_{50} (15 phr) TPV blends.

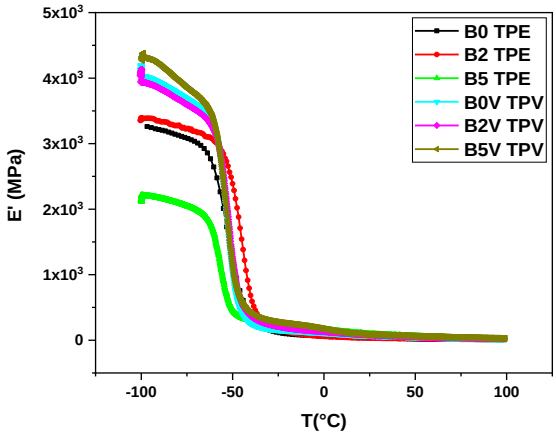

Figure IV.30 Variation of the storage modulus E' as a function of temperature for the control NR/PP, and those of the 10Phr of CA_{25}, and CA_{50}-containing TPE and TPV blends.

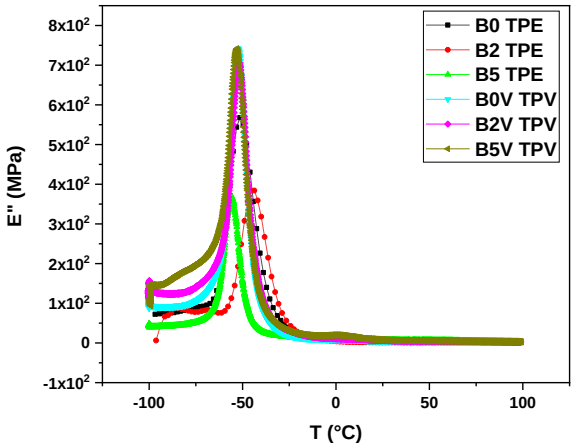

Figure IV.31 Variation of the loss modulus E" as a function of temperature for the control NR/PP, and those of the 10Phr of CA_{25}, and CA_{50}-containing TPE and TPV blends.

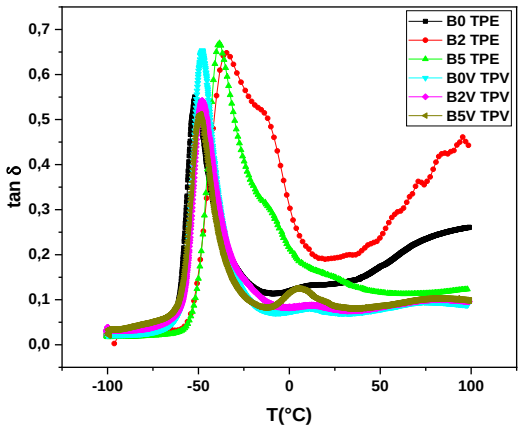

Figure IV.32 Variation of the damping factor tan δ as a function of temperature for the control NR/PP, and those of the 10Phr of CA_{25}, and CA_{50}-containing TPE and TPV blends.

IV.3 Morphological Examination

It has been established that the properties of polymer blends depend on the morphology and the interfacial adhesion which develop between the matrix and the blend components **[2].**Therefore, the morphology as characterized by the SEM can be an effective way to make correlations with the mechanical behavior of the material.

Morphology depends on blend composition, melt viscosity of the components and processing history. When the components have different melt viscosities the morphology of the resulting blends depends on whether the minor component has a lower or higher viscosity than the major one.

The results of the morphological analysis of the NR/PP based TPE is presented in this chapter. The morphology of the blends was investigated using Scanning Eelectron Microscopy (SEM) and also by Atomic Force Microscopy (AFM).

As mentioned earlier, the majority of polymer blends are immiscible due to thermodynamic limitations. Hence, blending usually leads to multiphase heterogeneous morphologies where the properties of the polymeric constituents, interface adhesion and the final morphology often dictate the ultimate properties of these materials **[17].** The morphology development during the melt mixing stage, i.e. the size, shape and distribution of one polymeric phase into another, strictly depends on the rheological properties of the constituent polymers, the presence of different types of additives, compatibilizers, the interfacial tension and processing conditions **[18].**

IV.3.1 SEM analysis

IV.3.1.1 Effect of the compatibilizing agents on the morphology of the TPE blends

Figure IV.33 (a) through (c) presents the SEM micrographs of the control NR/PP blend, those of the 10 phr CA_{25}, and CA_{50}-containing TPE blends, respectively. A dosage of 10 phr is considered as the medium amount of the CAs studied. These micrographs show co-continuous phases with dark voids left after the extraction of the PP phase. For the control blend, these voids are randomly dispersed throughout the NR matrix and have different irregular shapes and sizes **[19].**

However, in the CA-containing blends, the pores which are smaller in size, they seem to be dispersed in a more regular manner. This distinction could be due to the improved adhesion resulting from the interactions mentioned earlier. The presence of the polar groups in the CA

composed of a 1:1 ratio of ENR to PP-g-MA contributed to the reduction of the interfacial tension between the NR and PP phases and resulted in a more homogeneous morphology. These observations are consistent with the results of the mechanical properties where it was found that the blends with the CA exhibited higher tensile resistance. Choudhury and Bhowmick who investigated the compatibilization of NR/polyolefins TPE blends have reported similar observations **[20].**

In fact, the compatibilizer decreases the interfacial tension and the interaction between NR and PP is greatly enhanced. The ENR/PP-g-MA locates at the blend interface and thereby holds the two phases together. The localization of the compatibilizer at the interface makes the interface less mobile, more broad and stable. In the case of incompatible NR/PP blend, due to the presence of a sharp interface and poor interaction between the polymer phases there occurs high extent of inter layer slippage between the phases. Upon the addition of the CAs interfacial interaction between the phases increases and there will be less slippage at the interface. The ENR/PP-g-MA addition decreases the interfacial tension and this leads to a reduction in the dispersed phase size and an increase in interfacial adhesion. In addition to the increase in interfacial adhesion, the presence of the compatibilizer at the blend interface broadens the interface region through penetration of the CAs chains into the adjacent phases which stabilises the blend morphology.

(a)

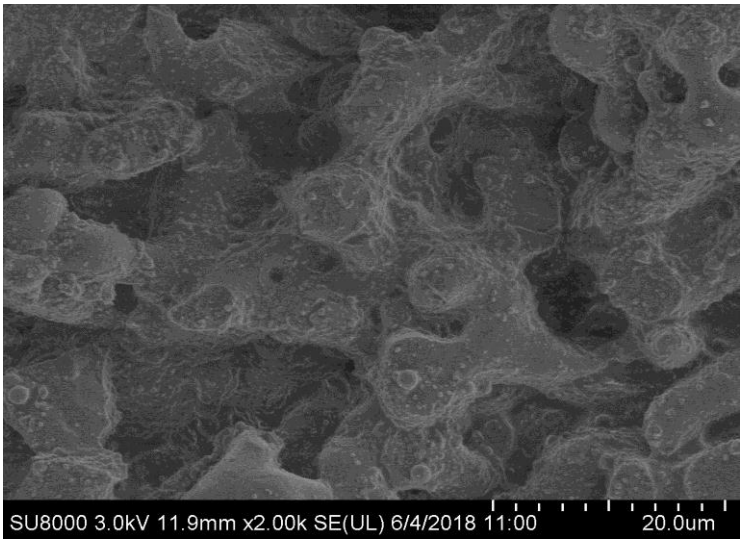

(b)

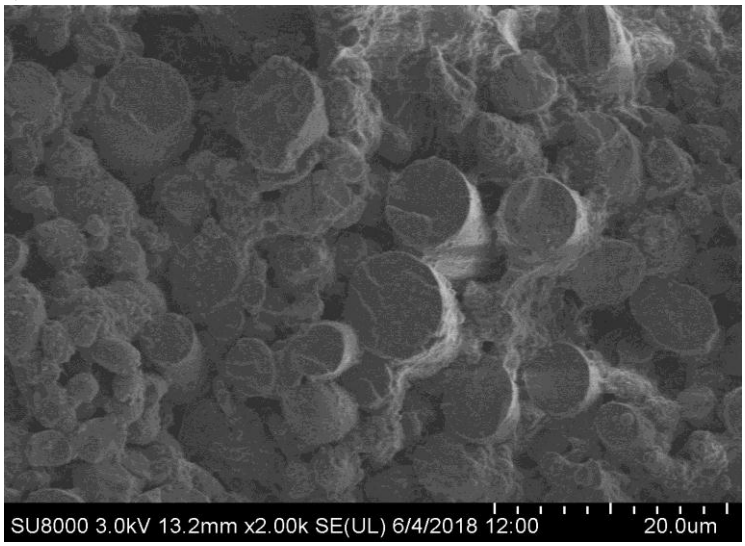

(c)

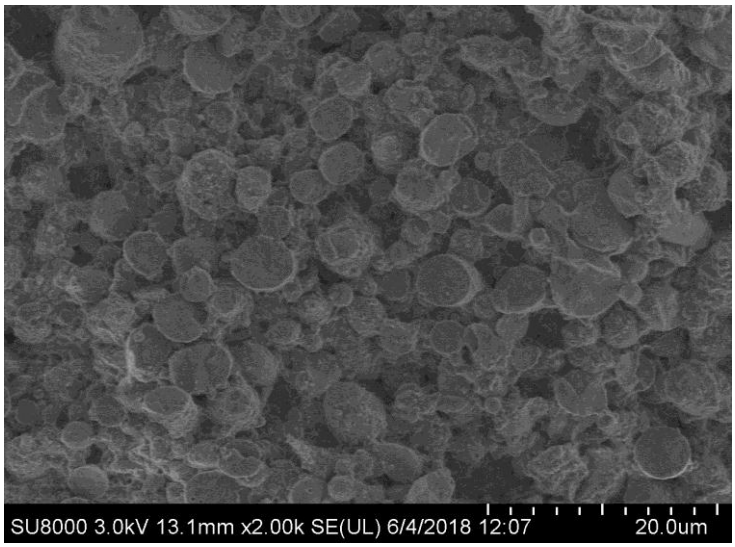

Figure IV.33 SEM micrographs of (a) the control NR/PP blend, (b) NR/PP/CA_{25} (10phr), and (c) NR/PP/CA_{50} (10phr).

IV.3.1.2 Effect of dynamic vulcanization on the morphology of the TPV blends

The evolution of phase morphology in polymer blends generally takes place while the rheological, interfacial, and thermodynamic properties of the components are changing. In the case of dynamic vulcanization of thermoplastic/elastomer blends, it is mainly the crosslinking reaction of the elastomeric component which influences all the aforementioned properties. The gradual formation of crosslinked elastomer network increases both the viscosity and the elasticity of the elastomer, and affects drastically the morphology development. Throughout this process, the elastomeric major phase, although within a co-continuous structure with its thermoplastic counterpart, is transformed into dispersed particles encapsulated by the thermoplastic polymer. This morphological transformation is widely known as phase inversion. The result is a material most likely with rubber-like properties **[21]**.

H.-J.Radusch reported that the elastomer phase in the initial stage of vulcanization is strongly deformed into continuous elastomeric threads and eventually breaks up and forms the final dispersed crosslinked domains **[21].** As mentioned earlier, the presence of an initial co-continuous morphology prior to dynamic vulcanization is a prerequisite in obtaining fine dispersed crosslinked elastomer phase at the end of vulcanization **[21-22].**The effectiveness of stress transfer and morphology transformation in an initially co-continuous morphology can be visualized by considering the complete opposite hypothetical situation, i.e., an initial dispersed/matrix morphology with the elastomeric component as the droplet phase. In this system, the viscosity and elasticity of the elastomeric component, which already forms the dispersed phase, increase during dynamic vulcanization. As a result, the stress transferred by the low viscosity thermo-plastic phase becomes less and less effective in deforming the elastomeric domains and coalescence of the elastomeric domains becomes more and more hindered due to increased viscosity and elasticity of this phase **[23-25].** SEM micrographs of the solvent-etched cryogenic fracture surfaces of the 70/30 NR/PP TPVs with different concentrations of the compatibilizers are shown in **Figure IV.34**. Xylene was used to extract the PP phase at high temperature. That is, the thermoplastic phase was dissolved in hot xylene, which left the vulcanized rubber adhered at the surface.

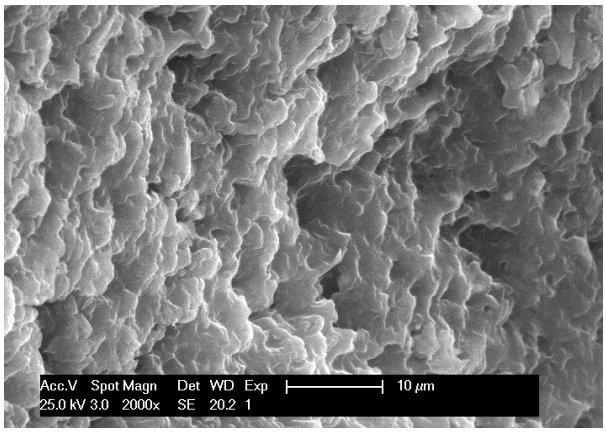

A: NR/PP without compatibilizer

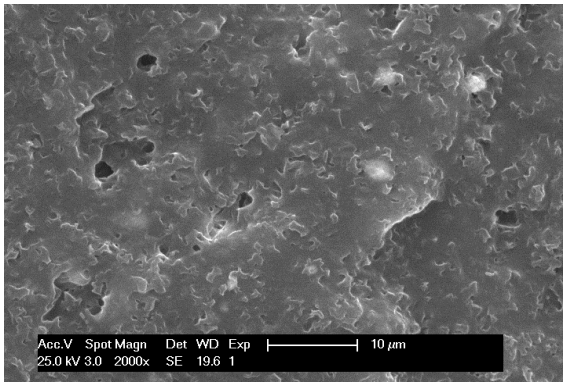

B: NR/PP with ENR_{25}/PP-g-MA (5Phr)

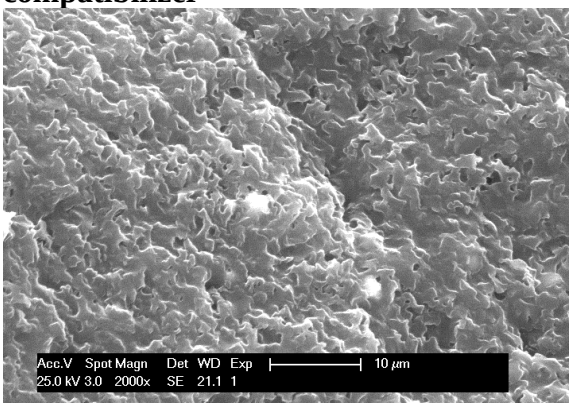

E: NR/PP with ENR_{50}/PP-g-MA (5Phr)

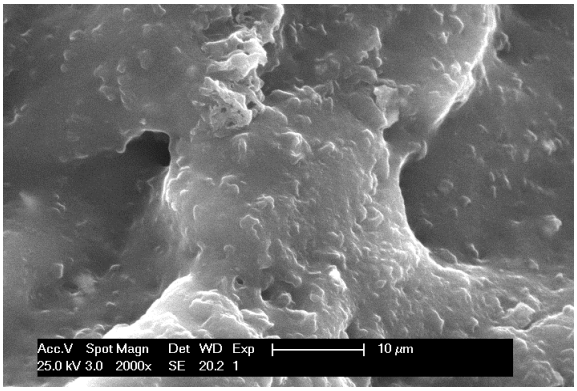

C: NR/PP with ENR_{25}/PP-g-MA (10Phr)

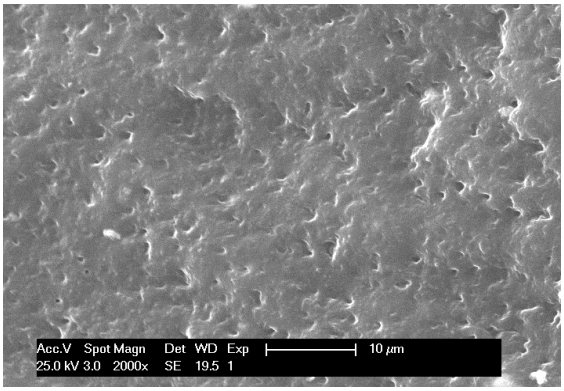

F: NR/PP with ENR_{50}/PP-g-MA (10 Phr)

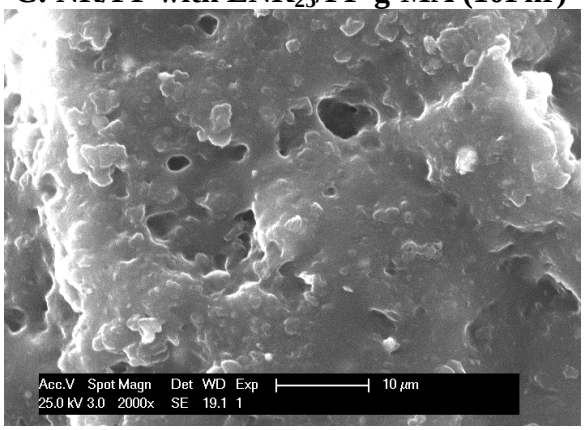

D: NR/PP with ENR_{25}/PP-g-MA (15 Phr)

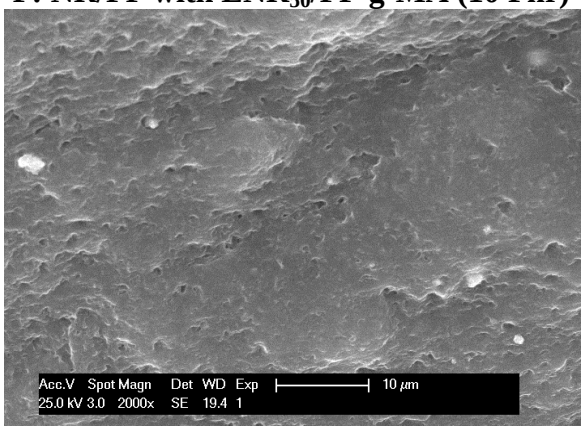

G: NR/PP with ENR_{50}/PP-g-MA (15 Phr)

Figure IV.34 SEM micrographs of NR/PP TPVs with two types and different concentrations of CAs.

According to **Figure IV.34**, it can be observed that the TPV without compatibilizer (Control NR/PP (**Figure IV.34** (**A**)) shows large and non-uniform rubber particles, whilst the other compatibilized and dynamically vulcanized TPVs show smaller and finely dispersed rubber particle morphology.

It can also be seen that the vulcanized rubber particles in the TPVs with ENR_{25}/PP-g-MA show larger sizes than those of the TPVs prepared with ENR_{50}/PP-g-MA at equal amount. Therefore, it can be stated that the size of the dispersed vulcanized rubber particles decreased with an increase in the level of epoxide groups in the ENR molecules.

IV.3.2 Atomic Force Microscopy

IV.3.2.1Effect of the compatibilizing agents on the morphology of the TPE blends

Atomic Force Microscopy is considered as one of the most perspective methods for studying polymer blends, because it allows to clearly define the phase boundary and its scale. In this research work, AFM was used to evaluate the effect of the compatibilizing agents on the interface morphology. **Figure IV.35** shows respectively the AFM Height and Phase images, of the 70/30 NR/PP TPE blend (a),(d),NR/PP/CA_{25} (10phr) (b),(e), and NR/PP/CA_{50} (10 phr) (c),(f). Height images reveal the surface roughness, while the measurement of the difference between the phase angle of the excitation signal and the phase angle of the cantilever response can be used to map compositional variations such as stiffness, hardness and viscoelasticity during scanning the surface sample in the AFM tapping mode. So the phase signal gives information about the size and shape of local heterogeneities at a nanometric scale, identifying regions with different stiffness. After the cryo-microtoming procedure, NR and PP expand differently, because they have different thermal coefficients and this fact provokes a high roughness in the AFM height image which corresponds to the NR/PP control blend compared to NR/PP/CA specimens. Garcia et al **[26]** reported that the morphology can be analyzed by the different color in the images, where these differences represent the hardness scale. Since the samples are mostly composed of natural rubber, PP and CA, depending on the formulation, two color scales were observed. With regard to AFM phase image of this specimen, two clearly different zones are observed, hence, the bright zones correspond to the PP phase and the dark zones correspond to the NR phase. The morphological properties are dramatically different in the case of AFM phase images, when the compatibilizer is added. So, a change in the bright zones is observed. In the case of NR/PP/CA_{25}, there are less bright zones than the control sample, due to the effect of the compatibilizing agent which promotes the adhesion between the two polymer phases. Nevertheless, the AFM phase image of NR/PP/CA_{50} shows the brightest zones. A possible explanation of this morphology is that it could be due to the fact that CA_{50} has more level of epoxide content compared to CA_{25}. Also ENR has higher viscosity than PP-g-MA (which has already been obtained through the RPA results), in addition to a higher compatibilizing effect due to the higher chemical interaction between the polar groups in ENR and PP-g-MA. The AFM phase image color depends on the rigidity of the components, in addition to other factors such as the type of tapping. However, since all the samples were prepared and measured under the same conditions, at moderate tapping, therefore, the changes in the rigidity can only be attributed to changes in the rigidity of the components as a result of the higher interactions induced by the CAs.

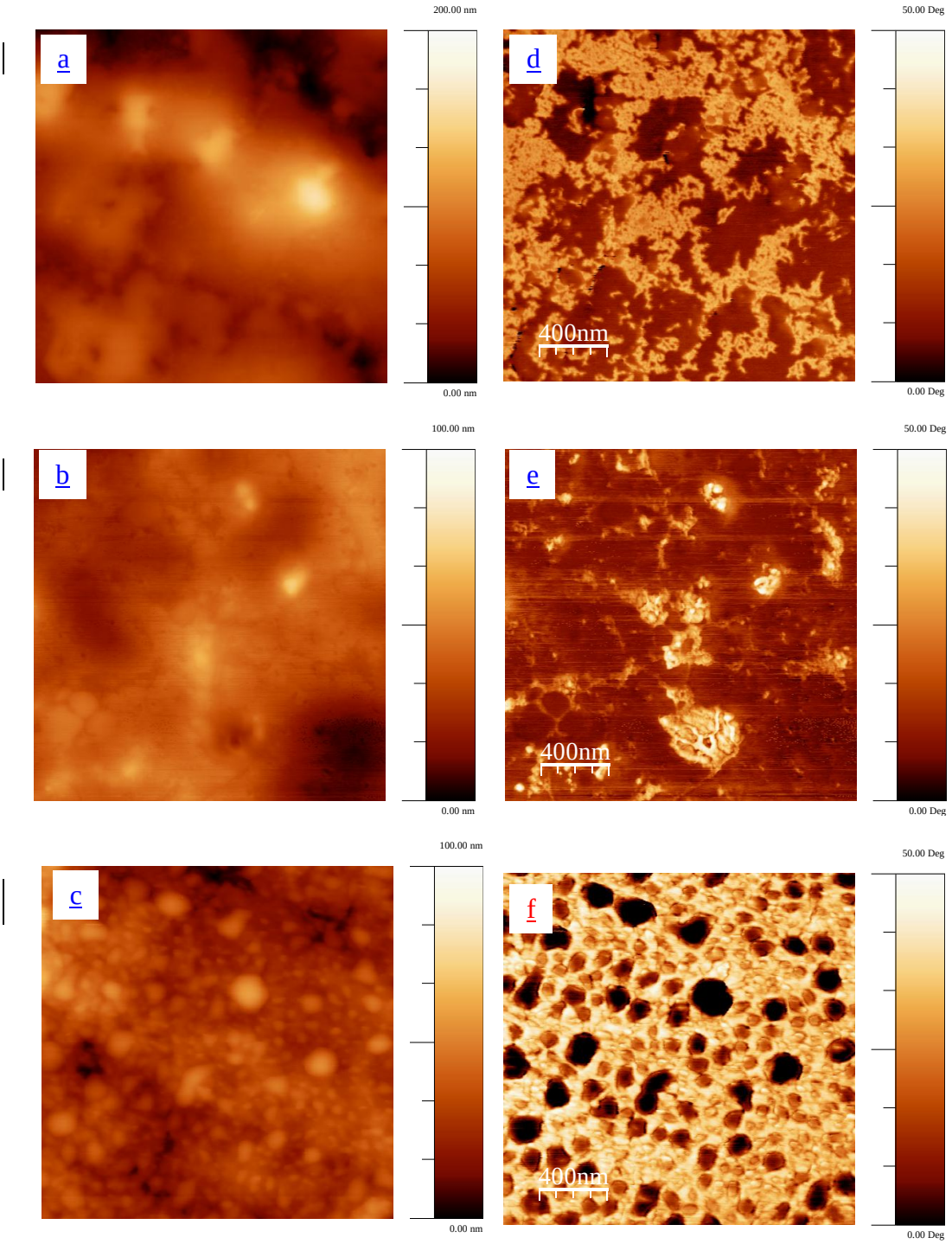

Figure IV.35 The AFM Height (a), (b), (c) and Phase (d), (e), (f) images of 70/30 NR/ PP TPE blends for the control NR/PP blend (a,d), NR/PP/CA_{25} (10phr) (b,e), and NR/PP/CA_{50} (10phr) (c,f). (Darker regions represent NR phase and lighter regions represent PP phase).

IV.3.2.2 Effect of dynamic vulcanization on the morphology of the TPV blends

For a 70/30 NR/PP composition, prior to dynamic vulcanization, PP is the minor component and is the dispersed phase in the NR matrix. During dynamic vulcanization of such a blend, NR and PP have to undergo a phase inversion to maintain the thermoplasticity of the blend. The usual way for preparing TPVs is, first, melt-mixing rubber with a thermoplastic, and co-continuous phase morphology is generated. Subsequently, a vulcanization agent for rubber is added to crosslink the rubber phase. Then, the rubber phase is no longer able to coalesce into a continuous phase. As the degree of crosslinking advances during mixing, the continuous rubber phase becomes elongated further and then breaks up into polymer droplets. As these droplets form, the thermoplastic polymer becomes the continuous phase. Thus, TPVs with fine dispersed rubber particles in the thermoplastic matrix will be obtained.

As noted in the Experimental part, NR/PP TPVs were prepared according to the following method, that is, NR was first compounded using a two-roll mill at room temperature. Then the PP was first preheated for 5 minutes in the mixing chamber without rotation. It was then melted for 2 minutes at a rotor speed of 60 rpm. The compatibilizer was incorporated and mixed for 2 minutes. The NR compound containing the curatives was added and mixing was continued until a plateau mixing torque was reached. The blend products were finally pelletized and the final product was cut into small pieces. AFM images were measured to check the occurrence of phase inversion.

To study the morphological changes of the dynamically cured NR/PP blend, the height and phase images of the three selected samples are shown in **Figure IV.36**. The darker regions represent the PP phase, and the lighter regions represent the NR phase. As shown in **Figure IV.36**, a co-continuous structure is observed in Height and Phase images, for the 70/30 control NR/PP TPV blend (a),(d),NR/PP/CA_{25} (10phr) (b),(e), and NR/PP/CA_{50} (10 phr) (c),(f) TPV blends, respectively. This morphology is ascribed to the coalescence of some NR rubber droplets.

Figure IV.36 (d) is an AFM image of the dynamically vulcanized NR/PP. In this micrograph, the morphology of large crosslinked NR particles (light) which are dispersed in the PP matrix (dark) can be observed, indicating the occurrence of phase inversion, and the large rubber particles have a tendency to be co-continuous because no compatibilizer was added.

Figure IV.36 (e, and f) presents the AFM images of the dynamically vulcanized NR/PP/CAs blends, wherein the light area represents the crosslinked rubber phase and the dark area is the

PP phase. From these AFM images, it can be seen that for a 10 Phr of ENR/PP-g-MA content, phase inversion exists and the rubber phase is finely dispersed in the PP matrix.

Furthermore, the size of the crosslinked rubber particles decreases especially for the CA_{50}-containig blends **(Figure IV.36 (f))** (higher epoxidation level in CA_{50} than in CA_{25})

A plausible explanation for this morphology is that the dynamic vulcanization which caused an increase of the viscosity of the NR phase, while that of PP maintaining its flow mobility, resulted in phase inversion.

Different forms and sizes of the two phases change as more interactions develop, especially for the CA_{50}-containing system compared to the control NR/PP thermoplastic vulcanizate blend **(Figure IV.36 (d)).**

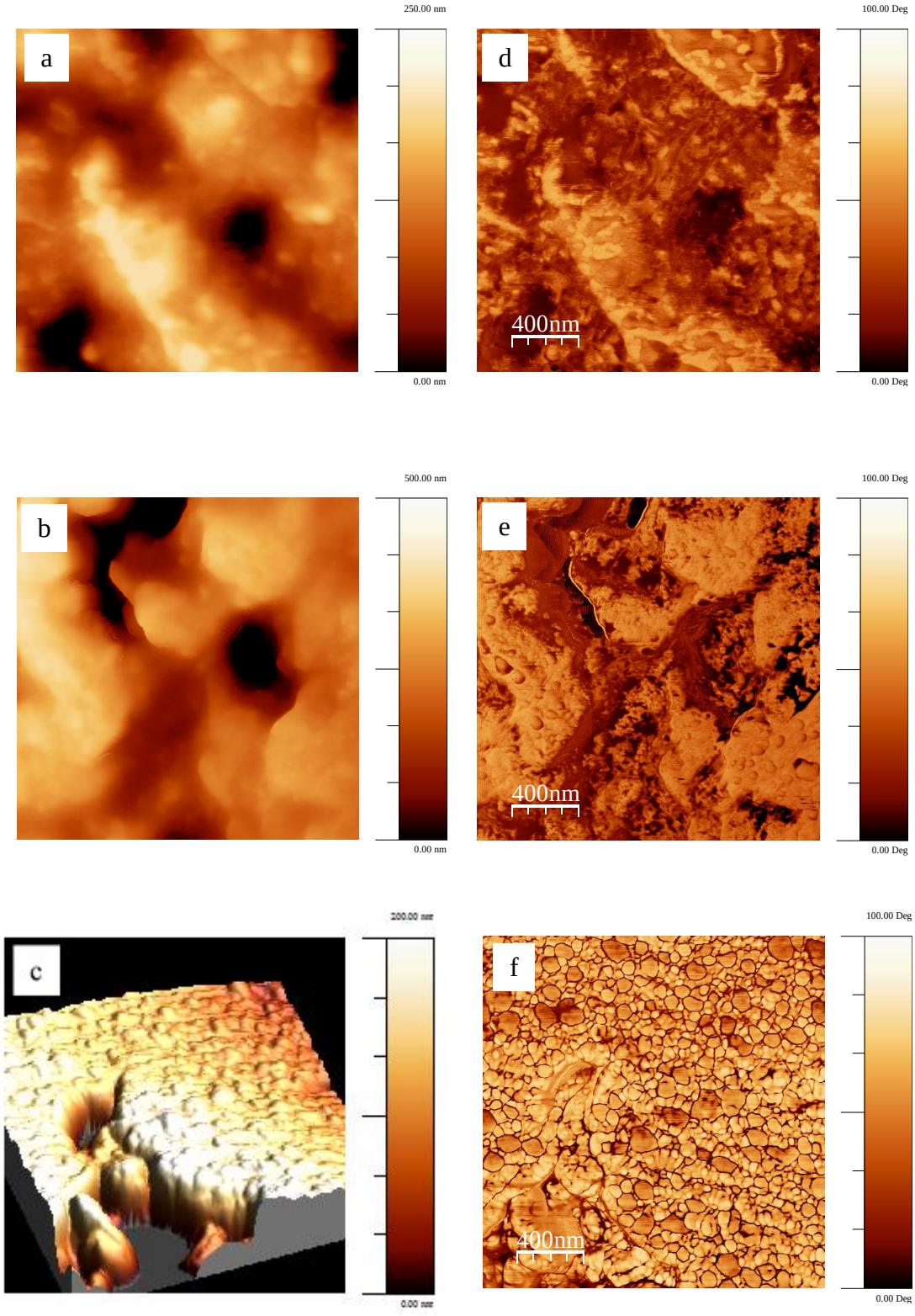

Figure IV.36 The AFM Height (a), (b), (c) and Phase (d), (e), (f) images of 70/30 NR/ PP TPV blends for the control NR/PP blend (a,d), NR/PP/CA_{25} (10phr) (b,e), and NR/PP/CA_{50} (10phr) (c,f). (Darker regions represent PP phase and lighter regions represent NR phase).

IV.4 Thermal properties

Thermal stability is relevant for the use of polymeric materials in a growing field of applications. A detailed understanding of the thermal degradation/ stability and of the kinetic parameters of polymers is important in the design of materials for specific use **[27,28].** Polymer blending has a great influence on the thermal stability of individual polymers **[29].** One of the widely accepted methods for studying the thermal properties of polymeric materials is thermogravimetry (TG). Thermogravimetric data will provide the number of stages of thermal breakdown, weight loss of the material in each stage, threshold temperature .etc. Both thermogravimetry (TG) and derivative thermogravimetry (DTG) provide information about the nature and conditions of degradation of the material. Compatibility of the polymer blends can be studied by differential scanning calorimetry (DSC). This will inform about the glass transition temperature (Tg) and melting temperature (Tm) of the polymeric material. Miscible blends will show single, sharp transition peak (Tg) intermediate between that of the blend components. Separate peaks will be obtained for immiscible blends. In the case of borderline miscible blends, broad transition peaks are obtained **[30-35].**

The aim of this chapter is to study the thermal properties of both the unvulcanized and dynamically vulcanized NR/PP blends with and without the addition of the compatibilizer (ENR/PP-g-MA).

IV.4.1 Differential scanning calorimetry

IV.4.1.1 Thermal properties of the parent polymers

Figure IV.37 shows the DSC thermograms of neat PP and PP-g-MA during the second heating and cooling cycles, respectively. The DSC thermograms of neat NR, neat ENR_{25}, and neat ENR_{50} are shown in **Figure IV.38**. According to **Figure IV.37**, it is seen that the crystallization temperature (Tc) and melting temperature (Tm) of PP and PP-g-MA were observed in these thermograms. The melting temperature of PP and its heat of fusion ΔH_f, Tm= 159°C,ΔH_f= 88 J/g are slightly higher than those of PP-g-MA, Tm= 157°C,ΔH_f= 85 J/g, respectively. On the other hand, it is observed that the crystallization temperature of PP-g-MA as well as its heat of crystallization ΔHc,Tc=112°C,ΔHc= -83 J/g are lower than those of PP, Tc=116 °C,ΔHc = -78 J/g. This is probably due to the fact that the grafted branches disrupted the regularity of the chain structures in PP and increased the spacing's between the chains; consequently, the percentage crystallization and therefore ΔH decreased.

According to **Figure IV.38**, it is seen that the Tg of neat NR, neat ENR_{25}, and neat ENR_{50} is −66°C, −41°C, and −22°C, respectively. The Tg of ENRs (either ENR_{25} or ENR_{50}) is higher than that of NR due to the insertion of the epoxy group in the polyisoprene chain, which decreases the rotational freedom of the polymer backbone. The Tg of ENR_{50} is higher than that of ENR_{25} due to higher polarity of ENR_{50}. This means that the higher the epoxidation level the higher is the Tg.

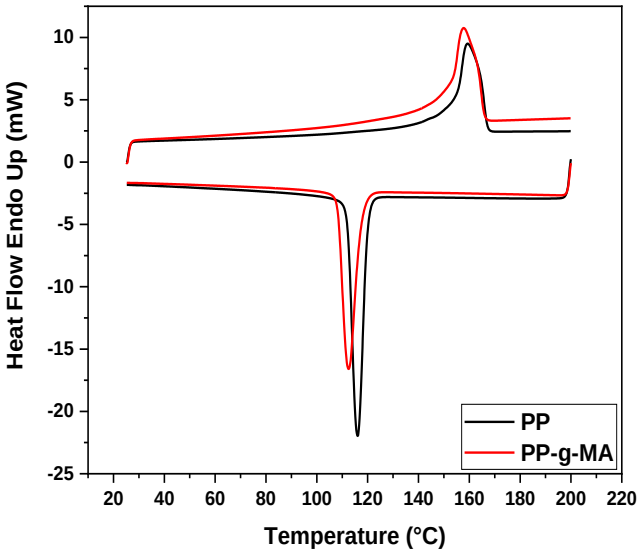

Figure IV.37 DSC thermograms of PP, and PP-g-MA.

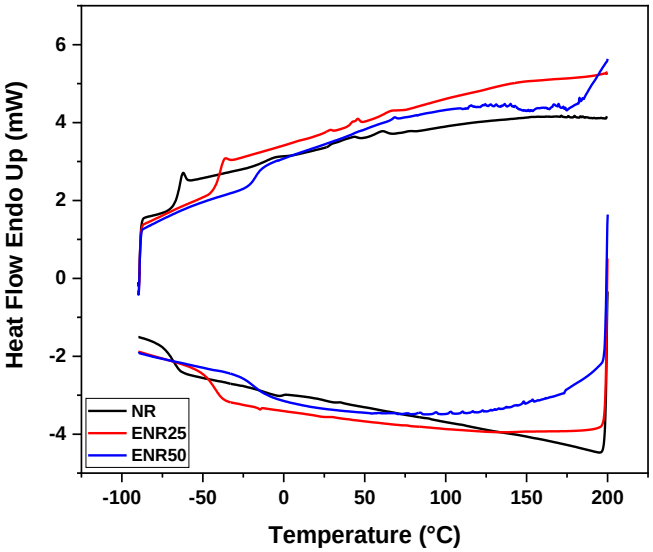

Figure IV.38 DSC thermograms of NR, ENR_{25}, and ENR_{50}.

IV.4.1.2 Thermal properties of the compatibilizing agents

Figure IV.39 shows the DSC thermograms for PP-g-MA, ENR_{25}, ENR_{50}, CA_{25}: ENR_{25}/PP-g-MA, and CA_{50}:ENR_{50}/PP-g-MA. It was found that the crystallization temperature (Tc) of neat PP-g-MA is about 112°C, and that of the PP-g-MA phase in CA_{25}, and CA_{50} blends shifted toward higher temperatures (118°C). On the other hand, the Tg of neat ENR_{25}, ENR_{50}, ENR_{25}/PP-g-MA, and ENR_{50}/PP-g-MA were found to be −41°C, −22°C, −42°C, and −16°C, respectively. It is also observed that the crystalline melting temperature (Tm) of ENRs/PP-g-MA (CAs) remained unchanged compared with neat PP-g-MA.

The decrease in crystallinity and increase of Tc in the CAs compared to neat PP is due to the fact that ENR reacted with PP-g-MA and resulted in a crosslinked structure. This is evidenced also by the increase of the glass transition temperature of the CAs since the crosslinked structure reduced the chain mobility. The increase of Tg was more pronounced in the case of CA_{50} due to a higher epoxydation level. This alteration of the degree of crystallization could also be due to the presence of some impurities in the ENR.

The DSC results are summarized in **Table IV.3**

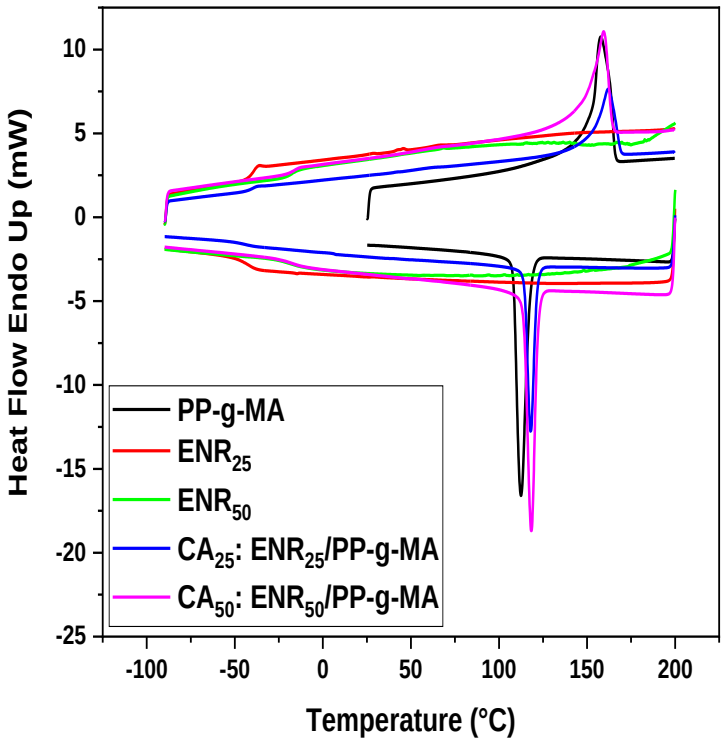

Figure IV.39 DSC thermograms of PP-g-MA, ENR_{25}, ENR_{50}, CA_{25}: ENR_{25}/PP-g-MA, and CA_{50}:ENR_{50}/PP-g-MA.

Table IV.3 Thermal properties of parent polymers and CAs.

	First heating run -90°C to 200°C				Cooling run 200 °C to -90°C			Second heating run -90°C to 200°C			
Parent polymers and CAs	**T_{g1} (°C)**	**T_{m1} (°C)**	**ΔH_{f1} (J/g)**	**Xc1 (%)**	**T_C (°C)**	**ΔH_C (J/g)**	**Xc C**	**T_{g2} (°C)**	**T_{m2} (°C)**	**ΔH_{f2} (J/g)**	**Xc2 (%)**
NR	**-66.02**	/	/	/	/	/	/	**-66.09**	/	/	/
ENR_{25}	**-41.26**	/	/	/	/	/	/	**-41.44**	/	/	/
ENR_{50}	**-22.01**	/	/	/	/	/	/	**-22.04**	/	/	/
PP	/	**164.04**	**89.09**	**43**	**116.06**	**-78.94**	**-38**	/	**159.23**	**87.69**	**42**
PP-g-MA (0.6 wt% of MA)	/	**163.30**	**72.06**	**35**	**112.50**	**-83.42**	**-40**	/	**157.67**	**80.62**	**38**
ENR_{25}/PP-g-MA (50/50)	**-41.24**	**161.98**	**46.41**	**44**	**118.02**	**-39.89**	**-38**	**-42.00**	**157.84**	**41.49**	**40**
ENR_{50}/PP-g-MA (50/50)	**-17.41**	**159.32**	**45.59**	**44**	**118.44**	**-42.40**	**-41**	**-16.66**	**157.84**	**42.76**	**41**

IV.4.1.3 Thermal properties of the CA-containing TPE blends

The DSC thermograms for the CA_{25} and CA_{50}-containing TPE blends are presented in **Figure IV.40** and **Figure IV.41**, respectively.

Table IV.4 presents the melting temperature T_m, heat of fusion ΔH_f, and the fractional crystallinity χ_c obtained by DSC. The percentage crystallinity of the control NR/PP thermoplastic elastomer blend and those of the CA-containing blends at different CA_{25} and CA_{50} contents are presented in **Figure IV.42**. It can be observed that while T_m and ΔH_f remained almost unchanged, the crystallization temperature increased for both the CA_{25} and CA_{50}-based blends. On the other hand, the addition of the compatibilizing agents caused a decrease of χ_c values compared to that of the unmodified blend. The crystallization behavior of the dispersed PP phase in the blend has been altered as a result of a reduction of the spherulite size and a reduced thickness of the crystalline lamellae. It can therefore be deduced that this alteration of the crystallization behavior resulted from the addition of the compatibilizing agents containing ENR and PP-g-MA.

It has been established that the factors that reduce the ability to crystallize depends on the mobility of the macromolecular chains, the presence of a rigid structure, and also on the interchain interactions. Therefore, this alteration of the crystallization behavior noted with the blends studied could be attributed to the crosslinked structure of the CAs, which reduced the

mobility of PP chains, to the interactions that developed between the blend constituents, and also due to the presence of the OH functional group present on the chains of the compatibilizing agents. The mechanism mentioned by Nakason C et al **[1]** is in favor of this explanation.

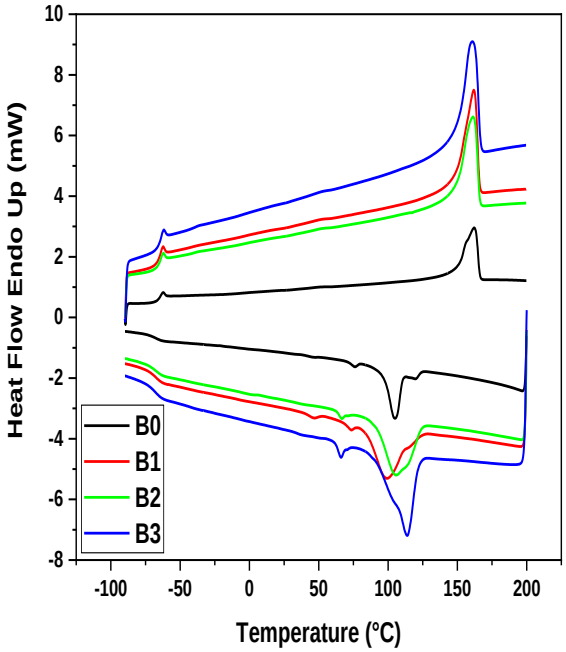

Figure IV.40 DSC thermograms of B0: NR/PP, B1: NR/PP/CA_{25} (5 phr), B2: NR/PP/CA_{25} (10 phr), B3: NR/PP/CA_{25} (15 phr).

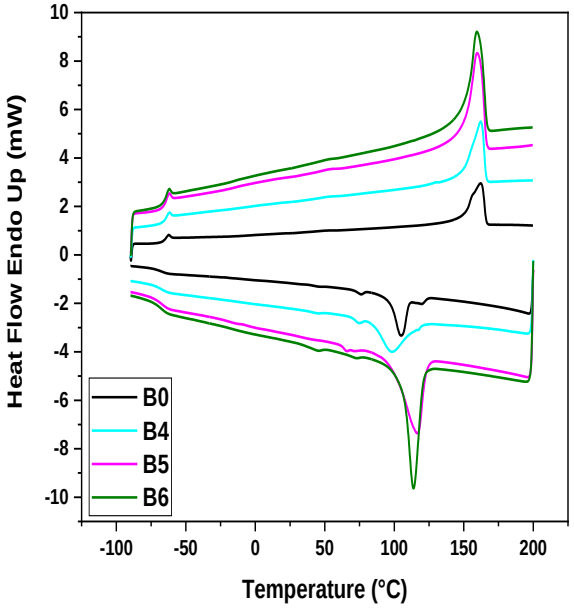

Figure IV.41 DSC thermograms of B0: NR/PP, B4: NR/PP/CA_{50} (5 phr), B5: NR/PP/CA_{50} (10 phr), B6: NR/PP/CA_{50} (15 phr).

Table IV.4 Thermal properties of the CA-containing TPE blends.

TPE blends	T_m (°C)	ΔH_f(J/g)	χ_c(%)
B0	162.20	24.94	48
B1	161.82	25.35	39
B2	161.19	24.71	37
B3	160.74	24.96	36
B4	162.24	23.43	36
B5	159.61	26.15	39
B6	159.41	25.16	37

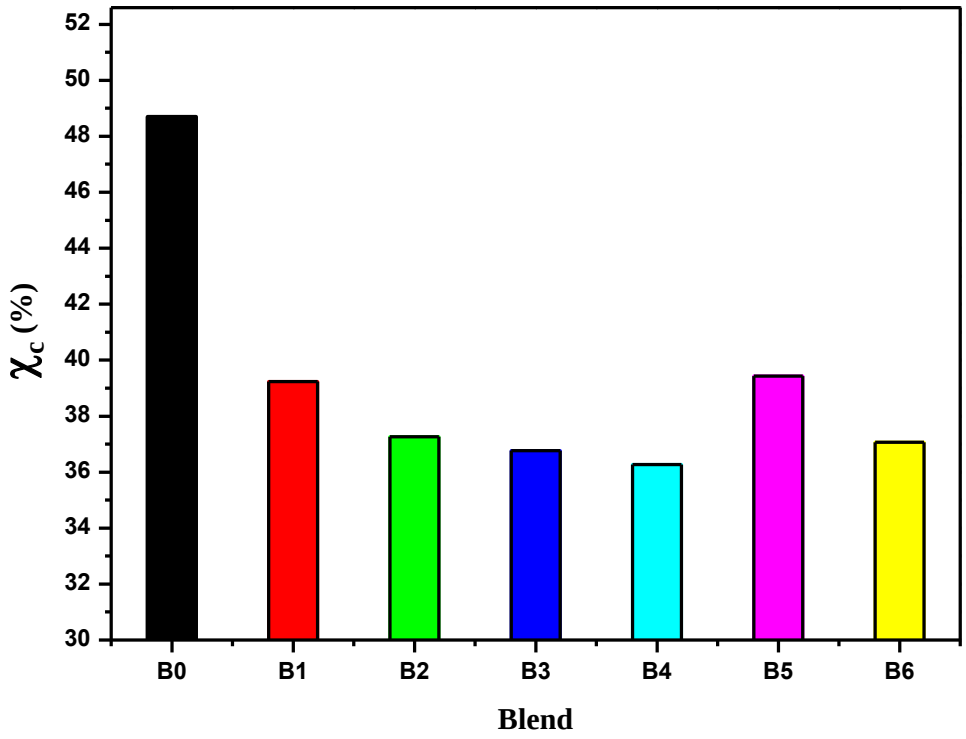

Figure IV.42 Percentage crystallinity (χ_c) of the control NR/PP blend, and those of the CA_{25}, and CA_{50}-containing blends.

IV.4.1.4 Effect of dynamic vulcanization

Figure IV.43 and **FigureIV.44** show the DSC thermograms of NR/PP TPV blends prepared with different CA_{25} and CA_{50} contents, respectively. The different thermal entities such as glass transition temperature (Tg), melting temperature (Tm), heat of fusion (ΔH_f),

% crystallinity (Xc), and heat of crystallization (ΔH_c) of the control NR/PP and the CA-containing TPV blends are presented in **Table IV.5**. The crystallization temperature (Tc) and melting temperature (Tm) of the control NR/PP TPV blend were around 117 °C and 160 °C, respectively. Increasing the CAs contents (either CA_{25}, or CA_{50}), in the blends did not change significantly the melting peak (Tm),the crystallization temperature (Tc), and the glass transition temperature (Tg) compared to the control NR/PP TPV blend. Also, it can be observed that a slight increase in ΔH_f was observed when 15 Phr of CA was present in the TPVs blend compared to the control NR/PP blend value. However, the most striking result noted for the dynamically vulcanized CA-containing blends is the increase of the percentage crystallinity especially for the CA_{50} containing TPV. In fact, χ_c increased by 3% compared to the control 70/30 NR/PP TPV without CA (52 % for the 10Phr of CA_{50}, 49% for the control NR/PP TPV blend).

On the other hand, it is shown that the percentage crystallinity of the CA-containing TPV blends is higher than that of the CA-containing TPE blends. This could be attributed to phase inversion caused after dynamic vulcanization, which means that the PP chains becoming the continuous phase with a lower viscosity and higher mobility had no barrier anymore against their ability to crystallize. It can therefore be considered that these DSC findings confirm the rheology results as well as the SEM and AFM observations.

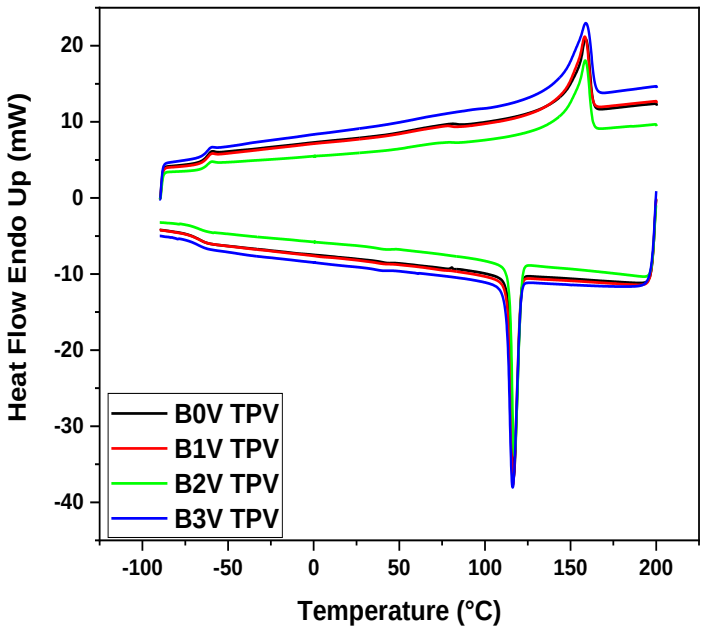

Figure IV.43 DSC thermograms of B0V:NR/PP, B1V: NR/PP/CA_{25} (5 phr), B2V: NR/PP/CA_{25} (10 phr), and B3V: NR/PP/CA_{25} (15 phr).

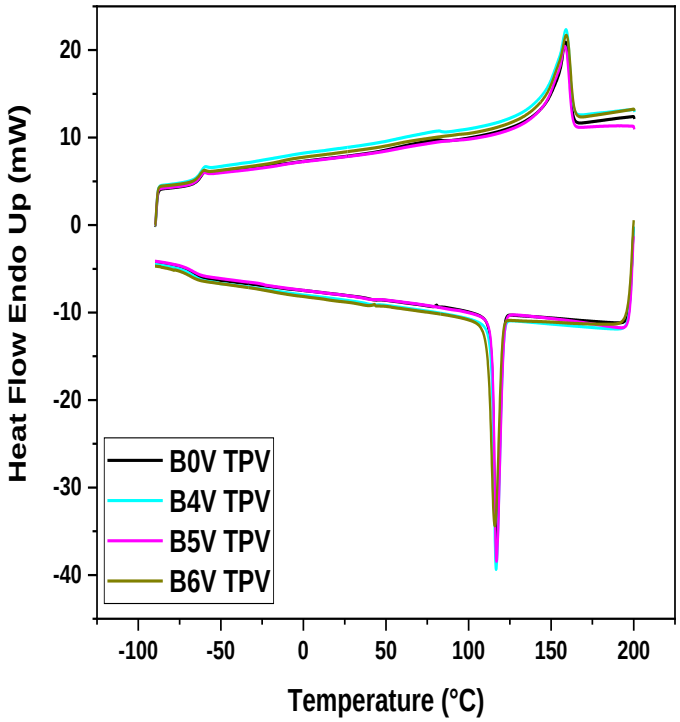

Figure IV.44 DSC thermograms of B0V:NR/PP, B4V: NR/PP/CA_{50} (5 phr), B5V: NR/PP/CA_{50} (10 phr), and B6V: NR/PP/CA_{50} (15 phr).

Table IV.5 Thermal properties of the CA-containing TPV blends.

TPV blends	T_C (°C)	ΔH_C (J/g)	χ_c (%)	T_g (°C)	T_m (°C)	ΔH_f (J/g)	χ_c (%)
B0V	117.33	-28.63	-45	-62.69	160.05	30.72	49
B1V	117.12	-30.04	-46	-63.29	159.41	32.04	50
B2V	117.77	-27.75	-42.	-62.94	159.58	31.66	48
B3V	116.77	-32.87	-48	-63.12	160.49	34.14	50
B4V	117.22	-31.07	-48	-63.33	160.11	33.05	51
B5V	117.59	-30.91	-46	-63.63	159.53	34.40	52
B6V	116.59	-31.94	-46	-62.49	160.74	33.37	49

IV.4.2 Thermogravimetric analysis

IV.4.2.1 TGA and DTG analysis of the CAs

The thermal stability of any polymeric material is largely dependent on the strength of the covalent bonds between the atoms forming the polymeric molecules. The dissociation energy of the bonds C–H, C–C, C–O, C=C,O–H, and C=O bonds were reported to be 414, 347, 351, 611,464, and 732 kJ/mol, respectively **[36].** PP-g-MA contains C–C and C–H, and C=O bonds, whereas, ENR contains all the above bonds except C=O bond. Thus, it may be expected that the blends of PP-g-MA with ENR will possess higher thermal stability than PP-g-MA.

TGA is the most widely used method to investigate the thermal stability of polymers over a wide range of temperature. In this work, TGA was used to investigate the thermal stability of PP-g-MA, ENR_{25}, ENR_{50}, CA_{25}: ENR_{25}/PP-g-MA, and CA_{50}: ENR_{50}/PP-g-MA. The TGA thermograms of the compatibilizers are shown in **Figure IV.45 (A).** It can be observed that neat PP-g-MA and neat ENRs decomposed in one step. However, the degradation of their blends, occurs in two stages corresponding each to the decomposition of ENR followed by PP-g-MA.

The temperatures of the decomposition for the first stage ranged from 340°C to 390°C, which corresponded to the decomposition of ENR. For the second stage, the temperatures ranged from 400°C to 450°C corresponding to the PP-g-MA decomposition. The maximum peak position temperatures of the first and the second decomposition steps of CAs (**Figure IV.45 (B))** are summarized in **Table IV.6.**

Table IV.6 Temperature of the first and the second decomposition steps of the CAs.

Samples	$Tdmax_1$(°C)	$Tdmax_2$(°C)
PP-g-MA	415	/
ENR_{25}	355	/
ENR_{50}	400	/
ENR_{25}/PP-g-MA	356	430
ENR_{50}/PP-g-MA	352	430

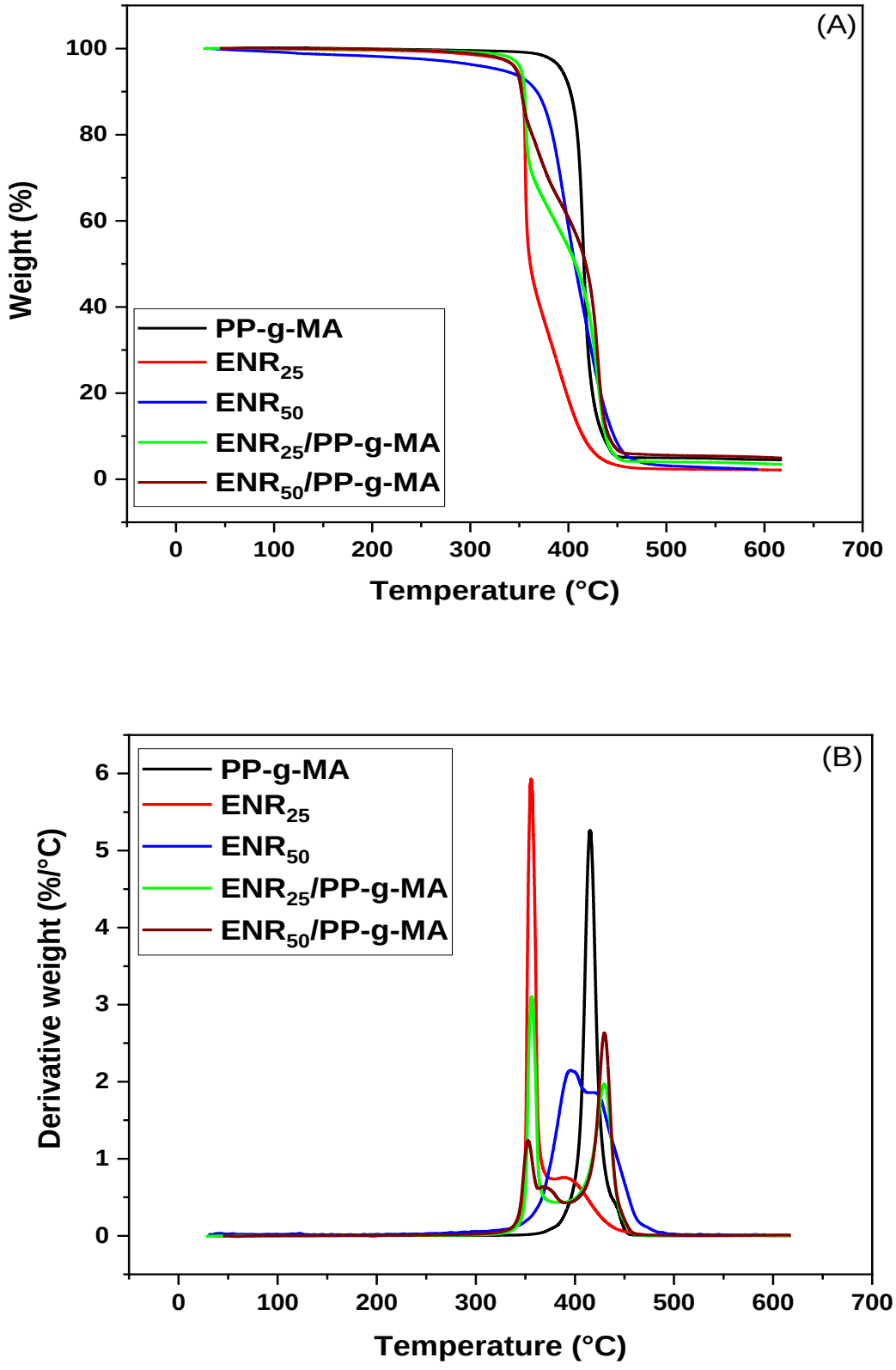

Figure IV.45 TGA (A) and DTG (B) thermograms of PP-g-MA, ENR_{25}, ENR_{50}, ENR_{25}/PP-g-MA, and ENR_{50}/PP-g-MA.

IV.4.2.2 Thermogravimetric analysis of the CA-containing TPE blends

The thermal stability was studied by means of the thermogravimetric analysis over the temperature range between room temperature and 600°C. As shown in **Figure IV.46**, and **Figure IV.47** the TGA and DTG curves of the blends based on CA_{25} (B1, B2, B3) were found to have the same form as those of the CA_{50} compounds (B4, B5, B6). These thermograms show that all the samples exhibited a two-step degradation pattern. We can also observe that for either the CA_{25} or CA_{50}-based blends which exhibited the same general degradation pattern, at the three contents, the curves superimpose on that of the control NR/PP blend. Moreover, as shown in **Figure IV.46** and **Figure IV.47**, from which the decomposition temperatures(T_d) were obtained, it was found that while the temperature of the onset of degradation of NR in the blend remained unchanged (T_{d1} = 347 °C), that of PP insignificantly decreased by 2 degrees (from T_{d2} = 432 °C for neat NR/PP to 430 °C for the15 phr CA-containing blend). These findings mean that the addition of the compatibilizing agents did not influence much the thermal stability.

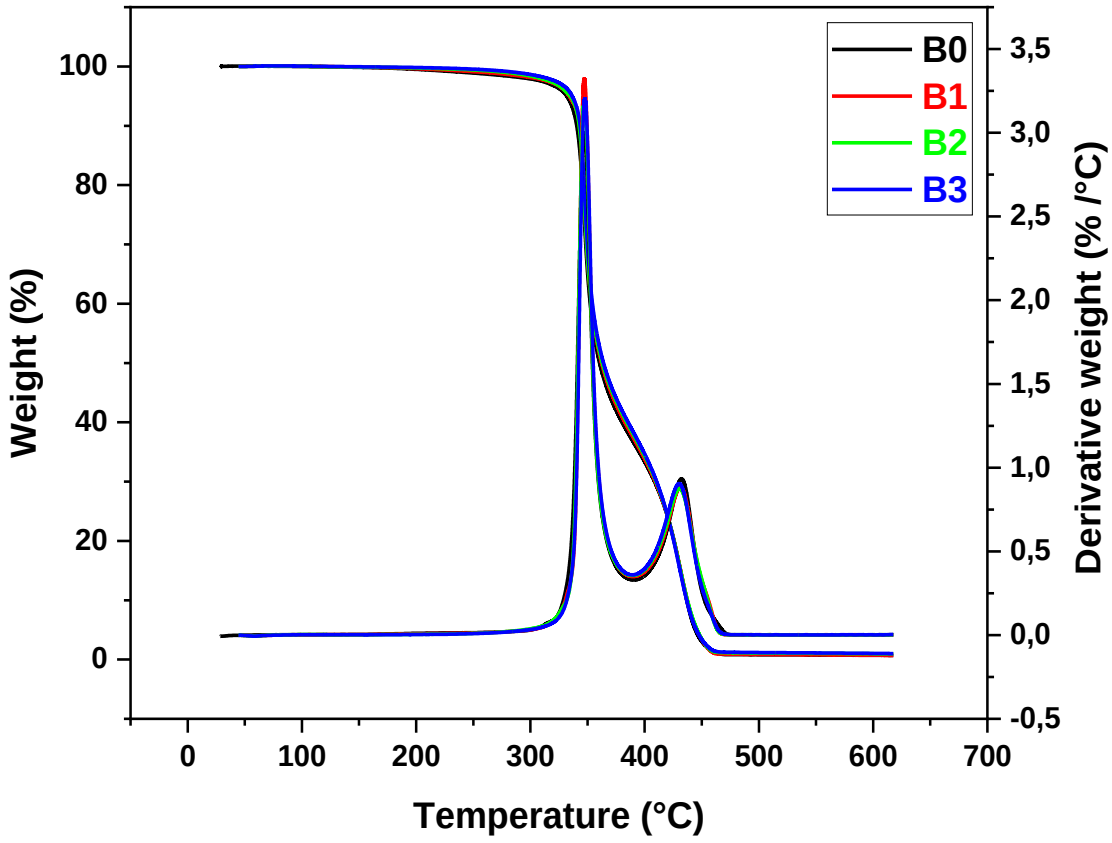

Figure IV.46 TGA and DTG thermograms of B0: NR/PP, B1: NR/PP/CA_{25} (5 phr), B2: NR/PP/CA_{25} (10 phr), B3: NR/PP/CA_{25} (15 phr) TPE blends.

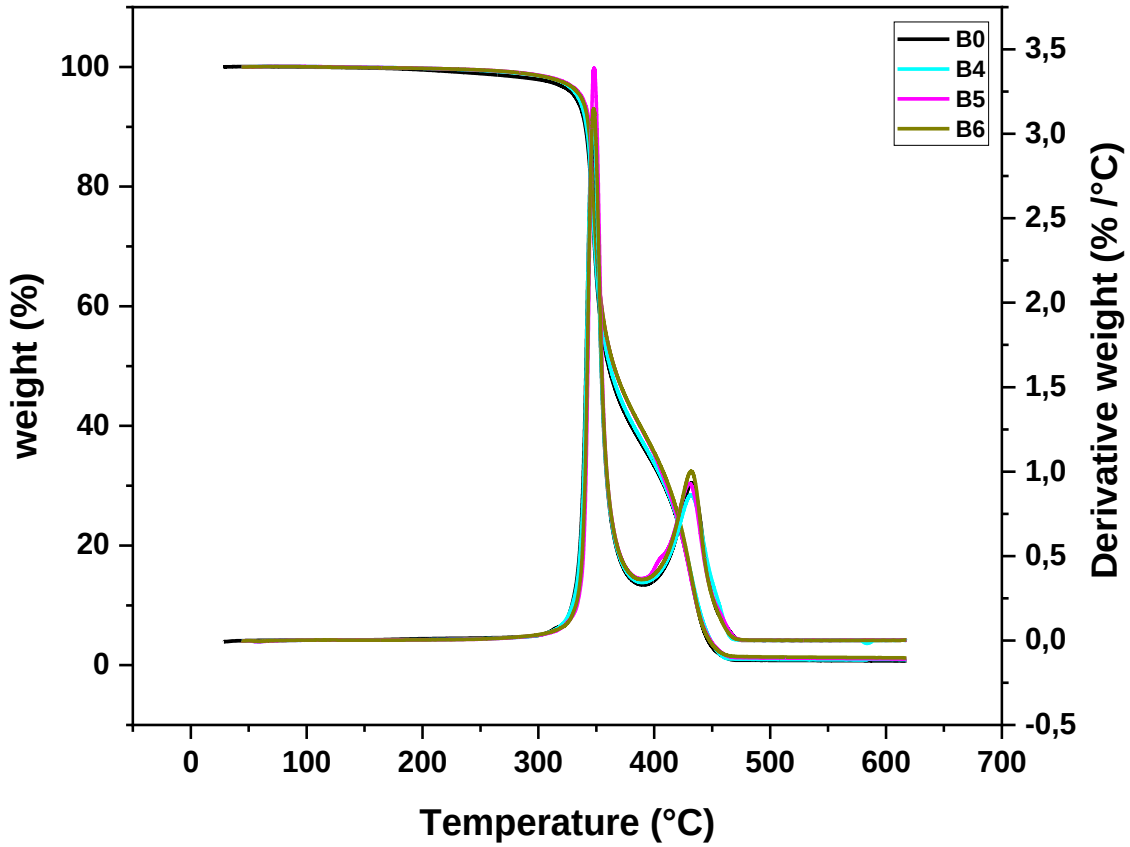

Figure IV.47 TGA and DTG thermograms of B0: NR/PP, B4: NR/PP/CA_{50} (5 phr), B5: NR/PP/CA_{50} (10 phr), B6: NR/PP/CA_{50} (15 phr) TPE blends.

IV.4.2.3 Thermogravimetric analysis of the dynamically vulcanized blends

The thermograms of the dynamically vulcanized TPVs for the CA_{25} and CA_{50}- containing blends are shown in **Figure IV.48**, and **Figure IV.49**, respectively. These curves exhibited the same patterns as those of their TPE counterparts. However, as shown in **Table IV.7**, it was found that the decomposition temperature Td_1, which corresponds to the onset of degradation of the elastomer phase, for the 10 Phr CA_{25}, and CA_{50}-based TPV decreased by 5°C and the decomposition temperature Td_2 , which corresponds to the onset of decomposition of the thermoplastic phase decreased by 7°C compared to the control NR/PP TPE blend.

Eventhough no plausible explanation can be made concerning these effects, these results reflect the complexity of the system studied. This contrast becomes significant if we include the possible vulcanization reaction that could occur in the ENR phase in addition to that in NR. In reality, vulcanization of single phase rubbers improves the thermal stability since more energy is required to break the bonds of the network formed.

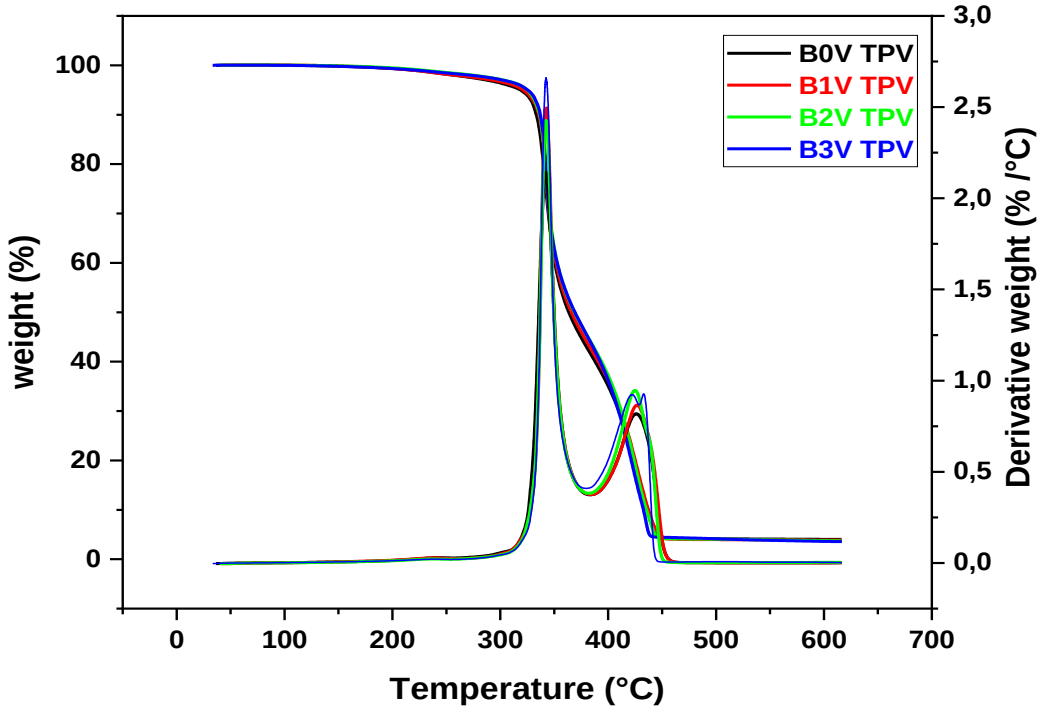

Figure IV.48 TGA and DTG thermograms of B0V: NR/PP, B1V: NR/PP/CA_{25} (5 phr), B2V: NR/PP/CA_{25} (10 phr), B3V: NR/PP/CA_{25} (15 phr) TPV blends.

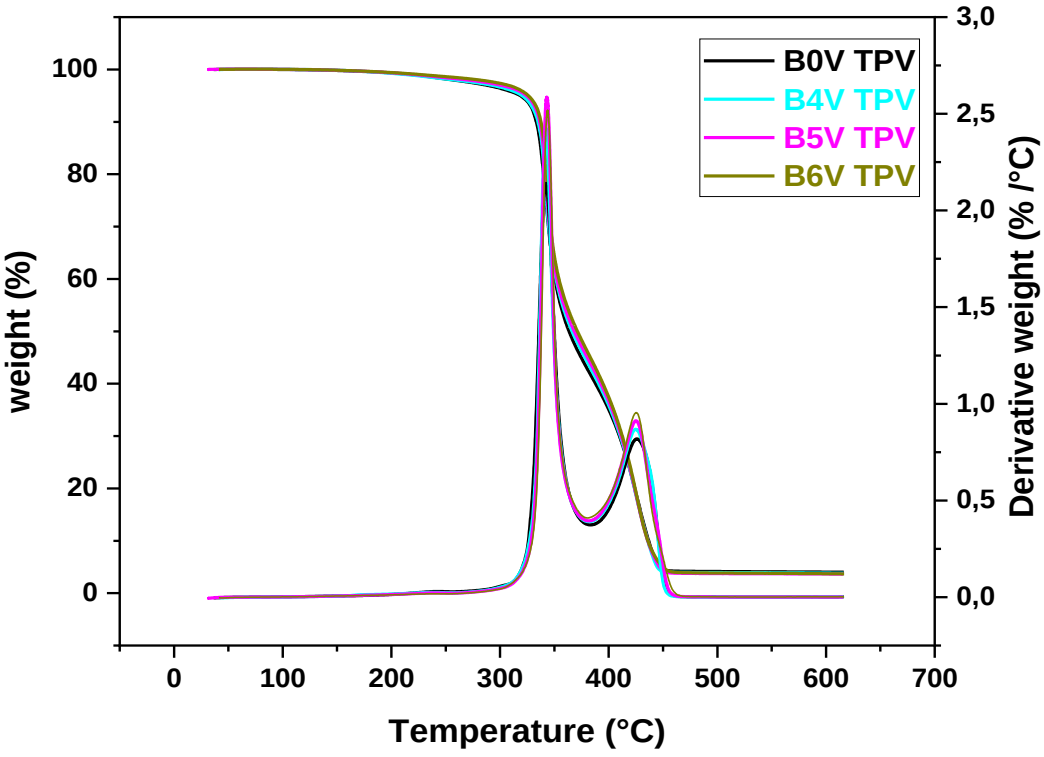

Figure IV.49 TGA and DTG thermograms of B0V: NR/PP, B4V: NR/PP/CA_{50} (5 phr), B5V: NR/PP/CA_{50} (10 phr), B6V: NR/PP/CA_{50} (15 phr) TPV blends.

Table IV.7 TGA and DTG results of the TPE and TPV blends with and without CAs.

Blends	T_{d1} (°C)	T_{d2} (°C)
B0	347	432
B2	347	430
B5	348	430
B0V	342	425
B2V	342	425
B5V	343	425

IV.5 Conclusions

In this chapter, the following conclusions were drawn:

1- The presence of compatibilizers at different concentrations caused an improvement in the mechanical properties of both TPE and TPV blends compared with the control 70/30 NR/PP blend without compatibilizer. This was reflected by the increase of tensile strength and Young's modulus and a decrease of the elongation at break with the increase of the amount of the CA.

2- The dynamic mechanical characterization of the TPE and TPV blends pointed out the increase in the elastic modulus and decrease of the loss modulus with increasing concentration of the compatibilizing agents. The addition of the CA at different contents caused also an increase and shift in the glass transition temperature (Tg) along with larger tan δ peaks. The DMA results revealed also that the T_β transition peak, relative to the PP phase in the blend, disappeared for the unvulcanized CA_{25} or CA_{50}-containing blends but was more pronounced and shifted by almost 9°C for the dynamically vulcanized system with respect to the control 70/30 NR/PP blend.

3- The morphology as observed by SEM and AFM revealed a more homogeneous distribution of the dispersed PP phase for the CA-containing TPE systems compared to the control NR/PP blend. The morphology of the TPVs was characterized by the dispersion of small particles of the vulcanized elastomeric phase in the thermoplastic phase indicating the occurrence of phase inversion.

4- The study of the thermal properties by DSC showed that the increase of the CA concentration led to a decrease in the percentage crystallinity for the unvulcanized TPEs but an increase for the TPVs; which was attributed to phase inversion.

The TGA measurements showed that the incorporation of the compatibilizer did not have any significant effect on the thermal stability of the TPE blends. However, it was found that the decomposition temperatures of the two phases decreased for the dynamically vulcanized blends compared to the TPE blends, an unexpected result that reflects the complexity of the system studied which involves many conflicting factors.

References

[1] Nakason, C.; Wannavilai, P.; Kaesaman, A. Thermoplastic Vulcanizates Based on Epoxidized Natural Rubber/Polypropylene Blends: Effect of Compatibilizers and Reactive Blending. *J. Appl. Polym. Sci.***2006**, *100* (6), 4729–4740. https://doi.org/10.1002/app.23260.

[2] Balakrishnan, H.; Attaran, S. A.; Imran, M.; Hassan, A.; Wahit, M. U. Epoxidized Natural Rubber–Toughened Polypropylene/Organically Modified Montmorillonite Nanocomposites. *J Thermoplast Compos Mater.***2014**, *27* (2),233–250. https://doi.org/10.1177/0892705712443252.

[3] Thitithammawong, A.; Noordermeer, J. W. M.; Kaesaman, A.; Nakason, C. Influence of Compatibilizers on the Rheological, Mechanical, and Morphological Properties of Epoxidized Natural Rubber/Polypropylene Thermoplastic Vulcanizates. *J. Appl. Polym. Sci.***2008**, *107* (4), 2436–2443. https://doi.org/10.1002/app.27233.

[4] Mohamad, N.; Nur Sharafina, Z.; Ab Maulod, H. E.; Yuhazri, M. Y.; Jeefferie, A. R. Morphological and Mechanical Properties of Polypropylene/Epoxidized Natural Rubber Thermoplastic Vulcanizates Treated with Maleic Anhydride-Grafted Polypropylene. *Int J Automot Mech Eng.***2013**, *8*, 1305–1315. https://doi.org/10.15282/ijame.8.2013.19.0107.

[5] Mahendra, I. P.; Wirjosentono, B.; Tamrin; Ismail, H.; Mendez, J. A.; Causin, V. The Influence of Maleic Anhydride-Grafted Polymers as Compatibilizer on the Properties of Polypropylene and Cyclic Natural Rubber Blends. *J Polym Res.***2019**, *26* (9), 215-225. https://doi.org/10.1007/s10965-019-1878-2.

[6] Nakason, C.; Jarnthong, M.; Kaesaman, A.; Kiatkamjornwong, S. Thermoplastic Elastomers Based on Epoxidized Natural Rubber and High-Density Polyethylene Blends: Effect of Blend Compatibilizers on the Mechanical and Morphological

Properties. *J. Appl. Polym. Sci.***2008**, *109* (4), 2694–2702. https://doi.org/10.1002/app.28265.

[7] Nakason, C.; Wannavilai, P.; Kaesaman, A. Thermoplastic Vulcanizates Based on Epoxidized Natural Rubber/Polypropylene Blends: Effect of Epoxide Levels in ENR Molecules. *J. Appl. Polym. Sci.***2006**, *101* (5), 3046–3052. https://doi.org/10.1002/app.23926.

[8] Wetton, R. E.; Marsh, R. D. L.; Van-de-Velde, J. G. Theory and Application of Dynamic Mechanical Thermal Analysis. *Thermo Acta.***1991,** 175(1), 1-11 https://doi.org/10.1016/0040-6031(91)80240-J

[9] Zhang, X.; Loo, L. S. Study of Glass Transition and Reinforcement Mechanism in Polymer/Layered Silicate Nanocomposites. *Macromol.***2009**, *42* (14), 5196–5207. https://doi.org/10.1021/ma9004154.

[10] Liau, W. B. Dynamic Mechanical Relaxation of Lightly Crosslinked Epoxidized Natural Rubber. *Polymer.***1999**, *40* (3), 599–605. https://doi.org/10.1016/S0032-3861(98)00286-9.

[11] Nakason, C.; Panklieng, Y.; Kaesaman, A. Rheological and Thermal Properties of Thermoplastic Natural Rubbers Based on Poly(Methyl Methacrylate)/Epoxidized-Natural-Rubber Blends. *J. Appl. Polym. Sci.***2004**, *92* (6), 3561–3572. https://doi.org/10.1002/app.20384.

[12] Gelling, I.R. Epoxidised natural rubber. *J Natural Rubber Research.***1991**,6(3), 184-205, https://doi.org/10.5254/1.3536059.

[13] Thomas, S.; George, A. Dynamic Mechanical Properties of Thermoplastic Elastomers from Blends of Polypropylene with Copolymers of Ethylene with Vinyl Acetate. *Eur Polym J.***1992**, *28* (11), 1451–1458. https://doi.org/10.1016/0014-3057(92)90291-9.

[14] Roy Choudhury, N.; Chaki, T. K.; Bhowmick, A. K. Thermal Characterization of Thermoplastic Elastomeric Natural Rubber-Polypropylene Blends. *Thermo Acta.***1991**, *176*, 149–161. https://doi.org/10.1016/0040-6031(91)80270-S.

[15] Oommen, Z.; Groeninckx, G.; Thomas, S. Dynamic Mechanical and Thermal Properties of Physically Compatibilized Natural Rubber/Poly(Methyl Methacrylate) Blends by the Addition of Natural Rubber-graft- Poly(Methyl Methacrylate). 12.*J Polym Sci: Part B:Polym Phys.***2000**, 38, 525–536.https://doi.org/10.1002/(SICI)1099-0488(20000215)38:4<525::AID-POLB4>3.0.CO;2-T

[16] Benmesli, S.; Riahi, F. Dynamic Mechanical and Thermal Properties of a Chemically Modified Polypropylene/Natural Rubber Thermoplastic Elastomer Blend. *Polym Test.* **2014**, *36*, 54–61. https://doi.org/10.1016/j.polymertesting.2014.03.016.

[17] Utracki, L. A. Analysis of Polymer Blends by Rheological Techniques. *J Elastomers Plast.***1986**, *18* (3), 177–186. https://doi.org/10.1177/009524438601800305.

[18] B. D. Favis, "Factors influencing the morphology of immiscible polymer blends in melt processing," in Polymer Blends, D.R. Paul and C.B. Bucknall, John Wiley & Sons, Inc., , New York, **2000.**

[19] Belhaoues, A.; Benmesli, S.; Riahi, F. Compatibilization of Natural Rubber–Polypropylene Thermoplastic Elastomer Blend. *J Elastomers Plast.***2020**, *52* (8), 728–746. https://doi.org/10.1177/0095244319891231.

[20] Choudhury, N. R.; Bhowmick, A. K. Compatibilization of Natural Rubber–Polyolefin Thermoplastic Elastomeric Blends by Phase Modification. *J. Appl. Polym. Sci.***1989**, *38* (6), 1091–1109. https://doi.org/10.1002/app.1989.070380609.

[21] H.-J. Radusch, Chapter ‘‘Phase Morphology of Dynamically Vulcanized Thermoplastic Vulcanizates,’’ in Micro- and Nanostructured Polymer Blend Systems: Phase Morphology and Interfaces, C. Harrats, S. Thomas, and G. Groeninckx, CRC/Taylor &

Francis: Boca Raton, FL **2006**. Pages 36, ISBN 9780429115486.

[22] Naskar, K.; Noordermeer, J. W. M. Thermoplastic Elastomers by Dynamic Vulcanization. *Prog Rubber Plast Recycl Technol.***2005**, *21* (1), 1–26. https://doi.org/10.1177/147776060502100101.

[23] Dufaure, N.; Carreau, P. J.; Heuzey, M.-C.; Michel, A. Phase Inversion in Immiscible Blends of PE and Reactive EVA. *J Polym Eng.***2005**, *25* (3),187- 216 https://doi.org/10.1515/POLYENG.2005.25.3.187.

[24] Joubert, C.; Cassagnau, P.; Michel, A.; Choplin, L. Influence of the Processing Conditions on a Two-Phase Reactive Blend System: EVA/PP Thermoplastic Vulcanizate. *Polym. Eng. Sci.***2002**, *42* (11), 2222–2233. https://doi.org/10.1002/pen.11112.

[25] Oderkerk, J.; Groeninckx, G. Morphology Development by Reactive Compatibilization and Dynamic Vulcanization of Nylon 6/EPDM Blends with a High Rubber Fraction, *Polymer*. **2002**; 43(8): 2219-2228. https://doi.org/10.1016/S0032-3861(01)00816-3.

[26] Garcia, P. S.; de Sousa, F. D. B.; de Lima, J. A.; Cruz, S. A.; Scuracchio, C. H. Devulcanization of Ground Tire Rubber: Physical and Chemical Changes after Different Microwave Exposure Times. *Express Polym. Lett.***2015**, *9* (11), 1015–1026. https://doi.org/10.3144/expresspolymlett.2015.91.

[27] Schneider, H. A. Are Kinetic Parameters of Non-Isothermal Thermogravimetric Degradation of Polymers Unequivocal. *J Thermal Analys.***1993**, *40* (2),677–687. https://doi.org/10.1007/BF02546639.

[28] Gupta, M. C.; Viswanath, S. G. Kinetic Compensation Effect in the Thermal Degradation of Polymers. *J Thermal Analys.***1996**, *47* (4), 1081–1091. https://doi.org/10.1007/BF01979449.

[29] Lizymol, P. P.; Thomas, S. Thermal Behaviour of Polymer Blends: A Comparison of the Thermal Properties of Miscible and Immiscible Systems. *Polym Deg Stab.***1993**, *41* (1), 59–64. https://doi.org/10.1016/0141-3910(93)90061-M.

[30] Tomić, N. Z.; Marinković, A. D.; Veljović, Đ.; Trifković, K.; Lević, S.; Radojević, V.; Jančić Heinemann, R. A New Approach to Compatibilization Study of EVA/PMMA Polymer Blend Used as an Optical Fibers Adhesive: Mechanical, Morphological and Thermal Properties. *Inter J Adhestion and Adhesives.***2018**, *81*, 11–20. https://doi.org/10.1016/j.ijadhadh.2017.11.002.

[31] Tomić, N. Z.; Marinković, A. D.; Radovanović, Ž.; Trifković, K.; Marinović-Cincović, M.; Jančić Heinemann, R. A New Method in Designing Compatibility and Adhesion of EVA/PMMA Blend by Using EVA-g-PMMA with Controlled Graft Chain Length. *J Polym Res.***2018**, *25* (4), 96. https://doi.org/10.1007/s10965-018-1493-7.

[32] Silva R, Carvalho GM, Muniz EC, Rubira AF. Miscibility influence in the thermal stability and kinetic parameters of poly (3-hydroxybutyrate)/poly (ethylene terephthalate) sulphonated blends. *Polímeros.***2010**, 20(2), 153-158.https://doi.org/10.1590/S0104-14282010005000023.

[33] Pielichowski, J.; Pielichowski, K. Application of Thermal Analysis for the Investigation of Polymer Degradation Processes. *J Thermal Analys.***1995**, *43* (2), 505–508. https://doi.org/10.1007/BF02546839.

[34] Howell, B. A.; Ray, J. A. Comparison of Isothermal and Dynamic Methods for the Determination of Activation Energy by Thermogravimetry. *J Therm Anal Calorim.***2006**, *83* (1), 63–66. https://doi.org/10.1007/s10973-005-7251-1.

[35] Núñez-Regueira, L.; Villanueva, M.; Fraga-Rivas, I. Activation Energies for the Thermo-degradation Process of an Epoxy-Diamine System: Influence of the Curing Cycle Selection. *J Therm Anal Calorim.***2006**, *83* (3), 727–733. https://doi.org/10.1007/s10973-005-6980-5.

[36] Vasile, C., Ed.; *Handbook of Polyolefins*, 2nd ed., rev.expanded.; Plastics engineering; Marcel Dekker: New York, **2000**.

General Conclusions

General Conclusions

The objective of this work was to investigate the effect of the addition of a 50/50 blend of ENR/PP-g-MA as a compatibilizing agent on the rheological, mechanical, dynamic mechanical, morphological and thermal properties of a 70/30 NR/PP thermoplastic elastomer blend.

The following results were obtained:

1- The FTIR analysis revealed that upon blending, ENR reacted with PP-g-MA and produced ENR-grafted PP with an ester and acid-based linkage. This crosslinked reaction was confirmed during the preparation of the compatibilizer by the rise of the mixing torque noted when ENR was added to PP-g-MA. Confirmation of this reaction was obtained also from the ^{1}H-NMR characterization since dissolving the CAs in hot xylene produced a swollen gel.

2- Evidence to suggest compatibilization was then observed from the Brabender plastograms of the NR/PP blends containing the compatibilizers. These plastograms showed a moderate increase of the torque when the CAs were added. This increase was attributed to the interactions that developed with the blend constituents through the functional groups of ENR and PP-g-MA. From the Brabender plastograms, it was also found that, compared to ENR_{25}; the ENR_{50}-based CA caused a plastization effect by reducing the viscosity which was reflected by the value of the final torque. For the TPVs, it was found that the torque increased also as a result of the incorporation of the CA as well as the dynamic vulcanization which was carried out using a mixture of TMTD, DTDM, and CBS.

3- The RPA measurements indicated that the viscosity of both types of the compatibilizing agents was higher than that of their respective individual values, confirming hence the crosslinking reaction which results upon blending ENR with PP-g-MA. Moreover, the RPA results revealed that, the viscosity of both TPEs and that of TPVs increased with increasing the concentration of both types of the CAs. The same trends were observed for the effects on the storage modulus.

4- The degree of crosslinking of the elastomer phase in the blends dynamically vulcanized by sulfur donors at different amounts of CAs was estimated by measuring the swelling index. It was found that the swelling index decreases continuously with increasing the CA concentration. It can therefore be inferred that changes down to the molecular level have taken place due to the interaction of CA_{25} and CA_{50} with PP and

NR, and that the vulcanizates changed to a stiffer and less penetrable material by the solvent.

5- The mechanical properties results confirmed the enhancement of the interphase interactions for both the unvulcanized blends and the dynamically vulcanized ones. This was reflected by the increase of tensile strength and Young's modulus and a decrease of the elongation at break with the increase of the amount of the CA.

6- The dynamic mechanical characterization of the TPE and TPV blends pointed out the increase in the elastic modulus and decrease of the loss modulus with increasing concentration of the compatibilizing agents. The addition of the CA at different contents caused also an increase and shift in the glass transition temperature (Tg) along with larger tan δ peaks. The DMA results revealed also that the T_β transition peak, relative to the PP phase in the blend, disappeared for the unvulcanized CA_{25} or CA_{50}-containing blends but was more pronounced and shifted by almost 9°C for the dynamically vulcanized system with respect to the control blend.

7- The morphology as observed by SEM and AFM revealed a more homogeneous distribution of the dispersed PP phase for the CA-containing TPE systems compared to the control NR/PP blend. The morphology of the TPVs was characterized by the dispersion of small particles of the vulcanized elastomeric phase in the thermoplastic phase indicating the occurrence of phase inversion.

8- The study of the thermal properties by DSC showed that the increase of the CA concentration led to a decrease in the percentage crystallinity for the unvulcanized TPEs but an increase for the TPVs; which was attributed to phase inversion.

The TGA measurements showed that the incorporation of the compatibilizer did not have any significant effect on the thermal stability of the TPE blends. However, it was found that the decomposition temperatures of the two phases decreased for the dynamically vulcanized blends compared to the TPE blends, an unexpected result that reflects the complexity of the system studied which involves many conflicting factors.

Recommendations

Recommendations

For an eventual continuation of this work, it would be beneficial to further investigate:

1-Study of the chemical structure of the individual CAs as well as that of the resulting TPE using a solid-state NMR.

2- Study the mechanism of the vulcanization reaction.

3-Extend the study to:

3-1 A rigid type of TPNR; for example, a 50/50 NR/PP using a lower MFI grade of PP.
3-2 Another type of TPE such as a blend of a synthetic rubber with a polyolefin.
3-3 The use of other dynamic vulcanization systems.

Abstract

The objective of this work is to study the effects of the incorporation of a 50/50 blend of Epoxidized Natural Rubber / Polypropylene-grafted maleic anhydride (ENR/PP-g-MA) as a compatibilizing agent (CA) for a thermoplastic elastomer based on a 70/30 Natural Rubber / Polypropylene NR / PP blend on the rheological, mechanical, dynamic mechanical, morphological and thermal properties.

Several formulations of this type of elastomer containing different concentrations of CA (from 5 to 15 Phr) were prepared by mixing in the molten state Natural Rubber and Polypropylene using a Brabender plasticorder. The cure response of a vulcanization system based on sulfur donors; namely: tetramethylthiuram disulfide (TMTD), 4,4'-Dithiodimorpholine (DTDM), and N-Cyclohexyl-2-benzothiazole sulfenamide (CBS) and the CA effects were assessed through the Brabender plastograms and swelling index. The rheological behavior was examined by means of a Rubber Process Analyser (RPA). The mechanical properties were determined by the tensile measurements, and the dynamic mechanical properties were also investigated. Scanning Electron Microscopy (SEM) and Atomic Force Microscopy (AFM) were used for the morphological examination. The thermal properties were measured by means of the Differential Scanning Calorimetry (DSC) and Thermogravimetric Analysis (TGA).

The Brabender plastograms as well as FTIR analysis revealed that upon mixing ENR reacts with PP-g-MA and a crosslinked structure results. Evidence of compatibilizing effects was obtained from an improved mechanical and dynamic mechanical properties; which was attributed to a reduction of the interfacial tensions and an enhanced interphase interactions imparted by the CAs.

The study of the thermal properties by DSC showed that the increase in the concentration of CA led to a decrease in the percentage of crystallinity for the TPEs but an increase for the TPVs; which was attributed to phase inversion. On the other hand, the TGA showed that the incorporation of the compatibilizer did not have any significant effect on the thermal stability of the blends.

SEM and AFM examinations revealed a more homogenous distribution of the dispersed PP phase for the CA-containing blends compared to the control NR/PP system. The morphology of dynamically vulcanized blends is characterized by the dispersion of small particles of the vulcanized elastomeric phasein the thermoplastic phase.

Keywords: Natural Rubber, Polypropylene, Thermoplastic Elastomer, Epoxidized Natural Rubber,Polypropylene-grafted Maleic Anhydride,Compatibilizing Agent.

Résumé

L'objectif de ce travail est d'étudier les effets de l'addition d'un mélange de Caoutchouc Naturel Epoxydé/Polypropylène greffé par l'anhydrid maléique (ENR/PP-g-MA) en tant qu'agent compatibilisant (AC) sur les propriétés de l'elastomer thermoplastique à base du mélange Caoutchouc Naturel/Polypropylène (NR/PP). Les différents mélanges étudiésont été préparés à l'état fondu en utilisant un mélangeur BRABENDER.

Pour évaluer l'influence de l'AC, plusieurs techniques d'analyse ont été utilisés ; notamment la rhéologie par RPA (Rubber Process Analyser), détermination des propriétés mécaniques de traction, la DMA en mode de tension, la DSC, l'ATG et DTG, la MEB et l'AFM pour la caractérisation morphologique.

Le suivi des plastogrammes au cours de la préparation des AC a révélé que l'ENR réagit avec le PP-g-MA et produit une structure réticulée. Cette structure a été confirmée grâce à l'analyse par FTIR.

Les résultats ont montré que l'effet compatibilisant a été obtenue vu l'amélioration des propriétés mécaniques et mécaniques dynamiques. Ceci a été attribué à la réduction des tensions interfaciales et l'augmentation de l'adhésion interphases causées par les agents compatibilisant. D'autre part, la DSC a révélé que l'augmentation de la concentration des AC a conduit à une diminution du taux de cristallinité de la phase thermoplastique pour les mélanges non vulcanisés, mais a causé une augmentation de celui-ci pour les mélanges dynamiquement vulcanisés. Ceci a été attribué a l'inversion de phases en conséquence de la vulcanisation dynamique.

Par ailleurs, l'analyse thermogravimétriques a montré que l'incorporation des agents compatibilisant n'affect pas trop la stabilité thermique.

L'examen de la morphologie par MEB et AFM a révélé une distribution homogène de la phase dispersé pour les mélanges non vulcanisés. Celle des mélanges dynamiquement vulcanisés est caractérisée par la dispersion des particules de la phase élastomérique en raison de l'inversion de phases.

Mots clés : Caoutchouc Naturel, Polypropylène, Elastomère Thermoplastique, Caoutchouc Naturel Epoxydé, Anhydride Maléique,Agent Compatibilisant.

ملخص

الهدف من هذا العمل هو دراسة تأثير دمج ايبوكسيد المطاط الطبيعي/ البولي البروبيلين المطعم بالأنهيدريد ماليك (PP-g-MA/ENR) بنسبة 50/50 كعامل توافق (CA) للمطاط الطبيعي الترموبلاستيكي المتكون من خليط المطاط الطبيعي/البولي بروبيلين PP/NR 30/70 على الخصائص الريولوجية، الميكانيكية، الميكانيكية الديناميكية، المورفولوجية و الحرارية. تم تحضير عدة تركيبات من هذا النوع من اللدائن المحتوية على تراكيز مختلفة من عامل التوافق CA (من 5 إلى 15 Phr) عن طريق خلط المطاط الطبيعي والبولي بروبلين في الحالة المنصهرة باستخدام جهاز من نوع برابندر(Brabender).

تم تقييم استجابة العلاج لنظام الفلكنة الديناميكية المعتمدة على مانح الكبريت وتأثيرات CAs من خلال منحنيات جهاز البرابندر(Brabender plastograms) وقياس مؤشرالإنتفاخ. الخصائص التي تمت دراستها إضافة الى منحنيات البرابندر شملت دراسة السلوك الريولوجي للعينات عن طريق (RPA). كما تم أيضا دراسة كل من الخصائص الميكانيكية عن طريق اختبار الشد وكذا الخصائص الميكانيكية الديناميكية عن طريق (DMA). تم استخدام الفحص المجهري الإلكتروني (SEM) والفحص المجهري للقوة الذرية (AFM) من أجل تعيين الخصائص المورفولوجية. تم أيضًا قياس الخصائص الحرارية عن طريق استعمال جهاز المفارق الحراري (DSC) والتحليل الحراري الوزني (TGA).

أظهرت دراسة المنحنيات البيانية أثناء تحضير(CAs) أن ENR يتفاعل مع PP-g-MA وينتج بنية متشابكة. تم تأكيد هذا الهيكل المتشابك من خلال تحليل FTIR.

أظهرت هذه النتائج أيضا أن تأثير التوافق تم الحصول عليه من خلال تحسين الخواص الميكانيكية والميكانيكية الديناميكية. يعزى ذلك إلى انخفاض التوترات البينية بين الأسطح وزيادة التصاق الطور البيني الناتج عن أجهزة التوافق.

أظهرت دراسة الخصائص الحرارية باستعمال جهاز المفارق الحراري(DSC) بأن زيادة تركيز عامل التوافق أدى إلى انخفاض في درجة التبلور بينما أظهر التحليل الحراري الوزني (TGA) بأن تركيز هذا الأخير ليس له أي تأثير على الاستقرار الحراري لخليط المطاط الطبيعي والبولي بروبيلين.

كشفت فحوصات SEM وAFM عن توزيع أكثر تجانسًا لمرحلة PP المشتتة للخلطات المحتوية على CA مقارنة بخليط NR / PP. يتميز الشكل المورفولوجي للخلطات المفلكنة ديناميكيًا بتشتت الجزيئات الصغيرة من الطور المرن المفلكن في الطورالترموبلاستيكي بسبب انعكاس المرحلة.

الكلمات المفتاحية: المطاط الطبيعي ،البوليبروبلين ،المطاط الطبيعي الترموبلاستيكي، ايبوكسيد المطاط الطبيعي ،البولي البروبيلين المطعم بالأنهيدريد ماليك، عامل التوافق.